UNIVERSITÀ DI PISA

Department of Agriculture, Food and Environment

Master of Science
in
Plant and Microbe Biotechnology

Molecular networks controlling leaf cell differentiation during drought stress in *Brachypodium distachyon*

Candidate
Concetta De Quattro

Co-supervisor
Prof. Andrea Cavallini

Supervisors
Prof. Mario Enrico Pè
Dr. Rodolfo Bernardi

Academic Year 2013-2014

Gli ultimi saranno primi e i primi saranno ultimi.

Vangelo secondo Matteo 20, 1-16

Table of contents

Abstract

An important challenge for today agriculture is to intensify worldwide cereal production in a sustainable manner in order to respond to the increasing food demand.

Food production is limited mainly by biotic and abiotic stress and in particular by drought stress, the most common environmental factor affecting plant growth worldwide. For these reasons, the understanding of the complex molecular mechanisms involved in plant response during drought stresses is crucial for developing improved crop varieties better adapted to limiting environments.

Brachypodium distachyon (Bd), a drought-tolerant wild grass, is an interesting model species to deeply study the molecular mechanisms involved in drought-stress response. With this aim, in this study a reproducible soil assay to subject Bd to drought stress was applied, which resulted in a drastically leaf size reduction. This effect was mainly caused by a reduction in cell expansion instead of a reduction of cell proliferation, underlining the insensitivity of the meristem to drought stress.

Starting from this drastic phenotypic effect, the project, using Next Generation Sequencing (NGS) data provides a description of the molecular networks activated in response to drought, focusing on three different developmental zones (proliferation, expansion, and mature cells) of the third young developing *Brachypodium* leaf. More specifically, in order to investigate the mechanisms controlling leaf growth reduction during drought, the third emerging leaf was dissected in the three developmental zones and each zone was subjected to whole transcriptome analysis based on NGS. Eighteen libraries were sequenced, i.e. 3 cell types of leaf grown in control and drought condition, considering 3 biological replicates. Bioinformatics tools and statistical analyses were applied to NGS data, showing that distinct leaf cell zones respond differently to drought treatment. Moreover, the integration of mRNA-Seq data with small RNA-Seq data, previously produced by the lab, allowed to investigate the link between microRNAs and their putative target genes.

1 Introduction

1.1 Modern agriculture

Human population has been predicted to reach over 9.3 billion by the year 2050 (U.S. Census Bureau 2014) and it has been estimated that global food production must be increased over 50-70% due to the exponentially growing world population (FAO, 2009). At the same time, the industrial demand for crops is expected to rise with the growing use of renewable fuel worldwide (Baldos and Hertel, 2014).

Biotic and abiotic stress negatively affect food production, causing a reduction up to 70% (Boyer, 1982) and in particular drought stress, the most common environmental factor, has been shown to pose a critical challenge to agriculture in 45% of the world. ag (Bot, 2000). Thus, water represents a limiting resource in many environments and it has been expected to become even scarcer in the coming decades (UN, 2007).

In this context, the oncoming global climate changes are fuelling the current and future agricultural difficulties, especially water deficit.

The latest report of the Intergovernmental Panel on Climate Change (IPCC, 2013) highlighted that warming is unequivocal, many of the observed changes are unprecedented over decades to millennia: in the Northern Hemisphere, 1983–2012 was likely the warmest 30-year period of the last 1400 years and many extreme weather and climate events have been observed since 1950s (Fig.1.1).

A plausible climate change scenarios includes higher temperatures, changes in precipitation, and higher atmospheric CO2 concentrations (Adams et al., 1998). Climate change impacts agro-ecosystems, affecting plant growth by increasing the variability (frequency and intensity) of weather conditions, such as rainfall, drought, water-logging and elevated temperature. These changes affect both crop productivity and quality (Ortiz et al., 2014).

In this scenario, intensifying food production will be crucial to ensure food security in the coming future.

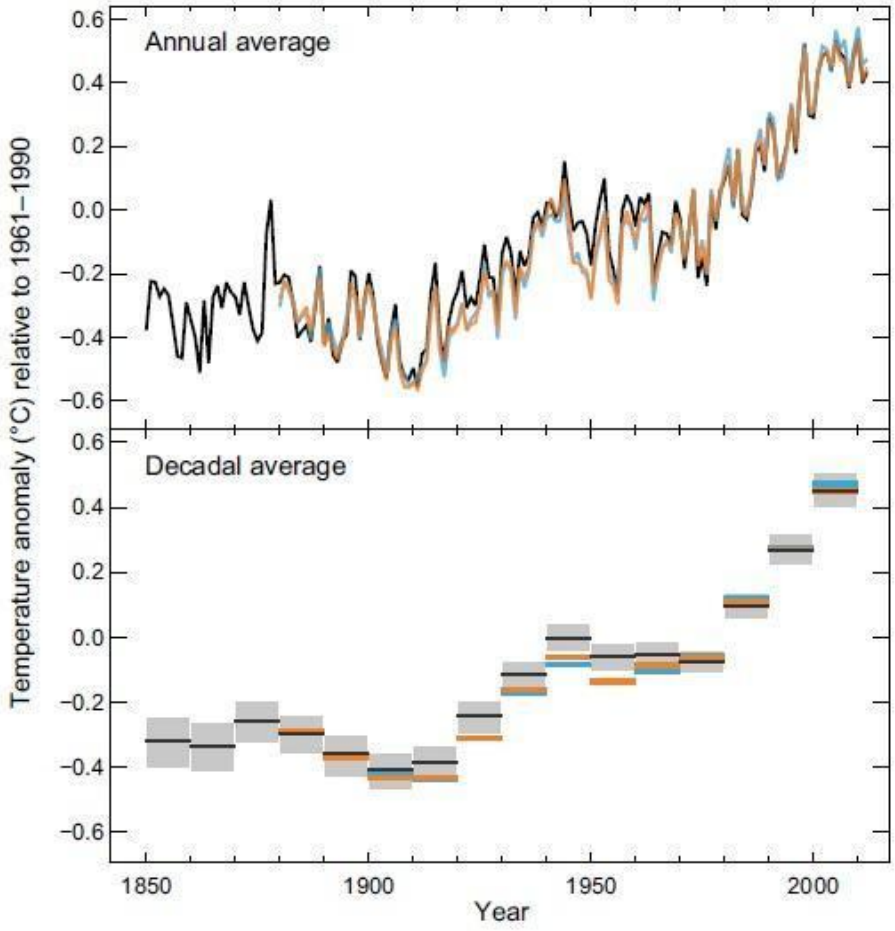

Figure 1.1. Observed global mean land surface temperature anomalies, from 1850 to 2012. Top panel: annual mean values. Bottom panel: decadal mean values including the estimate of uncertainty for one dataset (black). Anomalies are relative to the mean of 1961−1990. Source: IPPC, 2013.

Increasing the cultivated area is not a feasible option to improve global food production. Therefore, it will be important to improve production in a sustainable manner. Important results in improving crop production could be reached by optimizing agricultural practices, reducing the yield gap, reducing food waste, changing consumption patterns or increasing the effectiveness of the food systems. However, these practices represent a partial solution (Dempewolf et al., 2014, Ortiz et al., 2014).

The development of high-yielding crops that can tolerate adverse environmental conditions is now becoming a very important scientific and socio-economical challenge. Current crops are poorly adapted to more uncertain and extreme climatic conditions (Bevan et al., 2010). They have a low genetic diversity as compared to their wild

ancestors, due to domestication, which resulted in population bottlenecks. This lack of variation thwarts attempts to improve germplasm, such as increasing its yield and its stress tolerance.

With the aim to have crops better adapted to new environments, two strategies could be used: developing new crops varieties (genotypes) with conventional breeding programs or introducing target traits into existing crops through genetic engineering.

Conventional breeding approaches could use wild plant species closely related to crops as a source of genetic variability in order to characterize traits involved in stress tolerance. For example plant adaptation to drought, cold, salinity and plant resistance to biotic stresses have been improved through the use of wild plant. Recently the need to better explore plant biodiversity, including wild ancestors, seed banks around the world has emerged, with the objective to improve crops response to climate change (Dempewolf et al., 2014). However, breeding for abiotic stress tolerance is very demanding, time consuming and difficult to realize due to low hereditability.

On the other hand, plant genetic engineering could represent an option, but, besides its scarse acceptability in many Countries, its potential is reduced by the lack of precise and effective target genes to be transferred.

1.2 Monocots and Brachypodium distachyon as a model plant

The Poaceae family is the fourth largest plant family in the world, with over 10,000 species distributed worldwide. The top four agricultural commodities by quantity are grass crops, such as sugarcane, maize, rice, wheat (Bevan et al., 2010).

Unfortunately, the breeding of those crops is time consuming and difficult due to the large polyploid genomes, long generation times, demanding growth requirements, and restricted access to germplasm due to quarantine restrictions and intellectual property concerns (Brkljacic et al., 2011). However, model plants have allowed scientists to study and characterized complex biological processes, which can be used in breeding programs of non-model organisms. *Arabidopsis thaliana*, who was the first plant with a sequenced genome, was the plant model for higher plant for many years. However, t *Arabidopsis* is not a very effective model plant for monocots, especially when agronomic traits are concerned.

In 2001 the undomesticated grass *Brachypodium distachyon* (Bd), belonging to the Pooideae, was proposed as a model species for temperate cereals, such as wheat andbarley (Draper et al., 2001, Brkljacic et al., 2011). This plant is a good model system due to its small stature (30 cm at maturity), short generation time (12 weeks), small genome (~300 Mbp), the ability to self-pollinate, easy growth under simple conditions and easy to transformation (Fig.1.2). All these features are particularly suited for genetic studies and molecular experiments with direct relevance to gene discovery and breeding program of wheat.

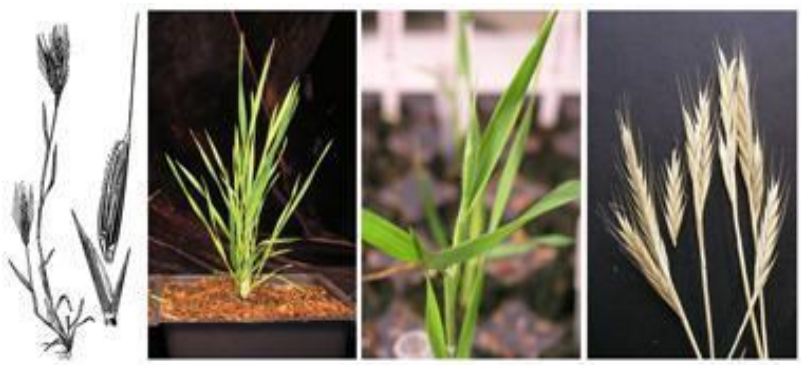

Figure 1.2. Images of Brachypodium plant, leaf and spike (from http://turboweed.org)

Brachypodium distachyon (Bd) belongs to the Poaceae family. Bd is a diploid species with a chromosome base number of *x*=5. Different polyploids species have been found: the autopolyploid series with diploid (2n=10), the tetraploid (2n=20) and the hexaploid (2n=30). The ploides 2n=20, 30, in contast with Bd (2n=10) tend to be taller, have a lesser requirement for vernalization exhibit prominent anthesis and larger seeds (Mur et al, 2011).

It was estimated that Bd diverged from a common wheat ancestor 32-39 million years ago (Mya), from the common rice ancestor 40-53 Mya and from that common sorghum ancestor 45-60 Mya (Fig.1.3). The phylogenetic survey showed that wheat is more closely related to Brachypodium than rice, sorghum or maize. Comparative genome analysis has highlighted a much higher synteny between Brachypodium and Triticaceae than that between rice or sorghum. Therefore, studies on Bd could be easily translated to cereal crops than studies of other model plant.

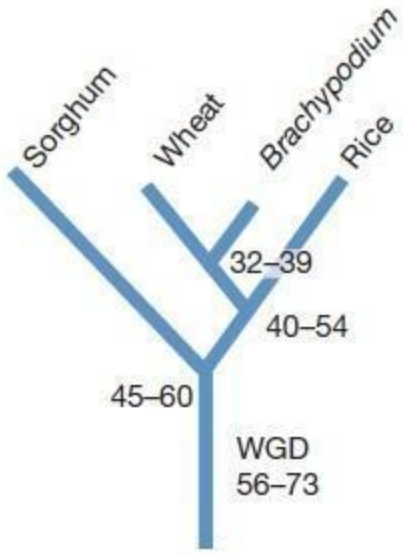

Figure 1.3. The distribution maxima of mean synonymous substitution rates (Ks) of Brachypodium, rice, sorghum and wheat orthologous gene pairs (Supplementary Table 16) were used to define the divergence times of these species and the age of interchromosomal duplications in Brachypodium. WGD, whole-genome duplication. The numbers refer to the predicted divergence times measured as Myr ago by the NG or ML methods (IBI, 2010).

Brachypodium displays many of the agronomic traits that are relevant for temperate cereals improvement, such as resistance to certain pathogens, cell wall composition, grain characteristics and abiotic stress tolerance.

Initially, Bd was proposed as model plant in order to study plant-pathogen response, in particular fungal rust pathogen (Xin-Chun, 2014). Recently many organizations, especially the U.S. Department of Energy, has proposed Brachypodium as a model system to study the genetic mechanisms controlling cell wall composition, biomass and stress tolerance (Bevan et al., 2010). Notably, along this topics, Bd has been also proposed as a model system for biofuel production, such as the wild grasses *Miscanthus* and switchgrass (*Panicum virgatum*).

Bd is also an interesting model plant for the identification and characterization of traits that could have been lost during domestication of cultivated crops, considering that it was never subjected to human selection. Moreover, these traits could be transferred easily to related grass crops (Jeong et al., 2013). An important Bd trait that could be studied is drough-tolerance. Originating from Iraq, Bd is an highly drough-tolerant plant. It may posses molecular mechanisms involved in drought stress response that may have been lost during domestication, therefore it could become a model system for studying drought tolerance in temperate cereal crops (Verelst et al., 2012).

A wide variety of genetic and genomic tools was developed (Mur, 2011).

In 2010, the International Brachypodium Initiative sequenced the entire genome of *Brachypodium distachyon*. It was the first sequenced genome of the Pooideae

subfamily. The diploid inbred line Bd21 was sequenced using a whole genome shot-gun sequencing approach and assembled to ten largest scaffolds, covering 99.6% of sequenced nucleotides. The genome contains 21.4% retrotrasposon sequences and about 25532 protein-coding gene loci annotated, similar to those predicted in rice and sorghum (Xin-Chun, 2014). Genome assembly is of high quality, due to the low level of repetitive DNA in the genome (28%) and to the BAC libraries sequences used during the assembly (Brkljacic et al., 2011). Recently, a revised version of Bd21 genome became available.

Agrobacterium tumefaciens-mediated transformation methods have been developed for Brachypodium. Combining this features with a rapid generation time, Bd is an excellent model for transgenic approaches in the grasses crops.

Several functional genetics platform are being developed for Bd, based on T-DNA tagging and chemical mutagenesis approaches.

The Brachypodium transformation has made feasible the creation of collections of sequence indexed T-DNA mutants. Two groups have been conducted projects to create T-DNA mutant collection: the BrachyTAG collection at John Innes Centre (Norwich, UK) currently is formed by 5000 T-DNA lines (genotype Bd21) that are available on the web site (http://www.brachytag.org/) and the USDA Brachypodium Genome Resources collection with 8491 lines (Dalmais et al., 2013).

By chemical mutagenesis it has been created two Brachypodium TILLING populations, one is BRACHYTIL at INRA in Versailles and Evry in France and the other is at the Boyce Thompson Institute. The BRACHYTIL is a tilling platform for the inbred line Bd21-3 formed by DNA isolated from 5530 different families (Dalmais et al., 2013).

Together with the development of biological and molecular tools were developed bioinformatics tools which allow the analysis of genomic data.

Many bioinformatics tools are available through the http://www.brachypodium.org website (Fig.1.4).

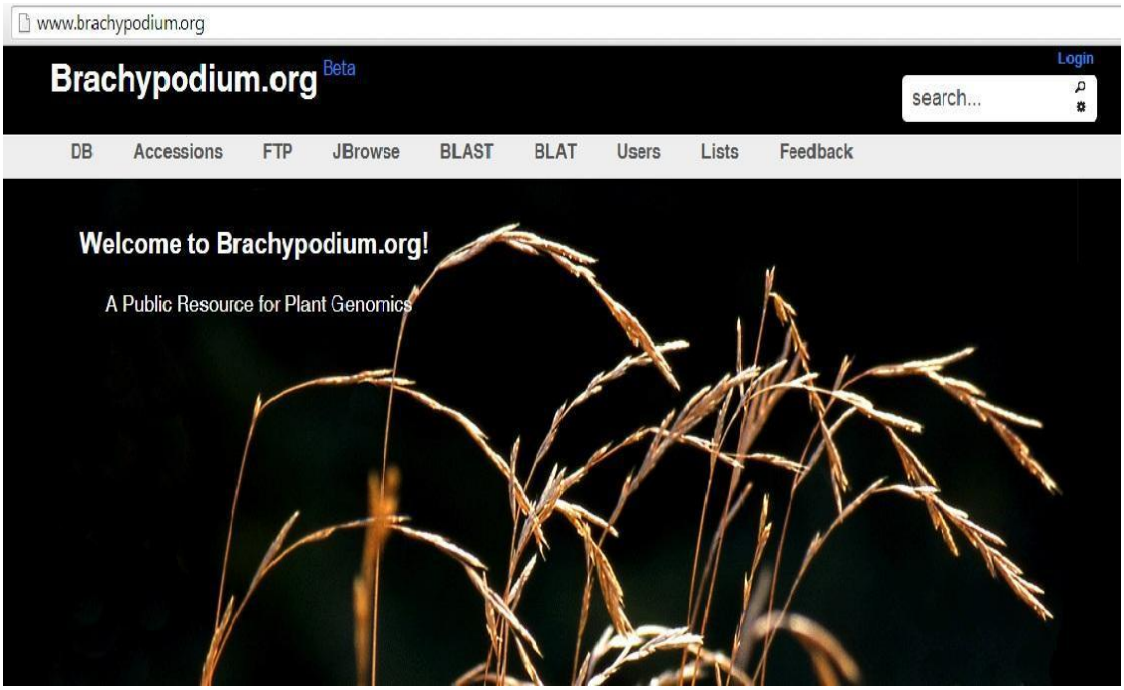

Figure 1.4. Frame of Brachypodium web site (www.brachypodium.org).

This is the reference web site for Brachypodium community, with links to many different resources and tools. It includes a BLAST tool, a genome annotation database, Brachypodium microarray analysis tools and resources, and BrachyBase, the Brachypodium genome browser, where the 8X assembly genome can be viewed and downloaded. BrachyBase contains standard genome information, EST database, and deduced protein and cDNA sequences. It also contains Illumina RNA-Seq transcriptome data and T-DNA mutant collection. Another Brachypodium genome browser is available at the Munich Information Center for Protein Sequences (http://mips.helmholtz-muenchen.de/).

The availability of the complete genome sequence enables genome wide analysis, such as the analyses of non coding and coding RNAs by means of next-generation sequencing (NGS) approaches. Moreover, the reference genome simplifies the computational identification and annotation of miRNAs and their mRNA target prediction. Currently the research about microRNAs (miRNAs) in Bd is underdeveloped: only 136 mature miRNAs from 135 miRNA precursors from different tissues and drought or cold stress-treated tissues were identified. Comparing to other model plants, such as Arabidopsis (338 miRNAs) and rice (708 miRNAs), the number

of annotated miRNAs in Bd is low, therefore it will be important to characterize with high confidence Bd miRNAs (Jeong et al., 2013).

The whole genome sequence also facilitates the analysis of coding RNAs. Indeed, reads generated by mRNA sequencing could be mapped to the reference genome and could be assembled into transcripts. The high-throughput mRNA sequencing (RNA-seq) makes it possible to discover new genes and transcripts and evaluate transcript expression in a single assay (Trapnell et al., 2012) and it could be used to improve genome annotation (Roberts et al., 2011). In addition, this approach allows to identify genes expressed at a very low level.

The whole transcriptome sequencing with NGS approach was conducted in this research project with the aim to identify molecular changes underlying growth reduction in Bd leaves under drought stress.

1.3 Plant abiotic stress response

Plant growth is affected by changing environmental conditions that could cause a reduction in crop yields. Indeed environmental stresses constitute the primary cause of crop losses worldwide, reducing average yields of most major crop plants by more than 50%. The ongoing climate change increases surface temperatures and aridity that will affect global agriculture in coming years. Together with the decline in arable farmland due to soil degradation and human activities, a strong pressure is put on crop production to feed the growing human population in the next decades (Danquah et al., 2014). For these reasons, it will be important to understand the molecular mechanisms involved in plants response to environmental stresses as an important aid in designing novel and efficient strategies to develop new and better adapted crop varieties.

Abiotic stress is defined as environmental conditions that reduce growth and yield below optimum levels (Cramer et al., 2011). Abiotic stress is characterized by intensity, duration, number of exposure, combination of more than one stress. The plant responses to abiotic stress are dependent on the tissue or organ affected by the stress and developmental stage. In addition, the level and the duration of stress (acute or chronic) can have a significant effect on the complexity of the response (Cramer et al., 2011). *In vitro* setups, used to study the effects of abiotic stress on plant, indicate that there is a

highly dose-dependent response of plants to stress and depends on the type of stress. This suggests the existence of a very sensitive machinery assessing the stress level and fine-tuning molecular responses (Claeys et al., 2014).

Due to their sessile nature, plants have developed adaptive mechanisms to cope environmental stresses: plants could be sensitive or resistant to stress. In the first instance plant are not able to response to stress, therefore plant might die. Instead resistant plant complete their life cycle under stress conditions, developing different adaptive responses that could be avoidance or tolerance mechanisms. When stress arises, plant growth is often affected by a rapid and acute ("acute response") inhibition, followed by recovery and adaptation to the new condition ("adaptation response"). While the acute response prepares plants for possibly more severe conditions, the adaptive response can be seen as the establishment of a new steady state to prolonged and stable stress (Skirycz and Inzé, 2010).

The abiotic stress response occurs in two stages: an initial sensory/activation stage, followed by a physiological stage during which the plant responds to the perceived stress. Once a stress is perceived by receptors and sensor proteins on the membrane, the information is transmitted to cytoplasmic target proteins through catalytic processes, such as phosphorylation. Ca^{2+} and inositol are secondary messangers involved in stress signalling. The increase in Ca^{2+} is sensed by various calcium binding proteins that initiate phosphorylation cascades that subsequently activate transcription factors. Transcription factors in turn activate expression of stress responsive genes. At this point starts the second phase and physiological changes occur that influence various cellular and whole plant process necessary to survive to the environmental stress. The genes expressed and subsequent physiological changes induced during the second phase are dependent upon the particular abiotic stress encountered. These changes can include modifications to cell membrane components – resulting in changes in membrane fluidity, stomatal closure, decreased photosynthetic activity, and increased production of heat shock proteins (HSPs) or dehydrin cryoprotectants. Thus, abiotic stress affects plant growth and development (Priest et al., 2014).

Stress sensors are not known and most of the signalling intermediates have not been identified. It is thought that different signalling pathways share one or more intermediates/components or have some common outputs, forming a "cross-talk" (Chinnusamy et al., 2004). Recent evidences indicate that plant hormones make a

crosstalk, through a synergic or antagonic interactions, playing a crucial role in plant response to environmental stress, by mediating growth, development, nutrient allocation, and source/sink transitions (Peleg and Blumwald, 2011). The two most important hormones are abscisic acid (ABA) and ethylene. ABA regulate many stress response, particularly osmotic stresses, inducing stomatal closure. Instead, ethylene is involved in many stress responses, such as drought, ozone, flooding, heat, chilling, wooding and UV-B light. Evidences show an interaction between ethylene and ABA during drought stress. Moreover, many abiotic stress affect synthesis, concentration, metabolism, transport and storage of sugars. Soluble sugars play a role as potential signals interacting with light, nitrogen and abiotic stress to regulate plant growth and development (Cramer et al., 2011).

The main abiotic stresses that affect plants and crops in the field include drought, salinity, heat, cold, chilling, freezing, nutrient, high light intensity, ozone (O3) and anaerobic stresses. Drought stress is one of the major factors limiting plant growth and development in agriculture (Boyer, 1982). For cereal crops, drought is the most important abiotic stress component reducing yield. A recent report showed that the extreme drought affected 80% of cultivated land in the United States in 2012 and reduced yield of maize by 27.5% and of soybean by 10%, causing an enormous economic damage (USDA, 2013). Due to climate change and urbanization and the depletion of aquifers, fresh water availability for irrigation will decrease in the coming decades. Hence, given its importance for agriculture, the effects of drought on plant development have been extensively studied in the past decades (Clays and Inzé, 2013).

Drought stress response could be subdivided into two strategies: avoidance stress and tolerance stress. Avoidance strategy is the maintenance of a high plant water potential during stress, balancing water uptake and water loss. Water uptake is maximized by the accumulation of compatible solutes, such as prolamines, raffinose, to lower the tissue water potential and by improving root growth, while water loss is limited by closing stomata, restricting shoot growth, trichomes presence, reduced leaf area, senescence of older leaves.

Tolerance strategy involves mechanisms that protect cells against damage. These mechanisms include the production of antioxidant to detoxify reactive oxygen species (ROS) and the synthesis of protective protein, such as dehydrin and late embryogenesis abundant (LEA) proteins, and compatible solutes, that has a dual role as osmolyte and

osmoprotectant. Long-term water stress can be accompanied by morphological changes, such as cuticle thickening, root architecture, hardening of cell walls. The balance between growth and survival is tightly regulated, and plants have evolved specific adaptations to growth under drought conditions (Fig.1.5) (Claeys and Inzé, 2013).

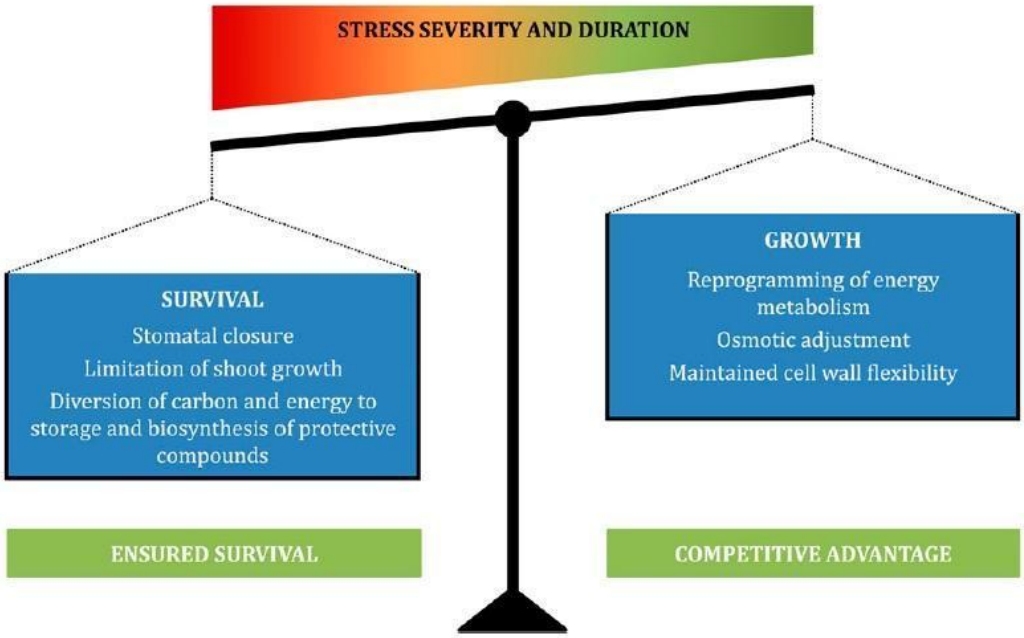

Figure 1.5 The balance between stress tolerance and maintained growth. In response to water limitation, stress avoidance and tolerance mechanisms are activated to ensure survival in case the stress is prolonged or becomes more severe, resulting in growth limitation and a potential competitive disadvantage. However, several adaptations allow plants to balance survival and continued growth depending on the stress level (Claeys and Inzé, 2013).

Until now, most of these drought responses have been studied only in mature tissues and under rather extreme stress conditions. These experiments have improved our knowledge of stress physiology and molecular responses, but they may not reflect physiological conditions that occur in the field. In addition, it was observed that plant response to severe drought conditions is different from a transient mild water deficit, therefore different mechanisms regulated this process (Skirycz et al., 2011).

Various molecular networks are involved in stress response. The common stress signalling pathways have been distinguished into abscisic acid (ABA) dependent and ABA independent pathway. The increase of ABA under drought stress induce stomatal

closure and regulate expression of transcriptions factors (TFs) that modulate downstream drought-responsive gene expression. TFs induce by ABA are AREB/ABFS, MYB2, MYC2 and RD26 (NAC) which bind their correspondent *cis*-active elements ABRE, MYB, MYC and NAC. AREB/ABFS is a major *cis*-acting element in ABA-responsive gene expression and the cis-element ABRE (ABA-responsive *cis*-element) has been found in the regulatory region of downstream genes. TFs of ABA-independent pathways include ZFHD, DREB2 and NAC(RD26). DRE (dehydration-responsive element)/CTR (C-RepeaT) is one the mayor *cis*-elements present in the promoter region of various ABA-independent abiotic stress-responsive genes. Recent studies have suggested that there are interactions between the major ABA signalling pathways and other signalling factors in stress responses (Shinozaki and Yamaguchi-Shinozaki, 2007, Nakashima et al., 2014).

After early signal perception events, signaling genes and molecules acting as secondary messengers, such as Ca^{2+} and reactive oxygen species. These regulatory mechanisms induce downstream functional genes and regulatory genes, such as transcription factors, which are needed to establish new cellular homeostasis that leads to drought tolerance and/or resistance.

Limited water availability affects plant growth. Initially that limiting growth was considered as a secondary effect of stress, caused by reduced photosynthetic activity and stomatal closure a lower rate of photosynthesis. However, carbohydrates are often accumulates in stressed plant, showing that growth reduction is not the consequence of carbon deficit (Claeys and Inzé, 2013).

However, after the onset of the stress, growth rates have been shown to decrease rapidly, independently of photosynthesis (referred to as "short-term adjustment"), followed by growth recovery and adaptation to the new condition. Therefore, it is now accepted that plants actively reduce their growth as part of the stress response. These growth changes allow plants to save and redistribute resources that can become limited; for example, smaller leaves lose less water due to a reduced transpiration area, while differential growth recovery leads to beneficially higher root-to-shoot ratios. Therefore, this phenotypic plasticity allows the plant to manage its resources under changing environmental conditions (Skirycz et al., 2010).

To study the mechanisms underlying stress-mediated growth inhibition, Inzé and co-worker at the University of Gent (BE) studied the *in vitro* effect of osmotic stress on

Arabidopsis leaf development (Skirycz et al., 2010). Those studies were conducted on the third leaf because its development is mostly seed-independent and it reaches maturity before the plant starts flowering. This experimental setup considered stage-specific sampling under prolonged drought stress, instead mature leaves or complete plant shoots like previous work. This study identified several hundred transcripts and multiple metabolites that respond to drought exclusively in the proliferating and/or expanding leaf zones. In addition the reduce leaf area is due to a combination of fewer and smaller cells (Skirycz et al., 2010).

In response to drought stress a pause and stop mechanisms has been proposed: when stress occurs, cell cycle rapidly stops with a decrease in CDKA activity and cells are block in a state allowing a quick recovery (pause); if the stress persists, cells initiate the differentiation process (stop). When proliferating cells completely disappeare, meristemoid division activity becomes higher in stressed leaves in order to create a small increase in cell numbers (Skirycz et al., 2011).

Surprisingly, ABA does not seem to be involved in the stress-response in proliferating and expanding cells, suggesting a central role of ethylene signaling in growing leaves. Results show that ethylene inhibits cell proliferation and CDKA activity by a post-transcriptional mechanism, whereas ABA would be responsible for drought tolerance in mature leaves (Fig.1.6) (Skirycz et al., 2011).

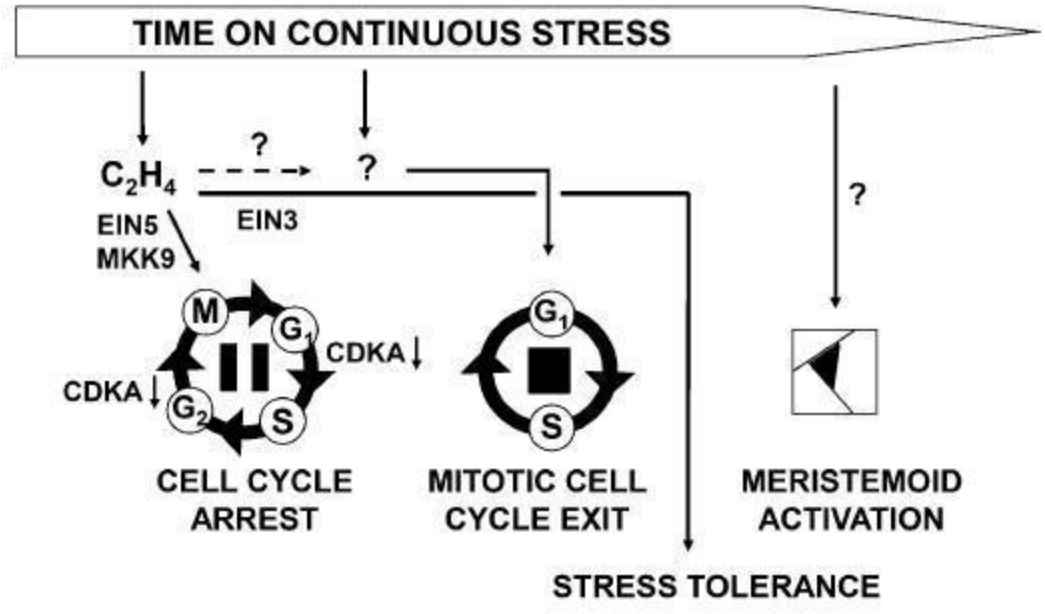

Figure 1.6 Simplified scheme depicting the regulation of cell cycle inhibition and cell differentiation in response to osmotic stress. Very rapidly (within hours) after the imposition of the stress, ethylene (C2H4) production is triggered, inhibiting CDKA activity through a posttranscriptional mechanism that reversibly inhibits the cell cycle by G1/S and G2/M arrest. Cell cycle arrest is independent of EIN3 transcriptional control and possibly mediated by a MAPK signaling pathway or the ribonuclease EIN5. In a later phase, a different signal leads to permanent inhibition and exit from the mitotic cell cycle in favor of the endocycle and cell differentiation. Later in leaf development, meristemoid division activity becomes higher in stressed leaves and the enhanced meristemoid division results in a small increase in cell numbers (Skirycz et al., 2011).

1.4 Small RNAs and abiotic stress

A very exciting area in abiotic stress research has emerged in recent years, focusing on epigenetic factors that mediate response to different stresses (Chinnusamy and Zhu, 2009). Plant small non coding RNAs play an important role in epigenetic regulation regulating gene expression by post-transcriptional degradation, and/or translational repression and/or chromatin modification.

For many years non-coding RNA (ncRNAs) genes were regarded as relics of an RNA-based origin of life. However, with the application of new technologies it was showed that these molecules have highly specialized biological roles so they could not considered as "molecular fossil". The involvement of many ncRNAs in functions requiring sequence-specific recognition of another nucleic acid sequence suggests their

function as regulatory molecules. During the 1990s, many experiments identified the presence of these small molecules. The first studies were conducted in petunia flowers and they showed that overexpression of gene to produce deep purple flowers gave white flowers instead. The explanation of this molecular mechanisms arrived in 1998 when it was first discovered in the worm *Caenorhabditis elegans* by studying RNA interference (Bonnet et al., 2006). Thus it was born the "Small RNA Era".

Small RNAs (sRNAs) are essential regulatory molecules that act to fine-tuning gene expression regulation through sequence complementary-dependent mechanisms at different levels: binding and cutting complementary target mRNAs, inhibiting translation of these mRNAs, and interacting with epigenetic DNA-methylation for RNA-directed DNA methylation (RdDM) (Humbeck, 2013).

Many studies focused on the characterization of the expression of sRNAs and their target transcripts, using mutant analyses to demonstrate the involvement of sRNAs in different stress pathways, e.g. drought, cold, salt, UV, heavy metal and biotic attack (Khraiwesh et al. 2012). The regulatory network of stress-responsive sRNAs also interacts with regulatory pathways under the control of the stress hormone abscisic acid (ABA) (Humbeck, 2013). It was shown that the role of sRNAs in a variety of phenomena is essential for genome stability, development, and adaptive responses to biotic and abiotic stresses (Vaucheret, 2006).

Plant small RNAs are 21-24-nt-long which, depending on their biogenesis and functions, are classified as microRNAs (miRNAs), trans-acting siRNAs (ta-siRNAs), natural antisense siRNAs (nat-siRNAs) and repeat-associated siRNAs (ra-siRNAs).

Micro-RNAs are the most abundantly expressed and well-studied class of small RNAs in plants. They are 20-22 nt long non coding RNAs that play a crucial role in regulations of gene expression in most eukaryotes (Schapire et al., 2014).

Plant microRNAs were first discovered in early 2002 in *Arabidopsis thaliana,* after that many plant miRNAs were found to be conserved in many plant genome such as *Oryza sativa, Zea mays* and more ancient vascular plants such as fern or in non vascular plant such as mosses (Bonnet et al., 2006).

miRNAs are coded by specific genes called MIR genes. Many differ MIR genes and precursors (between 50 and 900 nucleotides) may encode the same mature miRNA or highly similar molecules, therefore, these molecules are grouped into families.

The biogenesis of plant miRNAs happens within specialized regions of the nucleus,

called D-bodies, starting with the production of a primary miRNA (pri-miRNA) transcript from coding intergenic regions mediated by the activity of RNA polymerase II. Dicer-like 1 (DCL1), an RNase III enzyme, processes the pri-miRNA into a shorter, stem-loop formed by base-pairing between self-complementary regions called precursor-miRNA (pre-miRNA) and successively releasing a miRNA/miRNA* duplex with a 2-nucleotide 3' overhang at each end. After methylation by means of HUA ENHANCER 1 (HEN1), miRNA/miRNA* duplexes are exported to the cytoplasm by HASTY (HST), where ARGONAUTE 1 (AGO1), a member of the Argonaute family, recruits the processed RNA mature to form the RNA-induced silencing complexes (RISCs) and the miRNA* is usually degraded. RISC exerts its effect in RNA silencing by facilitating the recognition of RNA sequences showing complementarity to small RNAs incorporated into the complex. Target RNAs are cleaved, or rendered unavailable to translation.

Therefore, in plant miRNAs down-regulate expression of their target genes by complementary target mRNA cleavage between the 10-11 nucleotide or by a translational inhibition which presumably affects the pool of transcripts remaining after cleavage (Voinnet, 2009).

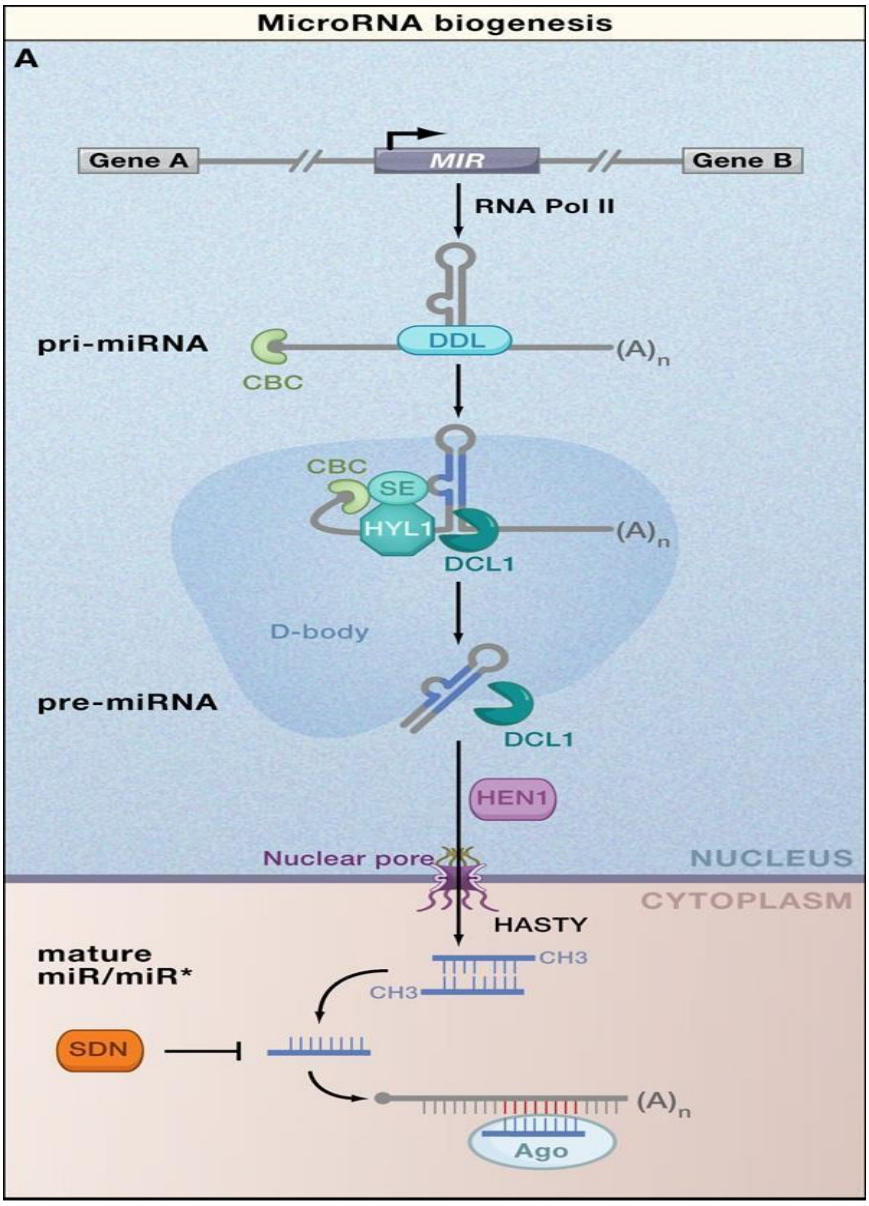

Figure 1.7. Biogenesis of plant miRNAs. Molecular pathway for the processing and stability of conserved plant microRNAs (miRNAs). Plant pri-miRNAs are mostly transcribed by RNA polymerase II (Pol II) from regions located between protein-coding genes. The RNA-binding protein DAWDLE (DDL) presumably stabilizes pri-miRNAs for their conversion in nuclear processing centers called D-bodies to stem-loop pre-miRNAs. This reaction entails the concerted action and physical interaction of the C2H2-zinc finger protein SERRATE (SE), the double-stranded RNA-binding protein HYPONASTIC LEAVES1 (HYL1), Dicer-like 1 (DCL1), and nuclear cap-binding complex (CBC). Pre-miRNAs, or mature miRNAs produced by DCL1, are then exported to the cytoplasm possibly through the action of the plant exportin 5 ortholog HASTY and other unknown factors. Mature RNA duplexes excised from pre-miRNAs (miRNA/miRNA*, where miRNA is the guide strand and miRNA* is the degraded strand) are methylated by HEN1, a reaction that protects them from being degraded by the SMALL RNA DEGRADING NUCLEASE (SDN) class of exonucleases. The guide miRNA strand is then incorporated into AGO proteins to carry out the silencing reactions (from Voinnet, 2009).

Most plant miRNA targets are transcription factors with important regulatory roles in

different physiological and developmental processes, such as leaf morphogenesis, patterning and polarity establishment, developmental timing, floral organ identity, phytohormone signaling (Wu, 2013). Moreover, in plant miRNAs have a crucial role in tolerance and response to biotic and abiotic stresses, including cold, drought, salinity, oxidative stress, hormone signaling, nutrient deficiency, bacterial infections, UV-B radiation and mechanical stress (Jiang et al., 2014). Hence, it is crucial the functional characterization of this molecules for understanding plant development and stress response. Recently, a large number of conserved and non-conserved miRNAs related to drought response was identified by means of a genome-wide approach in *Populus*, soybean, sugarcane, *Panicum virgatum* and *Medicago* (Yin et al., 2014).

Many stress-responsive miRNAs are induced or repressed during abiotic stress and can modulate the expression of target genes that may be involved in a particular stress response and/or tolerance. miRNA stress-induce reduce the expression of target gene by cleavage and it was observed that the expression patterns of miRNA target genes generally show an inverse correlation with those of miRNAs. Therefore this negative correlation between target mRNA and miRNA accumulation if often considered proof of miRNA targeting (Fig. a). Moreover a miRNA restricts the expression of its target in the cell type where they are expressed. Indeed, the target gene is abundant in a cell type in which the miRNA is lowly expressed and vice versa (Fig. 1.8). Therefore, in order to investigate cell type stress response the analysis should be conducted at cell-type level instead at the whole organ (Bertolini, 2013; Jeong and Green, 2013).

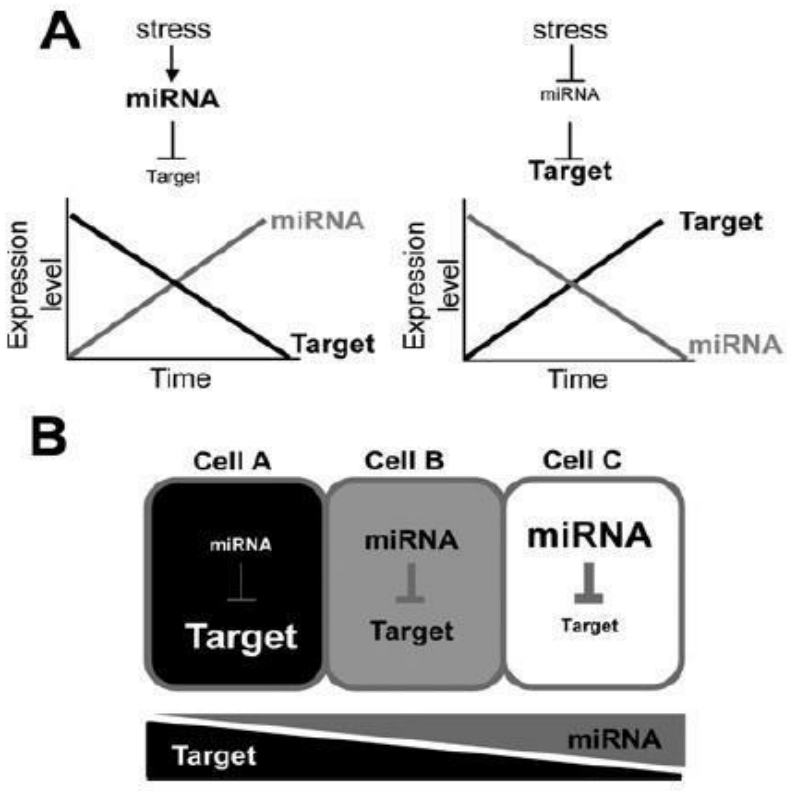

Figure 1.8. Spatio-temporal effects of stress-regulated miRNAs on target gene expression. A. Temporal regulation of target gene expression by stress-regulated miRNAs. Stress-induced miRNAs down-regulate the expression of their target genes during a given stress condition, while stress-repressed miRNAs up-regulate expression of their target genes during the stress condition. B. Spatial regulation of target gene expression by stress-regulated miRNAs. Stress-responsive miRNAs that are regulated in a cell type- specific manner can spatially restrict the expression of their targets in a particular cell or cell type (Jeong and Green, 2013

Various experimental and *in silico* approaches have been used to identify miRNA genes and their targets in plants. NGS revolutionized miRNAs discovery, providing an effective way to identify and profile small RNA populations in model and non model plants (Jiang et al., 2014) in a fast, accurate and less expensive way (Wu, 2014). Moreover, this approach provides a genome-wide view of interaction between miRNAs and their target genes. Indeed a computational prediction of miRNAs targets can be performed, based on complementary base pairing between the miRNA and its target. This target prediction requires an experimental validation. The most used technique is a modified 5'-RACE (Rapid Amplification of cDNA Ends) that allows to observe e the product of degradation after target cleavage by the miRNA. In the NGS era this validation approach is not sensitive due to the large amount of predicted targets produced by small RNA sequencing. Therefore, computational approaches were

developed that consent a global target identification and validation. The analysis of Parallel Analysis of RNA Ends (PARE) has been proposed for genome-wide identification of miRNA targets (Jeong and Green, 2013). Using PARE, also called degradoma analysis, target cleavage products can be cloned and sequenced. Moreover, the power of this methods is that it is possible to investigate site-specific cleavages at single-nucleotide level (Jeong et al., 2013).

In plants such as *Arabidopsis*, *Brachypodium*, rice and maize, several studies have described miRNA genes as well as their targets in a wide variety of tissues, developmental stages, and treatment conditions (Gentile et al., 2013). New miRNAs are deposited in miRBase (http://www.mirbase.org/), an online database of published precursor and mature miRNA sequences and annotation accessible since 2002. To date 28,645 precursor and 35,828 mature miRNAs from 223 species are available on the last release of miRBase database (miRBase release 21, June 2014,Van Peer et al., 2014).

1.5 Molecular regulation of leaf development

Leaves, the mayor organ where photosynthesis is performed, originate from shoot apical meristem (SAM), a small group of pluripotent stem cells that continuously divide and replenish themselves.The key functions of SAM is to maintain itself as a source of cells and to generate daughter cells that are displaced towards the meristem periphery and its base, where they enter specific differentiation pathways to form lateral organs (leaves and flowers) and the stem, respectively (Johnson and Lenhard, 2011). The pluripotent state of SAM is maintained by the activity of class *I KNOTTED1-LIKE HOMEOBOX (KNOXI)* genes. When these genes are down regulated, it occurred a switch from an indeterminate to a determinate fate in a small group of cells (founder cells) that loses indeterminacy and becomes the immediate precursor of the leaf primordia (Moon and Hake, 2011). The position of leaf primordium initiation is determined by local auxin accumulation. Usually these cells originate at the flank of SAM. Initially towards the outside cells form a peg, then divisions become localized to the margin between the upper and the lower side to form the leaf lamina (Kidner et al., 2010). During leaf growth three axes of development, proximo-distal, medio-lateral and adaxial-abaxial, are established and maintained throughout the entire process. The proximo-distal axis is

defined by the leaf petiole the lamina, the medio-lateral polarity is identified by the midvein and leaf margins. Whereas the adaxial–abaxial polarity is reflected in the two opposing sides of the leaf blade, which possesses cells with different functions: cells of the adaxial (upper) mainly conduct photosynthesis and cells of the abaxial (lower) part, with stomata, are specialized in transpiration optimized in gas exchange. This occurs concomitant with primordium outgrowth. This development is one of the main adaptations of land plants since it maximizes photosynthesis with a minimum water loss. (Pauline and Laufs, 2010).

Leaf development is extremely plastic and leaf size depends on genetic predisposition, leaf position and environmental conditions (Andriankaja et al, 2012).

During leaf growth two distinct, partially overlapping cellular phases can be recognized: cell proliferation and cell expansion. The rate and duration of these processes are responsible for the final leaf size. During cell proliferation, cells increase in size and accumulate cytoplasmic mass, and subsequently divide to form new cells. Subsequently, cells stop to divide and begin to increase cell size by cell expansion. During a transition phase, cell division first ceases at the tip of the leaf and gradually most cells start to expand from the tip to the base (basipetal direction). During cell expansion, most cells start to differentiate, however some cells, dispersed in the leaf and called meristemoids, continue to divide themselves and form stomatal guard cell (Gonzalez et al., 2012).

Leaf development can be divided into three phases: primordium initiation, primary morphogenesis, and secondary morphogenesis. During primary morphogenesis the leaf grows largely by cell proliferation, while during secondary morphogenesis the leaf cells stop dividing and begin to expand. Secondary morphogenesis does not occur in all leaf cells simultaneously, rather it begins in the tip of the leaf and progresses toward the leaf base (Andriankaia et al., 2012).

The final size and shape of plant organ is under the control of developmental genetic programs exhibiting species-specific characteristic. Indeed leaf morphogenesis involves a coordinated regulation among transcription factors (TFs), small non-coding RNAs (sRNAs) and hormones. Insight into leaf growth control has largely been achieved through the characterization of mutants with specific defects affecting cell differentiation, proliferation and expansion (Johnson and Lenhard, 2011).

To date, a growing number of organ growth regulators have been identified. They influence cell proliferation and/or cell expansion in different moments and in different

cell types during leaf development (Gonzalez et al., 2012). Thus, several transcription factors (TFs) involved in important pathway of leaf growth were largely characterized and investigated, such as: *AINTEGUMENTA*, *PEAPOD*, *JAGGED*, *BLADE ON PETIOLE*, *TCPs*, *GROWTH REGULATING FACTORs* (Fig.1.9).

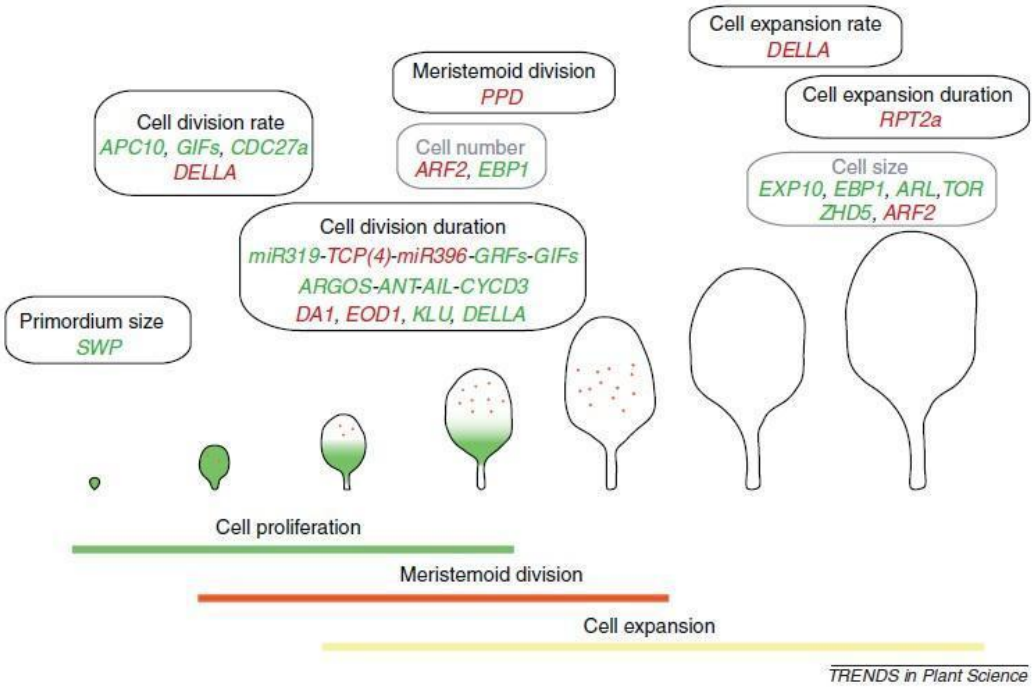

Figure 1.9 Molecular mechanisms regulating leaf size. The different processes occurring during leaf development (cell division and cell expansion) are represented. The different events that could influence the final leaf size (primordium size, cell division or expansion rate, cell division or expansion duration, and meristemoid division) and genes involved in positive (green) or negative (red) regulation are shown Abbreviations: SWP (STRUWWELPETER), APC10 (ANAPHASE PROMOTING COMPLEX10), GIF (GRF-INTERACTING FACTOR), CDC27a (CELL DIVISION CYCLE PROTEIN 27 HOMOLOG A), TCP (TEOSINTE BRANCHED1/CYCLOIDEA/PCF), GRF (GROWTH-REGULATING FACTOR), ARGOS (AUXIN-REGULATED GENE INVOLVED IN ORGAN SIZE), ANT (AINTEGUMENTA), AIL (AINTEGUMENTA-LIKE), CYCD3 (CYCLIN D3), EOD1 (ENHANCER OF DA1-1), ARF2 (AUXIN RESPONSE FACTOR2), KLU (KLUH), EXP10 (EXPANSIN10), EBP1 (ErbB-3 EPIDERMAL GROWTH FACTOR RECEPTOR BINDING PROTEIN), PPD (PEAPOD), RPT2a (REGULATORY PARTICLE AAA-ATPASE 2a), ARL (ARGOS-LIKE), TOR (TARGET OF RAPAMYCIN) and ZHD5 (ZINC FINGER HOMEODOMAIN5) (from Gonzalez et al., 2012).

Furthermore, it has been demonstrated the determinant role of several miRNA families in the spatial-temporal coordination of developmental processes by targeting a subset of TFs. Clear examples are those of mir164, miR159, miR166, miR319, miR396 that target CUC, GAMYB, HD-ZIPIII, TCP, and GRF respectively (Fig.1.10).

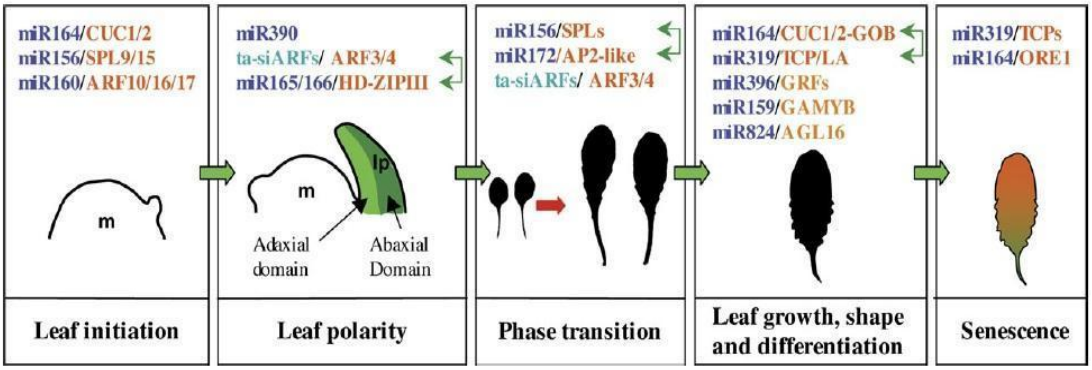

Figure 1.10 Small RNAs and their targets regulate the different stages of leaf development from initiation to senescence. MiRNAs and ta-siRNAs are in dark blue and light blue, respectively, and their targets in orange. Interactions between small RNA/target regulatory modules are shown by green double arrows. m, meristem; lp, leaf primordium (Pulido and Laaufs, 2010).

While several TFs underlying plant development and drought tolerance have been characterized, sRNAs have recently emerged as new regulator of leaf growth and development.

Plant hormones, such as gibberellin and auxin, play important roles in growth regulation. GAs is crucial in growth regulation, it stimulate cell division and cell expansion in leaves through the degradation of DELLA growth repressor, which inhibit leaf growth by altering cell proliferation and expansion. Similarly, in respond to auxin, the transcripion factors AUXIN RESPONSE FACTORS (ARF2) repress growth affecting cell division and cell expansion (Claeys et al., 2014). Regarding leaf development, auxin and cytockins are fundamental in the induction of leaf primordia. Auxin repress *KNOXI* genes expression promoting leaf differentiation from SAM. While cytockinins is required for maintenance the indeterminate group of cell in apical shoots Moreover *KNOXI* repress the expression of genes involved in GA biosynthesis and GA catabolism to maintain meristem (Blein et al., 2010).

1.6 Background information

Understanding the complex molecular mechanisms involved in plant stress response is crucial for future plant breeding programs, with the aim to develop new varieties

(genotypes) with better performance and a stable productivity.

When subjected to stress, plants rapidly reprogram their growth by not yet clatified mechanism, affecting cell number and size. To study the molecular basis underlining this process, particularly investigating monocot specific mechanism controlling leaf growth, we used *Brachypodium distachyo*n as the biological model.

With the aim of investigating the molecular basis of drought stress response, Verelst et al. (2012) developed a reproducible soil drought assay for *Brachypodium* plants (Fig.1. 11). This experiment allows to collect *Brachypodium* third leaf and dissect, according to fluorescence microscopy analysis, three type of cells: i) proliferating cells, ii) expanding cells and iii) mature cells.

This drought stress experiment results in 40% of stressed third leaf size reduction in comparison to control leaves. Leaf growth reduction is primarily caused by a reduction in cell expansion instead of a reduction in cell number, highlighting the insensitivity of the meristem to drought stress. This result is in contrast with previous observation made in different plant model species (e.g. *Arabidopsis* and rice) in which cell division and cell expansion is inhibited by drought resulting in smaller size and number cells per leaf.

To deeper investigate the genetic network at the basis of this phenomenon at organ and cellular level, kinematic and DNA-chip transcriptome analysis were performed. Kinematic analyses of proliferating and expanding cells were conducted to assess growth rate of the leaf under optimal and stress condition, and to understand how the processes that operate at the cellular level contribute to difference in growth rates at the whole organ level. The analysis of the transcriptome of each development zone showed that each area responds differently to drought. This may lead to identify key genes involved mainly in stress response.

Bertolini et al. (2013) utilized this drought stress experiment to perturb leaf growth along proximo-distal axis to investigate the role of miRNAs on the molecular regulatory networks underlying leaf development.

Eight small RNA libraries from expanding and proliferating cells grown in control and stress conditions were produced and sequenced using NGS technology. By applying a customed *ab initio* pipeline, a total of 270 miRNA and miRNA-like genes were identified, confirming 66 previous annotations and adding 28 new genes to know MIR families. In addition, 94 novel species-specific miRNAs and 82 siRNA-like miRNAs

were discovered. Differential expression analysis showed that a large proportion of mRNAs seemed to be involved in developmental programming, while only a few miRNAs modulate their expression during stress response. To describe the biological function of annotated miRNAs miRNAs target prediction based on sequence similarity between the miRNA and mRNA was performed. This genome-wide analysis of small RNA molecules provided additional evidence for a role of miRNAs in the regulatory network controlling cell division in normal and stressed conditions and demonstrated that drought causes a genetic reprogramming of leaf growth in which miRNAs are deeply involved (Bertolini et al., 2013).

This combined approach of studying both the transcriptomic profiles of coding genes and the characterization of the small RNAs allowed to shed light on the interplay between the different components of the system that act to establish a new growth leaf reprogramming during drought stress. Moreover using Brachypodium as model plant it was possible to identify stress-tolerance genes.

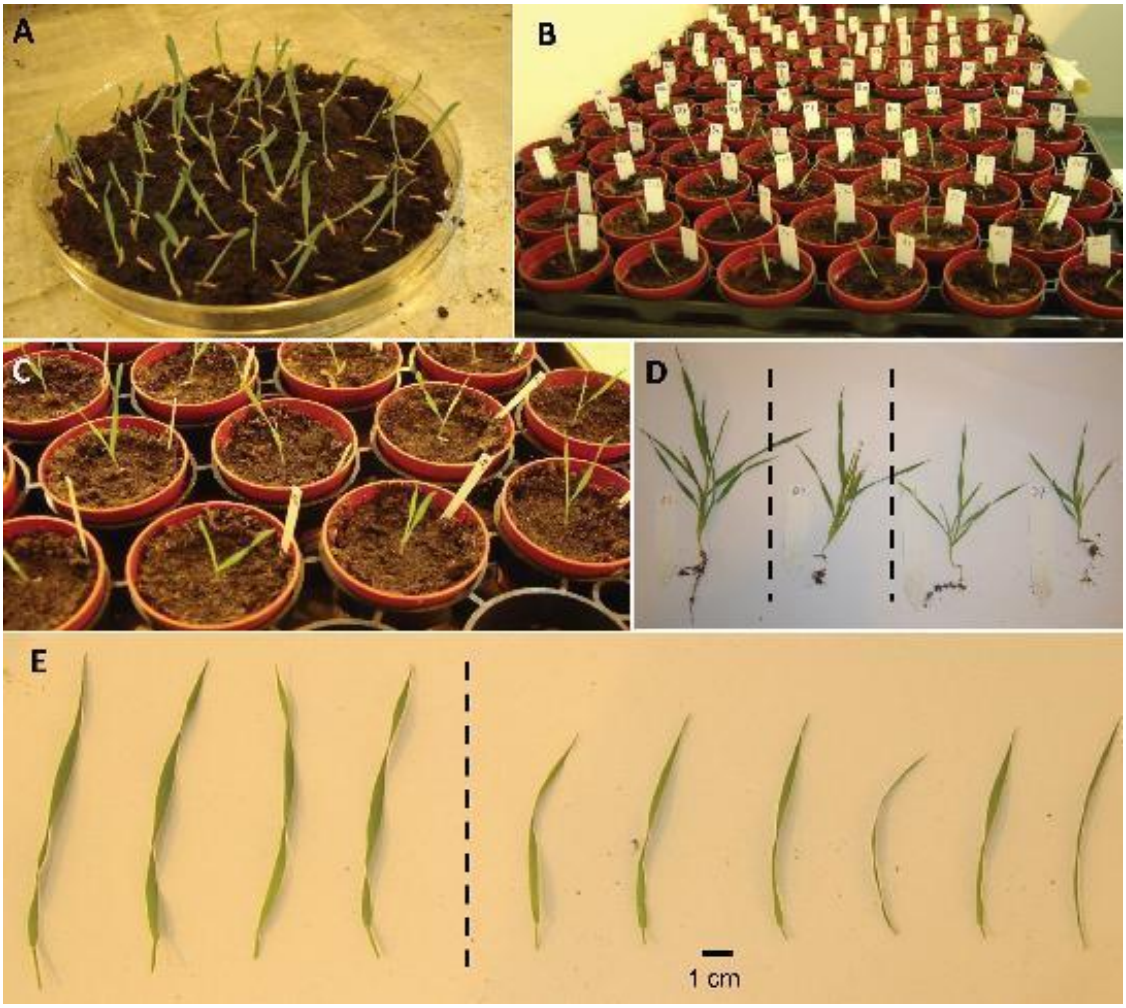

Figure 1.11 A Reproducible Drought Stress Protocol for *Brachypodium* in Soil. (A) shows Bd21 seedlings which have germinated synchronously on wet soil in a Petri dish. In (B), all seedlings have just been transferred to individual pots and, in (C), the second leaf has appeared in all plants. In (D), representative Bd21 plants are shown after 20 d of growth in the soil-based system; the plant on the left had been grown under control conditions, the second plant from the left had been grown under moderate drought stress, and the two plants on the right under severe drought stress. Plants from all conditions remained healthy and continued growing, although drought stress greatly slowed down vegetative growth and development. The effect of moderate drought stress on the length of the third leaf is presented in (E): four representative control leaves (left) are compared to six representative leaves from stressed plants (right), harvested 16 d after transfer of the seedlings to soil. Apart from being shorter, their width was clearly also reduced, resulting in a much smaller leaf surface overall (from Verelst et al., 2012).

2 Research objectives

Food production is limited mainly by biotic and abiotic stress and in particular by drought stress, the most common environmental factor affecting plant growth worldwide. Understanding the molecular mechanisms of plant response to stress is crucial for future agriculture which has to cope the growing demand for food and feed.

It was proposed that during drought stress response plants actively reduce their growth allowing to save and redistribute resources (Skirycz et al., 2010). To date underling mechanisms by which plants reprogram their growth are largely unknown. Therefore, it is important to dissect the molecular mechanisms that underlie drought tolerance in plants, in order to identify key regulators that are responsible for the drought-induced growth reduction.

The present project investigats the molecular mechanisms controlling leaf development, which has been shown to be extremely plastic and dependent on genetic predisposition, position, and environmental conditions by characterizing gene expression in leaf developmental zones of B. distachyon grown under severe drought stress. The project focuses specifically on the characterization of gene expression profiles of both coding and non-coding genes.

Deep sequencing of mRNAs, based on Illumina technologies, is applied to each developmental zone to obtain a complete picture of Bd transcriptome of young developing leaf subjected to drought stress. Cells in active proliferation, in expansion or that reached maturity are characterized both in stressed and controlled plants. The analysis of the whole transcriptome is expected to provide a comprehensive information on genome-wide transcription signals and genes differentially expressed during stress.

This project takes advantages of small RNA-Seq data, previously produced by the lab, that allows the analysis of the small RNAs population and describse their expression patterns in proliferation and expanding cells. Combining the next generation sequencing data (mRNASeq and small RNA-Seq) possible wish to investigate the link between microRNAs and their target genes.

3 Material and methods

3.1 Drought stress treatment

The drought stress experiment was conducted on January 2013 in Milano (Italy). *Brachypodium distachyon* inbred line 21 was grown under control and severe drought stress conditions, following the droughtstress protocol described by Verelst et al. (2013). Specifically, before starting the experiment Bd21 seeds were air dried and stored at room temperature for 2 weeks and then moved to 4°C for at least 2 weeks. Subsequently lemma and palea, were removed prior to sowing. Seeds were sown in Jiffy soil in a large petridish and incubated at 4 °C for 2 days in darkness. *Brachypodium* seeds were transferred into a growth chamber, with 16 hours of light, 24°C and 55% relative humidity. After 3 days, all seeds germinated synchronously, the petridish lid was removed to let plantlets accustom to the ambient atmosphere in the growth chamber. The next day, each plant with only the first leaf were transferred to small plastic pots (5.5 cm diameter, 5 cm high), containing an equal amount of soil. At the time of plantlet transfer, all pots contained 2.27 g water per g dry soil. After the transfer of the seedlings, water was withheld from all pots. Pots containing control plants were dried down until 1.82 g g^{-1}, while pots containing plants that would be subjected to drought stress were dried down to 0.45 g g^{-1} (severe drought stress). Pot weight was monitored every day, to compensate for evapotranspirative losses, adding water only to adjust the pot weight to the target level. Care was taken not to deposit the water in the direct vicinity of a plant, but rather on the outer edges of the pots, and watering always occurred at the same time during the afternoon, to not interfere with the time of most active plant growth (during the early morning hours).

Two to three days later the second leaf emerged in a highly reproductive manner, and another three days later the third leaf appeared. All plants grew synchronously, and the 3rd leaf (leaf3) of plants within the same experiment always appeared within a 24-h time window.

3.2 Plant material and leaf sampling for molecular analysis

All samples were collected from the third leaf Bd21 at fixed time point in the afternoon, about 24 h after the third leaf emergences. Hence, the growing third leaf , between 1.5 and 2 cm in size , was carefully collected from the leaf sheath of the older two leaves, without damaging the fragile meristem at its base. Samples were immediately stored in RNA-Later solution (Ambion, Austin, Texas). After an overnight incubation at 4°C, leaves were dissected into three distinct developmental zones (proliferating, expanding and mature). Based on microscopic observations, we defined the proliferation zone as the first 2 mm from the leaf base, the expansion zone as the next 4 mm, and the mature zone as the remaining distal part of the leaf. All the collected leaf zones were immediately frozen in liquid nitrogen and stored at –80°C until RNA extraction could be performed.

3.3 RNA extraction

Sample were grinded in liquid nitrogen using a mortar and pestle, total RNA was extracted from 100 mg of each tissue dissected from young leaf tissues using the Spectrum ^{TM} Plant Total RNA Kit (Sigma-Aldrich), following the manufactures's protocol .

RNA quality was evaluated by electrophoresis on 1% agarose gel. While RNA quantification was assesed using Nanodrop^{TM} 2000 UV spectrophotometer (Thermo Fisher Scientific Inc., MA) at 260 nm and 280 nm using 1 μl of RNA for each sample.

A total of 18 sample, were sent to IGA Technology Service (Udine) for RNA-Sequencing using the Illumina platform.

3.4 Illumina Library construction and Sequencing

RNA-Seq libraries were generated from each developmental zone for a total of 18 samples: three types of leaf cells (proliferation cells, expansion cells and mature cells) grown in control and drought condition, considering three biological replicates. RNA-

Seq libraries were constructed according to the Illumina protocol by IGA Technology Services (www.igatechnology.com). Brefly, mRNA is converted into first-strand cDNA using reverse transcriptase with either random hexamers and oligo (dT) as primers. The resulting first-strand cDNA is then converted into double-stranded cDNA, which is fragmented and ligated to Illumina adapters. The cDNA fragments are then amplified and sequenced using a sequencing by synthesis (SBS) approach.

Sequencing was performed at Applied Genomics Institute (IGA), Udine, Italy, using a 6-plex approach, producing 50 bp single end reads.

3.5 Bioinformatic analysis

mRNA reads were trimmed using ERNE-FILTER (v.1.3) and only for the library number 14 Cutadapt (v.1.2.1) was used to remove the presence of adapter contaminants. ERNE-FILTER was used to remove low quality bases from the ends of reads, setting a minimum Phred score of 33 and a minimum read length of 35 bp after trimming.

Filtered reads were then aligned to the reference genome version 2.0 of the 8x assembly of Bd21 and using the new annotation version 2.1, using the aligner TopHatversion 2.0.9 (Trapnell et al., 2010).

The following parameters were used for alignment:

- maximum number of mismatches = 0
- minimum intron length = 10
- maximum intron length = 500000
- library type = fr-firststrand

Secondly, Cufflinks algorithm (Trapnell et al., 2010, version 2.0.9) was used to reconstruct cell or stress specific transcripts not yet annotated in the annotation file .

Transcript quantification was achieved by counting the density of the reads that mapped to the exonic regions of a specific gene and reported as fragments per kilobase pair of exon model per million fragments mapped (FPKM).

Differential expression analysis was conducted testing two approaches: 1) Cuffdiff algorithm within the Cufflinks algorithm (Trapnell et al., 2010). Differential expression genes (DEGs) were determined considering a corrected p-value for multiple tests based on False Discovery Rate (FDR) adjustment < 5%.

2) DESeq2, available as an R/Bioconductor package at http://www.bioconductor.org (Bioconductor project version 2.4, Gentleman et al., 2004), a methods for differential analysis of count data (Love et al., 2014). This tool is based on the negative binomial distribution that makes possible the evaluation of the raw variance of data from experimental design with small numbers of biological replicates.

To identify differentially expressed loci between drought and control conditions in the same developing zone and during leaf development in the two growing condition , a series of pairwise comparisons were set up (Tab.3.1).

	Comparison
Leaf Development	Pc vs Ec
	Pc vs Mc
	Ec vs Mc
	Ps vs Es
	Ps vs Ms
	Es vs Ms
Drought Stress	Ps vs Pc
	Es vs Ec
	Ms vs Mc

Table 3.1 List of parwaise comparison performed during the analysis of differentially expressed loci. (P) proliferation, (E) expansion and (M) mature cells in (C) control and (S) drought stress conditions

To better proceed with DESeq2, an experimental design (Tab.3.2) and a count matrix of mapped reads were generated. Hence, differential expression analysis were performed, considering a p-value ≤ 0.05 and a FDR ≤ 0.1.

To better investigate differentially expressed genes highlighted in the pairwise comparisons, a Gene Ontology (GO) enrichment was applied using the bioconductor package GOSeq (Young et al., 2010) available on Biocondutor platform were subjected to.

Sample Name	File Name	Treatment	CellType
Pc_1	brachy_1_accepted_hits.bam	crtl	prolif
Pc_2	brachy_2_accepted_hits.bam	ctrl	prolif
Pc_3	brachy_3_accepted_hits.bam	ctrl	prolif
Ps_1	brachy_4_accepted_hits.bam	drought	prolif
Ps_2	brachy_5_accepted_hits.bam	drought	prolif
Ps_3	brachy_6_accepted_hits.bam	drought	prolif
Ec_1	brachy_7_accepted_hits.bam	ctrl	expans
Ec_2	brachy_8_accepted_hits.bam	ctrl	expans
Ec_3	brachy_9_accepted_hits.bam	ctrl	expans
Es_1	brachy_10_accepted_hits.bam	drought	expans
Es_2	brachy_11_accepted_hits.bam	drought	expans
Es_3	brachy_12_accepted_hits.bam	drought	expans
Mc_1	brachy_13_accepted_hits.bam	ctrl	mature
Mc_2	brachy_14_accepted_hits.bam	ctrl	mature
Mc_3	brachy_15_accepted_hits.bam	ctrl	mature
Ms_1	brachy_16_accepted_hits.bam	drought	mature
Ms_2	brachy_17_accepted_hits.bam	drought	mature
Ms_3	brachy_18_accepted_hits.bam	drought	mature

Table 3.2. Experimental design created for the differential expression analysis using DESeq2.
Ps: Proliferating cells under drought stress; Pc: proliferating cells under control conditions; Es: expanding cells under drought stress; Ec: expanding cells under control condition; Ms: maturation cells under drought stress conditions; Mc: maturation cells under control conditions. Biological replicates are indicated in the sample name column.

Moreover, to investigate the link between microRNAs and their putative target genes, mRNA-Seq data were interpolated with small RNA-Seq data, previously produced by the lab. These data analysis were conducted using R functions.

3.6 microRNA validation with 5'-RACE

To unambiguously diagnose endonucleolytic cleavage at the pairing sites between miRNA and presumptive targets, 5' RACE PCR, was performed.

Target genes were selected based on the target prediction analysis published by Bertolini et al. (2013), moreover the expression data of both small RNA-Seq and mRNA-Seq were used to get indication on the sampled to be tested with the 5' RACE PCR.Based on this observation, four target genes with opposite expression level to their miRNA and with important biological role in controlling cell proliferation were selected.

The first subset of genes subjected to target validation by 5'-RACE was :

- Bradi1g12650 Growth-Regulation Factor (GRF2) regulated by miR5049
- Bradi1g14820 Cyclin (CycA3) regulated by miR166g
- Bradi2g55320 Cell Division Cycle 6 (CDC6) regulated by R7754
- Bradi4g16450 No Apical Meristem (NAM) regulated by miR164a

Primers were designed with Primer3 version 4.0.0 (Tab.3.3). For each gene two gene specific primers were designed to amplify the predicted miRNA binding site region.

The total RNA was extracted from Brachypodium plants subjected to drought stress experiment in January 2013 at Milan (Italy). 5'-RACE was performed using the GeneRacer Kit (Invitrogen sing the GeneRacer® kit, catalog cumber: L1502-01) described by Kasschau et al. (2003). Two rounds of PCR were performed, first using the GeneRacer 5' Primer and Reverse outer gene specific primer followed by nested PCR employing GeneRacer 5' Nested Primer and gene-specific inner primer.

Amplified products were separated on 2% agarose gel electrophoresis and distinct bands with the appropriate size for miRNA-mediated cleavage were excised from the gel and purified through a DNA purification by centrifugation with Gel and PCR Clean-Up System kit (Promega). Purified products were subjected to PCR and electrophoresis agarose gel to verified the accuracy of the band height cut.

Primer	Sequence (5'-3')	Tm (°C)	Gene	Description
Fc+	GCTCATTATCAAGCCCTGTCTC	50		
Reverse out	CCTGAACCTTCTGGACATGAATA	60.32	**Bradi1g12650**	**Growth-Regulation Factor (GRF2)**
Reverse inn	TGTCCTTACTGCTCTGCTGGT	52.38		
Fc+	AGTATCCCAGCCTTTCTTTGG	59.60		
Reverse out	ATGCAGATACACCCTTGAActg	60.13	**Bradi1g14820**	**Cyclin (CYC)**
Reverse inn	TTTCCTCCTGAGCTGCAAGT	59.13		
Fc+	TTCCAAAGGATAGTGGTTTGTG	58.99		
Reverse out	TTTTTAATCAGCGAACAGTAAGGA	59.86	**Bradi2g55320**	**Cell Division Cycle 6 (CDC6)**
Reverse inn	CCTCAAGGAAAAAGAGGTCTGA	59.37		
Fc+	CAAGCCCTGATCTACAAGCAC	59.89		
Reverse out	TCAGCATACTAAGGACGGCATTT	60.30	**Bradi4g16450**	**No Apical Meristem (NAM)**
Reverse inn	CAACAGCAACCTGTCCCTAGA	61.23		
Fc+	CCTTTCATGTGACCATGTCTGT	59.89		
Reverse out	TGGAGAGAAATACTCCCTTCGTT	60.36	**Bradi4g30710**	**Tatraspanin (TETRA)**
Reverse inn	TCGTTTCATAATTCATTCTTGTCG	60.47		

Table 3.3. List of primers designed using Primer3. Fc+ = primer control positive; Reverse out = gene specific external primer; Reverse inn = gene specific inner primer

4 Results

4.1 Raw sequence results

mRNA-Seq libraries were generated from proliferating (P), expanding (E), and mature (M) leaf zones of Bd21 plants grown under drought stress (s) and control conditions (c). For each condition, three biological replicates were considered for a total of eighteen libraries (Ps1, Ps2, Ps3, Pc1, Pc2, Pc3, Es1, Es2, Es3, Ec1, Ec2, Ec3, Ms1, Ms2, Ms3, Mc1, Mc2, Mc3). Each library was subjected to deep sequencing using 6-plex approach on the Illumina HiSeq 2000, generating 436.6 million raw reads (Tab.4.1). The number of reads for each biological replicate vary from 15 to 30 million, guaranteeing the minimum number of raw read for approaching a transcriptomic analysis (Fig.4.1).

Libraries quality was assessed using FastQC tool and measured by different metrics, such as i) average PHRED error score, ii) quality per sequence length and iii) GC content biases (Fig.4.2). We observed that all library had 50 bp long reads with aPHRED score across all bases at each position greater than 30. Raw reads have almost 53% of GC content and few N's at 5' ends, between the 48-50 nucleotide. Lastly only in library Mc_2 was present an over representing sequences that was a True seq adapter, this adaptor was eliminated with CutAdapt tool.

Despite the high quality of raw libraries, a quality trimming step was performed to remove the few N's and the low quality nucleotide in the reads, with the aim to obtain a better alignment to the reference genome. ERNE-FILTER, an algorithm that operate trimming on both 5' and 3' ends of the read, was used (Tab.4.2). After trimming, we assessed libraries quality with FastQC. We observed that reads have a PHRED scores greater than 32 and a variable length from 35 bp to 50 bp. Moreover, Ns were eliminated at 5'ends (Fig.4.3).

Considering the good quality of reads, we expect a good alignment against Bd21 reference genome.

Library	Raw reds
Pc_1	31269797
Pc_2	23233575
Pc_3	21744665
Ps_1	26474091
Ps_2	29952467
Ps_3	26189736
Ec_1	38704916
Ec_2	20802248
Ec_3	18323053
Es_1	25483325
Es_2	21522887
Es_3	25596083
Mc_1	17146788
Mc_2	15333372
Mc_3	26109136
Ms_1	29017013
Ms_2	18658095
Ms_3	20996890
Total	436558137

Table 4.1. Total number of raw reads produced with independently sequencing of each library. Pc: Proliferating under drought stress; Pc: proliferating under control conditions; Es: expanding under drought stress; Ec: expanding under control condition; Ms: maturation under drought stress conditions; Mc: maturation under control conditions. Biological replicates are indicated with a number after the type of library.

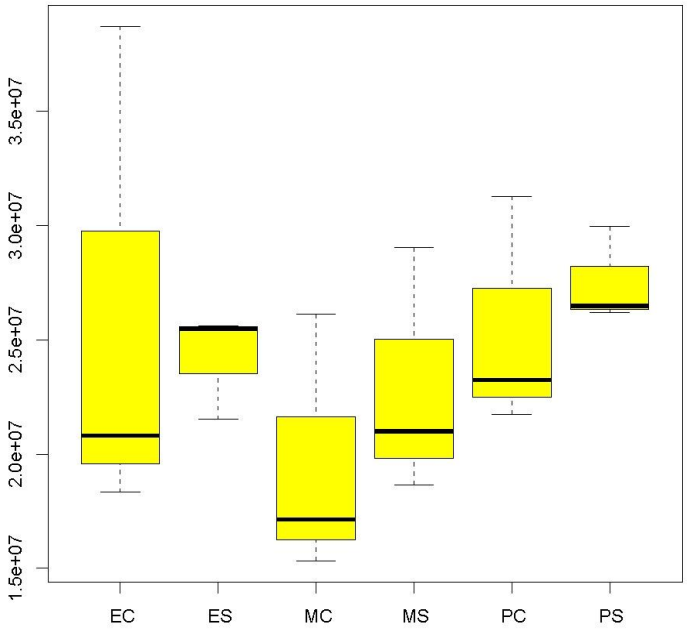

Figure 4.1. Boxplot of the number of raw reads produced by sequencing of each samples. Yellow bar represents the distribution on the three biological replicates in each samples.In Y-axis: number of million reads. X-axis: (P) proliferation, (E) expansion and (M) mature cells in (C) control and (S) drought stress conditions

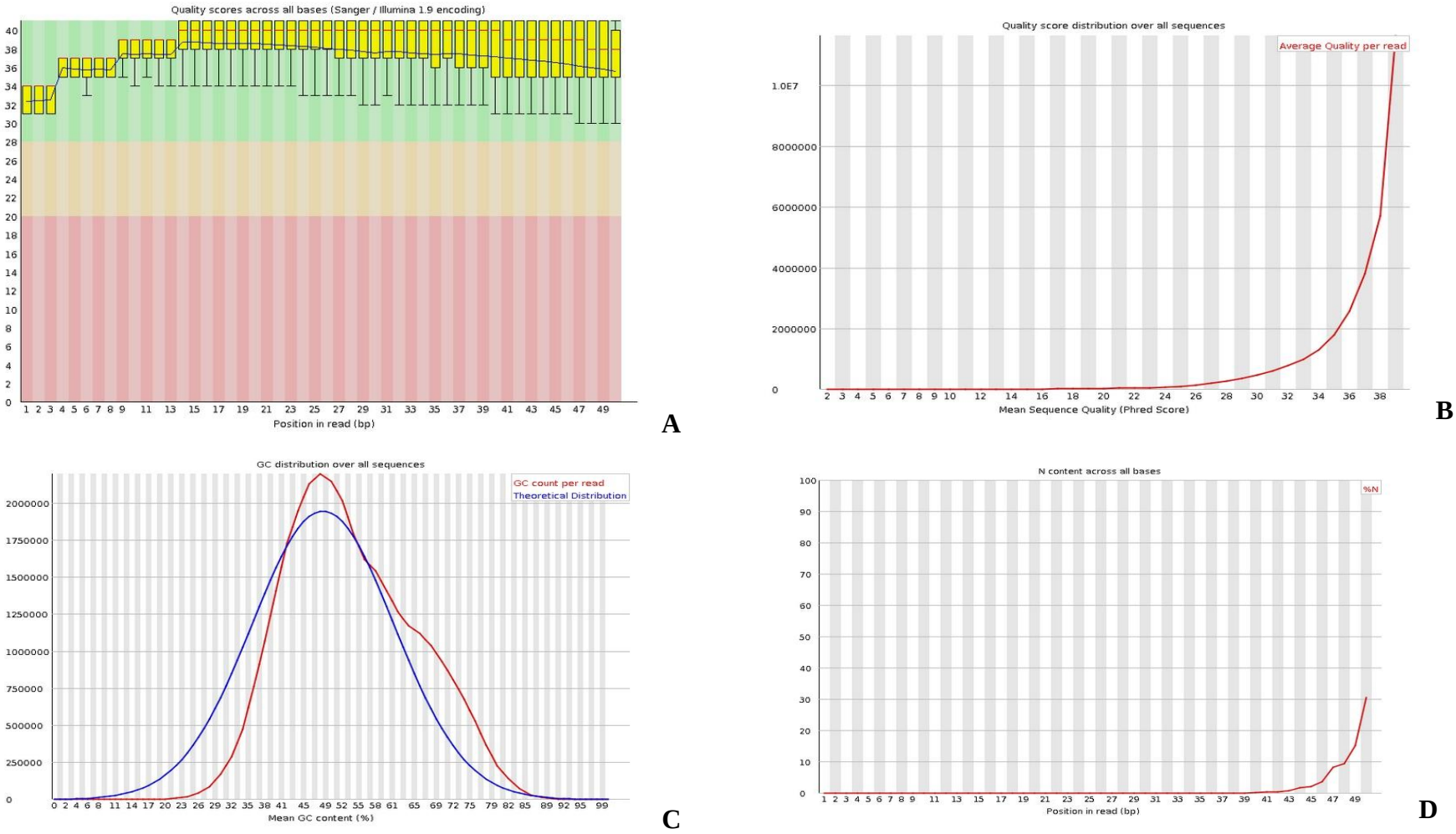

Figure 4.2. Visual output form FastQC of the raw library Pc_1. a. Per base sequence quality plot. Base positions in the reads are shown on x-axis and quality score (Q score) are shown on the Y-axis. b. Per sequences quality scores. Mean sequence quality are shown on x-axis. c. Per sequence GC content . It is shown GC distribution over all sequences. d. Per base N content. It is shown N content across all bases.

Library	Raw reads	Filtered reads	Percentage of filtered reads
Pc_1	31269797	28358946	90.69%
Pc_2	23233575	22080209	95.04%
Pc_3	21744665	20531207	94.42%
Ps_1	26474091	24222662	91.50%
Ps_2	29952467	28378904	94.75%
Ps_3	26189736	24632843	94.06%
Ec_1	38704916	35082051	90.64%
Ec_2	20802248	19721458	94.80%
Ec_3	18323053	17193323	93.83%
Es_1	25483325	23257421	91.27%
Es_2	21522887	20451327	95.02%
Es_3	25596083	24148377	94.34%
Mc_1	17146788	15682213	91.46%
Mc_2	15333372	14528288	94.75%
Mc_3	26109136	24602031	94.23%
Ms_1	29017013	26222948	90.37%
Ms_2	18658095	17710577	94.92%
Ms_3	20996890	19727074	93.95%
Total	436558137	406531859	93.12%

Table 4.2. Number of raw reads and trimmed reads of each library. (P) proliferation, (E) expansion and (M) mature cells in (C) control and (S) drought stress conditions.

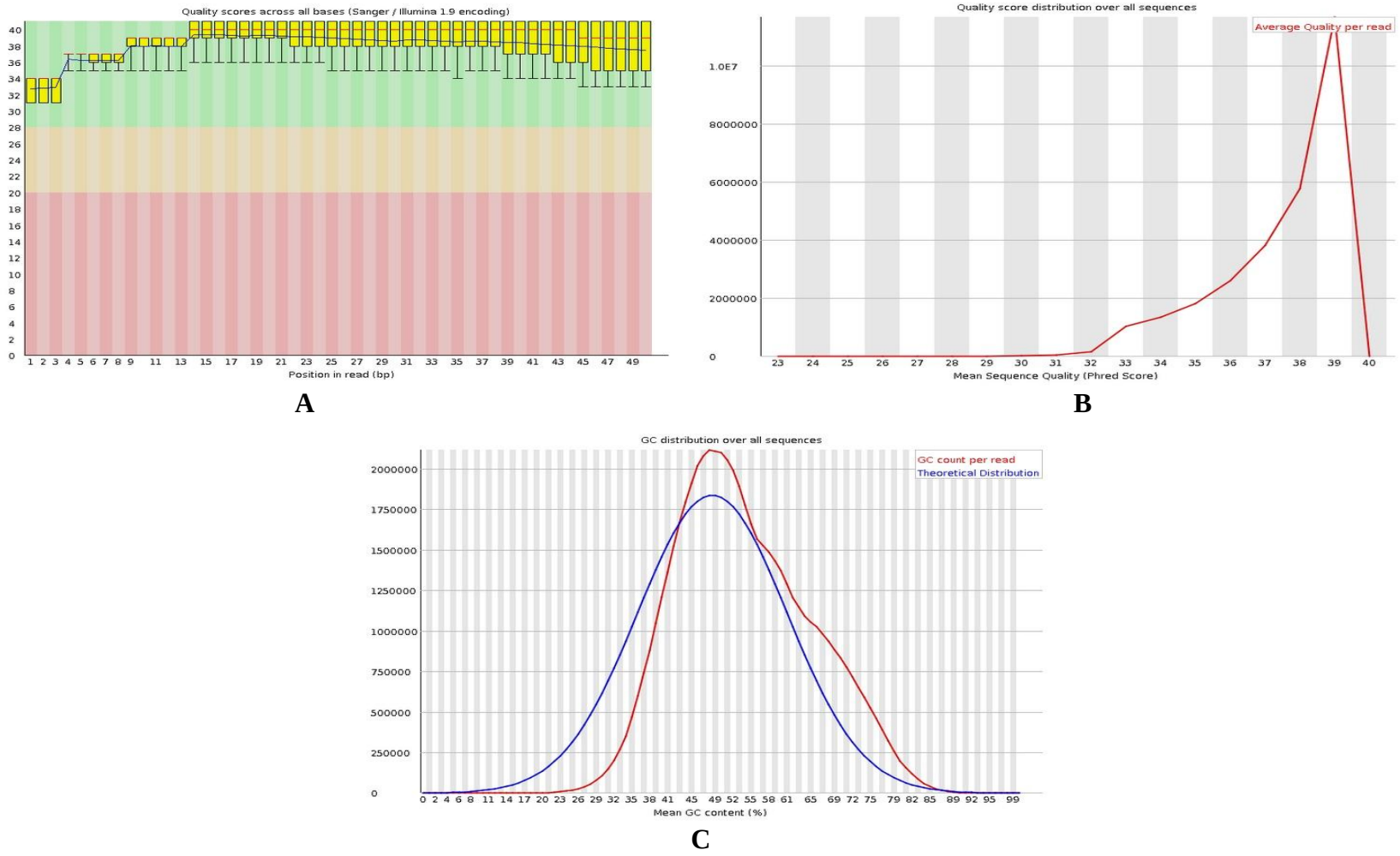

Figure 4.3. Visual output form FastQC of the trimmed library Pc_1 . a. Per base sequence quality plot. Base positions in the reads are shown on X-axis and quality score (Q score) are shown on the Y-axis. b. Per sequences quality scores. Mean sequence quality are shown on x-axis. c. Per sequence GC content . Mean GC content (%) are shown in X-axis. It is shown GC distribution over all sequences.

4.2 Reads alignments to reference genome

Reads were mapped against Bd21 genome reference version 2 (Vogel et al. 2010) using TopHat2 (Trapnell et al., 2012), retaining only sequences with a perfect match to the reference sequence .

TopHat2 is a fast splice junction read-mapping algorithm, designed to align reads from RNA-Seq experiment to a reference genome (Trapnell et al., 2009), allowing to discover new transcript splice sites. Indeed it is a spliced reads aligners with an exon-first approach. Brefely,TopHat first maps reads contained within exons (non-junction reads) to the whole genome, using Bowtie2, an unspliced short-read aligners program, and all reads that do not map to the genome are set aside as "initially unmapped reads" (IUM reads). Afterwards reads unmapped are aligned to each spliced junction with a seed-and-extend strategy (Trapnell et al., 2009). This approach allowed to reveal new alternative spliced transcripts and isoforms. To optimize the aligment procedure the Bd21 annotation file version 2.1, available on Phytozome 10 (http://www.phytozome.net/) was used. This new annotation file (GFF3) contained an improved annotation with a greater number of annotated genes compared to the previous version (33000 genes in contrast to 26000 genes of previous realise).

Statistic of the reads alignment to Bd21 genome is shown into Table 4.3. We observed that on average 97% of the reads were mapped to the references genome. This result confirmed reads high quality observed using FastQC.

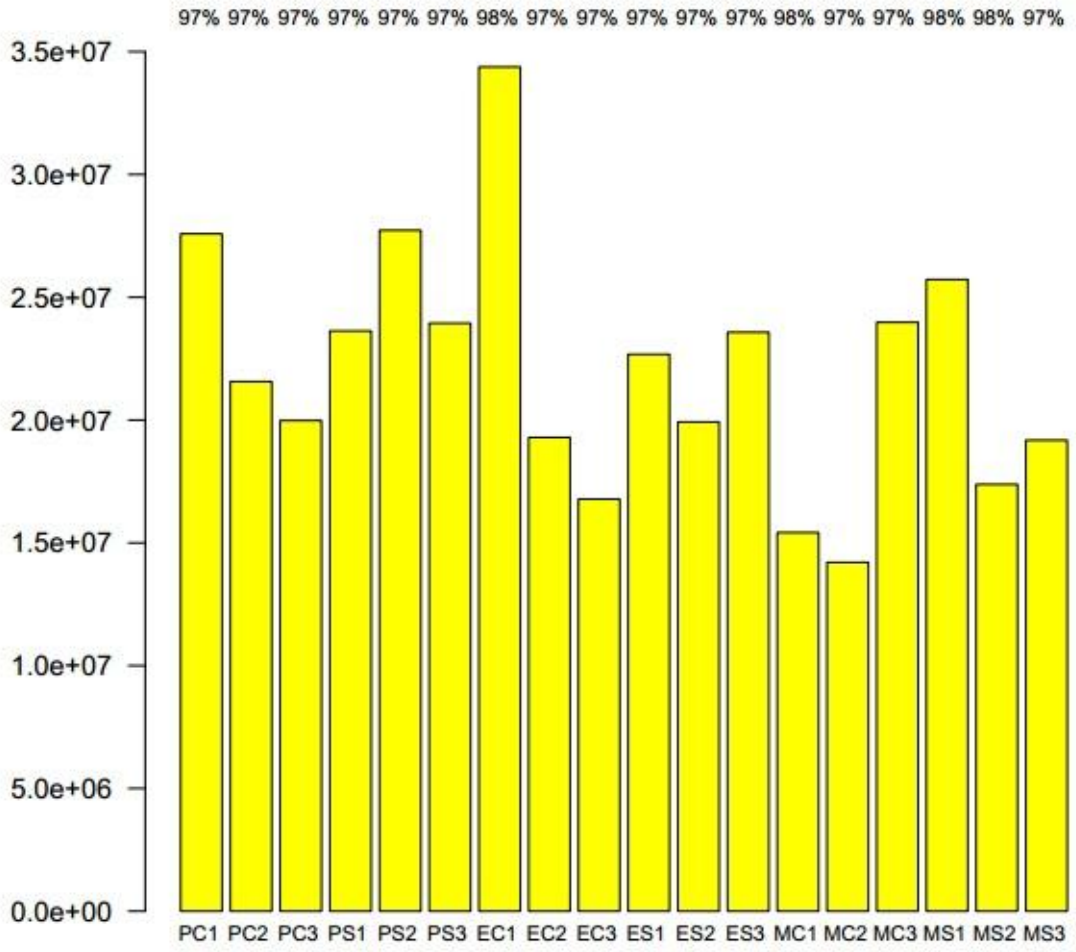

Figure 4.4. Barplot of mapped reads of each library to reference genome for each library the percentage of mapped reads is shown (P) proliferation, (E) expansion and (M) mature cells in (C) control and (S) drought stress conditions. Biological replicates are indicated with a number after the type of library.

Library	Raw reads	Filtered reads	Mapped reads	Percentage of mapped reads	Unmapped reads	Percentage of unmapped reads
Pc_1	31269797	28358946	27583072	97.30%	775874	2.70%
Pc_2	23233575	22080209	21567592	97.70%	512617	2.30%
Pc_3	21744665	20531207	19980766	97.30%	550441	2.70%
Ps_1	26474091	24222662	23628434	97.50%	594228	2.50%
Ps_2	29952467	28378904	27725572	97.70%	653332	2.30%
Ps_3	26189736	24632843	23943667	97.20%	689176	2.80%
Ec_1	38704916	35082051	34378437	98%	703614	2%
Ec_2	20802248	19721458	19293442	97.80%	428016	2.20%
Ec_3	18323053	17193323	16782020	97.60%	411303	2.40%
Es_1	25483325	23257421	22677330	97.50%	580091	2.50%
Es_2	21522887	20451327	19924089	97.45%	527238	2.60%
Es_3	25596083	24148377	23573192	97.60%	575185	2.40%
Mc_1	17146788	15682213	15417990	98.30%	264223	1.70%
Mc_2	15333372	14528288	14206606	97.80%	321682	2.20%
Mc_3	26109136	24602031	23980315	97.50%	621716	2.50%
Ms_1	29017013	26222948	25723044	98.10%	499904	1.90%
Ms_2	18658095	17710577	17379724	98.10%	330853	1.90%
Ms_3	20996890	19727074	19178321	97.20%	548753	2.80%
Total	436558137	406531859	396943613		9588246	

Table 4.3. List of statistic of libraries sequenced with Illumina HiSeq 2000. (P) proliferation, (E) expansion and (M) mature cells in (C) control and (S) drought stress conditions. Biological replicates are indicated with a number after the type of library.

4.3 Approaches of transcriptome analysis

After the alignment a transcriptome reconstruction was performed to identify expressed transcripts and isoforms in specific cell type and condition, followed by expression quantification for differential expression analysis across samples.

With this aim, we used two methods: i) GFF3 based approach based on DESeq2 and ii) the Tuxedo pipeline.

The first approach considers the GFF3 as a map of all coding genes to reconstruct the transcripts and counts the expression of each gene annotated. This method allows only to evaluate the expression of annotated genes..

The second approach called Tuxedo pipeline was proposed by Trapnell et al. (2012), includes a complete set of softwares such as Botwie, TopHat, Cufflinks and CummeRbund, able to conduct a transcriptomic analysis: from mapping to differentially expression analysis (Fig.4.5).

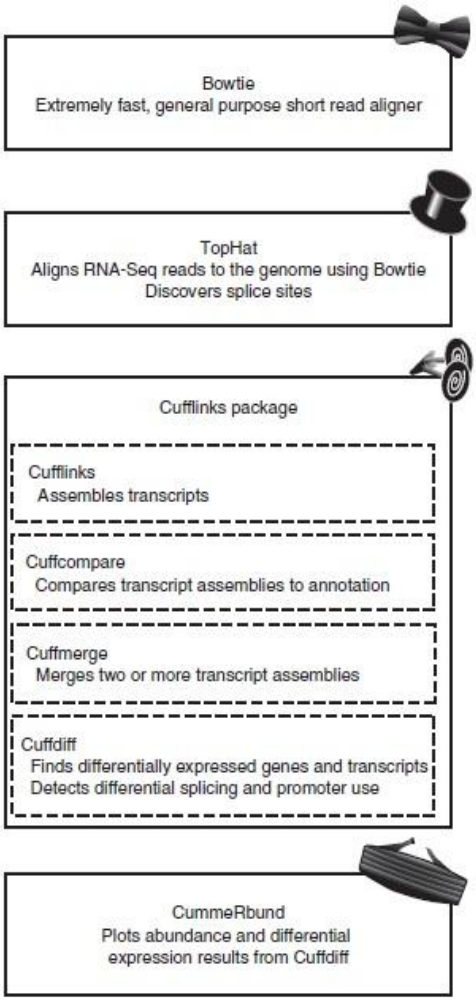

Figure 4.5. Softwares in the Tuxedo pipeline. Bowtie forms the algorithmic core of TopHat, which aligns millions of RNA-seq reads to the genome per CPU hour. TopHat's read alignments are assembled by Cufflinks and its associated utility program to produce a transcriptome annotation of the genome. Cuffdiff quantifies this transcriptome across multiple conditions using the TopHat read alignments. CummeRbund helps users rapidly explore and visualize the gene expression data produced by Cuffdiff, including differentially expressed genes and transcripts (Trapnell et al., 2012).

Advantage of using this method is to use Cufflinks allows to assembly individual transcripts from RNA-seq reads that have been aligned to the genome. Then, the assembly of each sample will be merged together using Cuffmerge to have produce the final assembly. Then, the final assembly is screened for transcripts that are differentially expressed using Cuffdiff.

This pipeline allows to identify new coding or non-coding transcripts tissues-specific and condition specific therefore it could integrate the genome annotation. However, novel genes must be validated.

In this project, the entire dataset was analysed using these two approaches; here I present data coming only from the first approach based on the annotation file.

4.4 Differential expression analysis

To investigate the molecular changes underlying leaf growth reduction during drought stress, we surveyed a gene expression analysis in responses to drought stress, using mRNA-Seq approach.

First we assessed overall similarity between 18 samples, calculating Pearson correlation, mRNA-Seq libraries showed high correlation (r=0.9) (Fig.4.6) between replicates. Moreover, libraries from the same cell type tend to cluster together indicating that the three type of cells were profiled correctly within the young leaf.

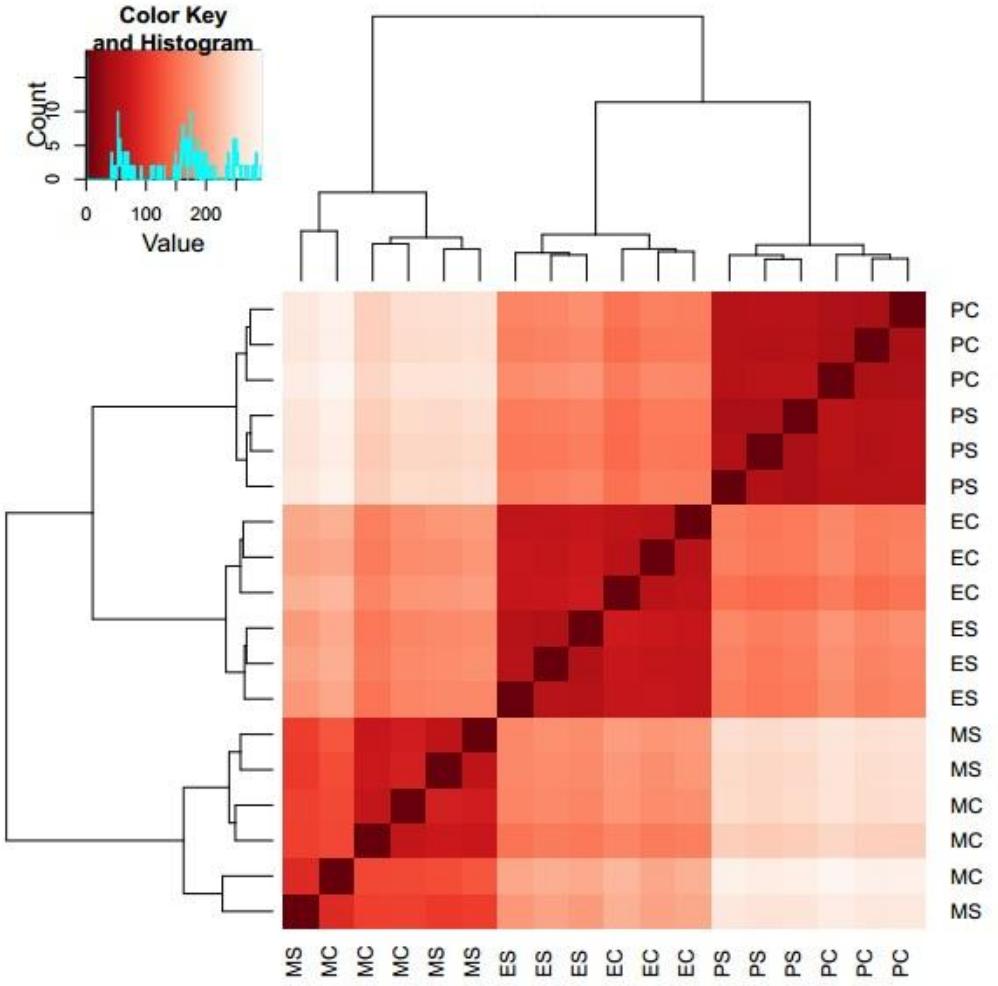

Figure 4.6. Sample to sample distance. Heatmap shows the distance between the 18 mRNA-Seqlibraries . (P) proliferation, (E) expansion and (M) mature cells in (C) control and (S) drought stress conditions.

We evaluated the expression level of 33000 genes included in the annotation v2.1. differentially expression analysis was performed using DESeq2 R/Bioconductor package (Anders et al., 2010), a method for differential analysis of count data by use of

negative binomial distribution (Love et al., 2014). This method allows us to gain statistical evidence for differential expression of genes.

Two classes of comparisons were performed:

1) during leaf developmental, evaluating expression profile between different cell type in the same growing condition
2) during drought stress, comparing the same developmental zone in different grown conditions: PS against PS, ES against EC, MS against MC

The first comparison addressed differentially expressed genes (DEGs) during leaf development in the same growing condition: stress and control (Pc vs Ec, Pc vs Mc, Ec vs Mc, Ps vs Es, Ps vs Ms, Es vs Ms). Based on FDR ≤ 0.1 and p-value ≤ 0.05 , shown in the volcano plot (Fig.4.7), we observed a high number of differentially expressed genes with high fold change. Whereas in second comparison (same developmental zone, different growth conditions) the number of gene differential expressed retrieved was drastically lower and with minor changes in the fold change (Fig.4.8).

Thus, it seems clear that development induces a drastic change in the expression profile between cells type in different leaf areas, both in control and stress conditions. Viceversa, drought treatment seems to have a minor influence in the expression profile.

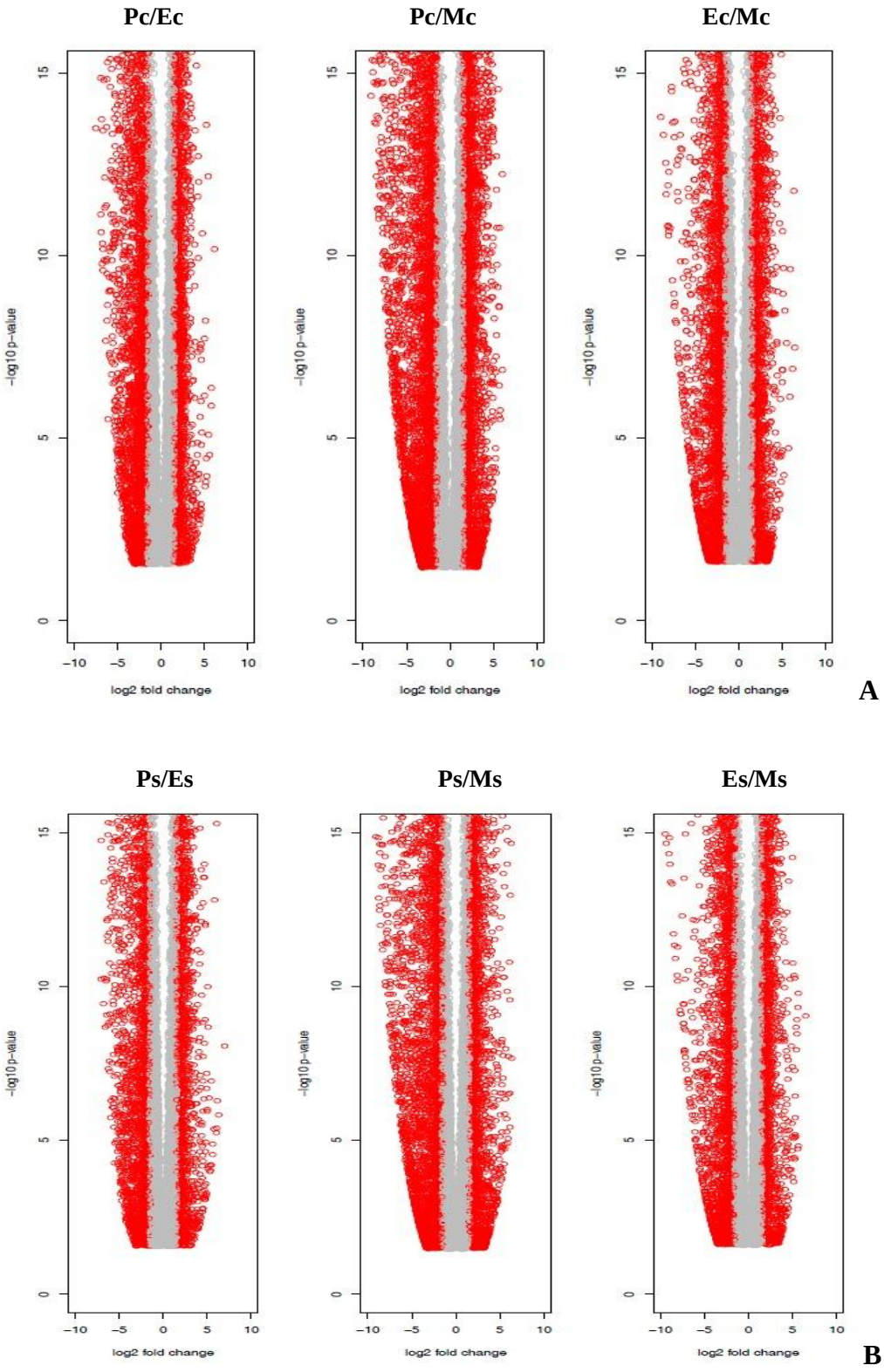

Figure 4.7. Differential expression of *B. distachyon* genes in response to development. Volcano plots of expression level between different leaf developmental zones in the same growth condition, control (a) and stress (b). Red dots indicate genes statistically significant with a fold change >2 or < -2. The Y-axes
display the negative log (base 10) of pValue, while the X-axes show the log (base 2) of the fold change.

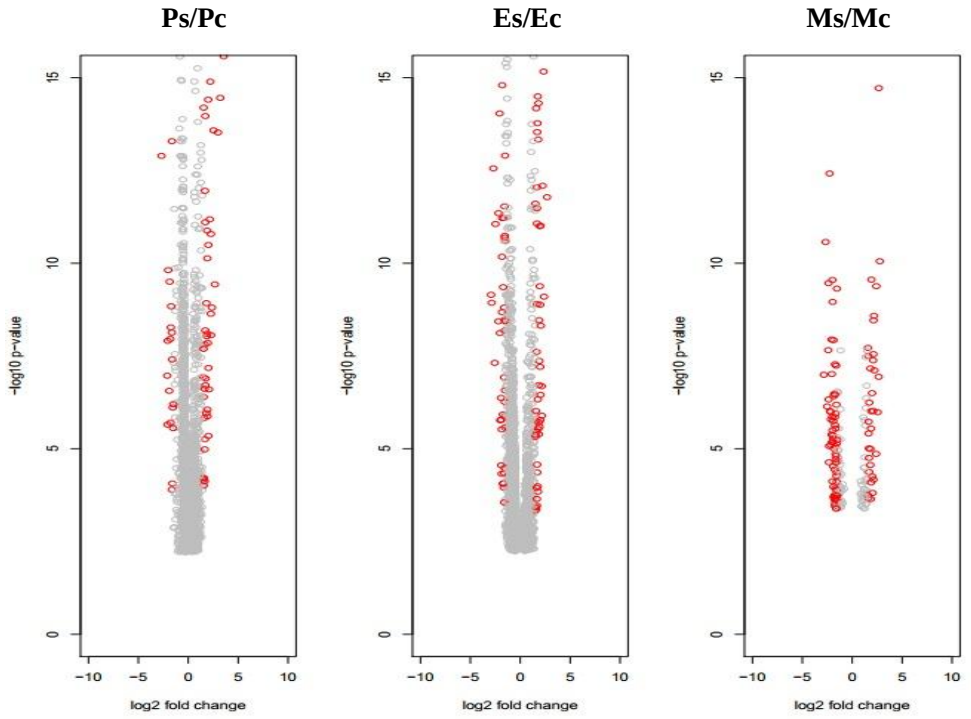

Figure 4.8. Differential expression of *B. distachyon* genes in response to drought stress. Volcano plots of expression differences between same developmental zone growing in different conditions same growth condition, drought and control. Red dots indicate genes statistically significant with a fold change >2 or <-2. The Y-axes display the negative log (base 10) of pValue, while the X-axes show the log (base 2) of the fold change.

In thesis we focus on the effect of drought stress in each single cell type in *Brachypodium* leaves, therefore it was considered the comparison between stress and control in three different developmental areas, such as proliferation, expansion and mature.

We identified genes differentially expressed using a FDR ≤ 0.1 and p-value ≤ 0.05 genes: 1090 up-regulated and 1890 down-regulated genes were found in proliferating cells (Ps vs Pc), 1134 genes up-regulated and 2080 down-regulated were found in expansion cells (Es vs Ec) and 90 up-regulated and 141 down-regulated genes were found in mature cells (Ms vs Mc).

To investigate shared expression profile between different developmental leaf zones when comparing severe drought stress against control condition, Venn diagrams were drawn using DEGs with FDR- ≤ 0.05 and p-value ≤ 0.05 genes (Fig.4.9). We detected 893 up and 567 down regulated genes exclusivelyin the proliferation zone, 971 up and 506 down regulated genes exclusively in the expansion zone and 75 and 32, respectively down and up regulated in the mature zone.

These expression data show that the molecular response to drought stress is highly dependent on the developmental stage, therefore response to drought stress is cell specific.

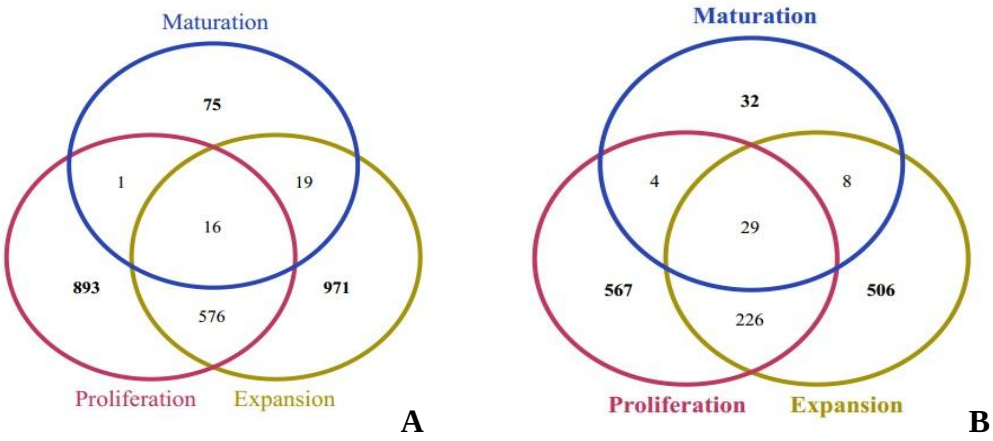

Figure 4.9. Response to drought stress in developmental zones of *Brachypodium* leaves. Venn diagrams show the number of down- (a) and up-regulated (b) genes with a pvalue ≤0.05 and a FDR ≤0.05 in the proliferation, expansion and mature zones of the third leaf of Bd21, when comparing control and severe drought stress conditions.

In order to investigate the expression profile of pivotal genes during leaf development. A set of genes involved in cell development have been selected belonging to: AUXIN RESPONSE FACTORS (ARF), CELL DIVISION CICLE (CDC6), GRF-interactive factors (GIF), ETHYLEN RESPONSIVE FACTOR (ERF), CYCLIN (CYC), EXPANSIN (EXP), GIBBERELLIN ACID (GA), GROWTH-REGULATING FACTOR (GRF), NAC domain protein (NAC), TEOSINTE BRANCHED1/CYCLOIDEA/PCF (TCP). Annotated genes belonging to these classes were retrieved and monitored the expression profile across cell type: in proliferating, expansing and mature.

In Brachypodium there are 22 genes annotated as ARF (Tab.4.4), 18 genes ERF (Tab.4.5), 34 genes CYC (Tab.4.6), 48 genes EXP (Tab.4.7), 34 genes GA (Tab 4.8), 14 genes GRF (Tab.4.9), 42 genes NAC (Tab.4.10) and 8 genes TCP (Tab.4.11).

ARF (Fig.4.8a), CYCLYN (Fig.4.8b) and GRF (Fig.4.8c) genes show a similar expression trend, showing a highly expression in proliferating cells and compared to expanding and maturate cells. ERF (Fig.4.8d), GA (Fig.4.8e), TCP (Fig.4.8f) and NAC (Fig.4.8g) genes are expressed mainly in proliferating and expanding cells . While the

majority of EXP (Fig.4.8h) genes are over expressed in expanding cells. Within profiles expression of NAC, TCP and GA genes, some genes have a different trend than the majority. These outliers genes will be subjected to further analysis in order to investigate their behaviour.

Bd ID	Ps_1	Ps_2	Ps_3	Es_1	Es_2	Es_3	Ms_1	Ms_2	Ms_3	Description
Bradi1g33160	25.06089949	24.42657896	25.37692479	79.83271731	73.6619593	48.26005098	53.26148775	28.54456218	41.99071958	ARF
Bradi1g34340	81.46292109	73.21205184	109.766066	114.4296537	111.5969116	144.7322155	173.8739736	71.8722244	299.9586296	ARF
Bradi2g08120	26.52934692	21.10327861	27.7199524	10.49223607	10.18053557	8.260986626	9.66993969	6.08149591	13.66944338	ARF
Bradi2g16610	656.8514701	746.539248	768.2314148	605.7580079	730.2191129	615.1545726	818.9057498	897.3247216	869.5489027	ARF
Bradi2g30567	66.53004942	64.67699177	76.23134766	84.90247277	104.4754444	108.3832171	253.9175274	192.5924897	242.6700192	ARF
Bradi2g36950	205.0718517	211.2646903	225.0656686	227.8782522	275.628574	273.1822819	327.2182818	682.1411246	363.8484193	ARF
Bradi2g46190	85.61683485	102.6523767	125.7125273	140.0221692	180.5065514	121.6501496	163.9288728	160.5895014	153.6606252	ARF
Bradi2g50120	237.0814037	250.9136759	310.2963479	128.9701911	133.6074096	134.2674841	133.1243218	63.24755747	240.1227263	ARF
Bradi2g59480	1037.965611	1115.012382	1339.317333	269.9564906	309.7173083	308.3257639	684.2666523	318.6778937	829.6667168	ARF
Bradi3g04920	649.6498643	632.2306432	752.4617162	500.9268389	475.7762058	515.879116	378.5192629	190.7929086	483.6971259	ARF
Bradi3g10777	7.211158845	3.562891195	5.109349025	3.874973549	5.347352014	3.029891647	1.474594909	2.994676017	0.47514108	ARF
Bradi3g28950	24.41730183	21.34418876	22.04362119	25.28832626	27.93881605	23.69606073	16.28111362	32.59209459	20.70323463	ARF
Bradi3g45880	1411.255139	1357.543766	1274.151427	2038.313586	1792.566079	1637.925759	568.5300671	281.319865	557.1504303	ARF
Bradi3g49320	28.67884625	30.58464808	33.20147661	17.55883537	17.11950757	17.48163496	27.70289071	29.92121922	17.98647065	ARF
Bradi4g01730	1180.162277	1306.523105	1476.275465	509.6631877	489.9631071	500.4497734	327.5503401	277.6998491	343.4912375	ARF
Bradi4g07470	853.2995614	838.4305187	939.8797806	474.9167582	449.5340593	475.8949813	452.995556	368.9440852	515.4330435	ARF
Bradi4g16547	249.1952357	217.0622943	227.906382	190.9949728	208.3760684	179.6446395	290.9344381	348.1979893	391.6577812	ARF
Bradi4g17410	1731.681414	1847.441305	2176.222025	600.775899	625.9966758	617.2899248	1135.143161	638.2253526	1114.87103	ARF
Bradi4g22180	211.4030445	185.7740357	197.558788	418.528562	457.0540742	498.430824	1156.700144	1276.169044	1370.910432	ARF
Bradi5g10950	365.4211199	384.8166107	498.9930514	296.2890886	355.9752041	333.1234944	565.9167572	477.8704342	666.6757286	ARF
Bradi5g23450	88.22902805	77.52224797	80.65307252	152.8868685	153.8392041	179.2186458	382.3413942	278.8800268	356.324482	ARF

Bd ID	Ps_1	Ps_2	Ps_3	Es_1	Es_2	Es_3	Ms_1	Ms_2	Ms_3	Description
Bradi5g27400	0.880548536	0.888143594	1.168750677	2.344010186	0.962698399	0.654575609	3.026419011	3.49362531	1.745035325	ARF

Table 4.4. List of Brachypodium genes annotated as AUXIN RESPONSE FACTORS (ARF2) with their expression in each developmental zone in drought stress conditions. The gene expression is expressed in FPKM. (P) proliferation, (E) expansion and (M) mature cells in (S) stress conditions.

Bd ID	Ps_1	Ps_2	Ps_3	Es_1	Es_2	Es_3	Ms_1	Ms_2	Ms_3	Description
Bradi1g48320	2.627127083	2.892970947	3.172499147	2.572241304	2.812539641	3.040715662	13.8402828	4.823082495	12.82293355	ERF
Bradi1g52000	0	0	0	0	0	0	0	0	0	Putative AP2/ERF
Bradi1g75040	0	0	0	0	0	0	0	0	0	ERF
Bradi1g76860	988.6389406	875.3163218	1018.201698	306.8979051	343.0761567	378.6565982	319.1297726	411.1091235	409.567191	PIN2/TERF1-interacting telomerase inhibitor 1
Bradi1g77150	0.619018095	0.618411095	0.635778725	1.420823635	1.382541867	1.424308039	5.354859076	3.547539281	3.283346693	Putative AP2/ERF and B3 domain
Bradi2g02710	1.919509177	2.542308437	2.063086324	0.862678581	0.413358202	0.249829435	0.27357207	0.11111658	0.088149856	Putative AP2/ERF and B3 domain
Bradi2g02720	0.987615233	1.109977641	0.901649828	1.104367461	1.136312303	1.035212979	2.156595054	2.425687573	1.995592536	Putative AP2/ERF and B3 domain
Bradi2g06180	0	0	0	0.162251073	0.093292422	0.105721834	0.077179432	0.062695834	0	ERF
Bradi2g17610	0	0	0	0	0	0	0	0	0.072928631	Putative AP2/ERF
Bradi2g47220	2.735412711	2.988923881	2.91353188	4.507680368	3.815797092	4.759315724	4.46710208	1.886975781	4.222183893	Putative AP2/ERF and B3 domain
Bradi2g52380	0.581409442	0.508234406	0.760011349	0	0.150244884	0.113508074	1.864430344	1.51454879	2.643313594	ERF
Bradi3g08790	0.220724166	0.289416392	0.26448395	3.478176258	2.666546204	3.199565579	4.411987967	2.951552682	2.843244222	ERF
Bradi3g16500	0	0.111143008	0	0.078570892	0.271063927	0	0	0	0.09634197	Putative AP2/ERF
Bradi3g32140	0	0.089992659	0.246720102	0	0	0.11054331	0.968390686	1.081659098	0.234024711	Putative AP2/ERF and B3 domain
Bradi3g51610	0.121306638	0.159058838	0.310093541	0.549727562	0.948260274	1.128870231	4.56425664	3.900832501	9.804572162	ERF
Bradi4g25170	18.18567445	21.27374129	21.34244472	31.81359544	23.66138476	28.78804966	1.729492575	0.766327433	1.01322492	Putative AP2/ERF and B3 domain
Bradi4g42167	20.72151147	27.47053932	25.35095118	32.89707835	32.54266786	29.9943907	2.22107034	2.296332481	1.648207232	Putative AP2/ERF and B3 domain
Bradi5g08380	0.223706925	0.065183872	0.214446446	0.460807665	0.423934214	0.320276835	7.277325144	1.709393445	4.068234976	ERF

Table 4.5. List of Brachypodium genes annotated as ETHYLEN RESPONSIVE FACTOR (ERF) with their expression in each developmental zone in drought stress conditions. The gene expression is expressed in FPKM. (P) proliferation, (E) expansion and (M) mature cells in (S) stress conditions.

Bd ID	Ps_1	Ps_2	Ps_3	Es_1	Es_2	Es_3	Ms_1	Ms_2	Ms_3	Description
Bradi1g09370	201.3362329	201.418165	195.6823816	97.46082121	98.5647047	94.88201229	79.5683442	172.0077154	72.88920999	Cyclin-H1-1
Bradi1g21230	17.46555904	15.48864486	16.98520777	1.564209506	1.079282058	2.446151054	2.380997284	2.901264104	2.301600828	Cyclin-D2-2
Bradi1g21237	168.0743652	165.7284999	173.4917651	26.9044035	26.98205145	35.60508757	22.32184954	31.91390514	17.64560634	Putative
Bradi1g22590	171.0350768	169.0548359	187.4576998	148.6006444	169.7720907	158.3776537	119.2325296	115.404311	128.112447	phase
Bradi1g24990	188.2932033	208.1767033	177.4826503	96.31688639	76.707921	80.56086172	15.6514021	11.55839866	9.902940403	Cyclin-D6-1
Bradi1g27370	7.563722182	7.824405661	7.218955366	8.735854175	9.905190762	7.412312738	31.57374845	32.11592852	31.08401006	Cyclin-U4
Bradi1g29537	192.059763	162.4717772	161.3035345	166.6192219	160.6126809	142.6286718	94.4093938	81.899906	116.0482297	Cyclin-L1-1
Bradi1g29830	675.9677596	698.1121857	769.3033141	127.5034775	90.36249926	170.9912764	23.97819547	12.03078539	14.99793148	Cyclin-B2-2
Bradi1g47510	817.3691786	687.363932	799.5379849	517.5995918	472.2380248	471.400642	517.8592995	229.9911181	574.0892098	Cyclin-T1-4
Bradi1g55310	207.9900799	206.7741825	198.0855314	180.0372326	177.6966208	168.6380718	122.0510863	193.1335671	123.9752725	Cyclin-L1-1
Bradi1g69380	50.09857724	55.0060395	73.77710171	9.272743721	10.66343296	16.89179359	14.22854737	16.18175812	19.43910524	Cyclin-SDS-like
Bradi1g70627	57.1928504	59.29016373	68.87602852	5.683294539	4.901739346	10.18380248	5.744775999	5.490239364	6.097643859	g2/mitotic-specific
Bradi1g70907	9.399482509	13.61238117	7.531068393	11.79042799	7.975711479	10.99662369	14.84592162	7.771945621	14.88238501	Cyclin-D5-3
Bradi2g10890	30.0567126	29.3054308	25.48797838	5.429292548	3.286082243	6.454741236	1.902968849	1.325018662	2.452683563	Cyclin-B1-3
Bradi2g13487	110.8181249	88.49922744	110.8209607	116.6719309	120.5584818	125.3579413	296.5276307	264.4026679	341.4104633	Cyclin-T1
Bradi2g17220	63.51513887	63.25893005	51.060785	12.28359345	14.5672704	15.00734324	12.5990717	26.99590868	10.59038655	Cyclin-D1-binding
Bradi2g21330	797.8901168	812.4678056	927.9840475	125.4452331	68.02190244	126.3639727	32.35047043	13.25018662	9.810734254	Cyclin-B1
Bradi2g22097	202.4611228	205.1403123	199.264612	117.9929446	136.6916859	135.5876512	97.87623707	176.9853526	128.2880916	Cyclin-T1-4
Bradi2g26090	96.8475403	99.06622154	92.72315207	101.7045383	99.0037354	115.1006513	73.13390622	199.9468568	83.8679255	Cyclin-P3-1
Bradi2g52760	1010.136749	953.1338734	1102.410473	188.3107257	100.8827249	199.848719	37.78752428	23.85033592	16.11763485	Cyclin-B1-1
Bradi3g02530	2.561705851	2.040246233	1.909959746	47.13929308	48.2217879	41.62662691	53.01239689	77.210739	44.25674466	Cyclin-U2-1
Bradi3g38417	329.5096484	338.57124	340.8064607	138.9971464	134.4477078	139.6635769	20.39154102	10.03929484	15.13211211	Cyclin-D4-2
Bradi3g50350	1.745900645	2.323933161	1.93988707	8.14078815	9.869273852	6.561376094	4.012368505	5.912403503	3.006645376	Cyclin-P4-1

Bd ID	Ps_1	Ps_2	Ps_3	Es_1	Es_2	Es_3	Ms_1	Ms_2	Ms_3	Description
Bradi3g53770	208.1512708	201.1871336	210.2480004	157.1179148	150.4027364	164.6283743	85.82515684	113.4186157	104.266402	Cyclin-C1-1
Bradi3g54360	813.2092677	827.2236578	761.5501763	512.5511405	455.6090922	511.576207	409.3597083	927.5221701	401.3129732	Cyclin-B1-2
Bradi3g58300	362.5087872	311.5245891	304.4014345	184.3913339	173.1947902	192.5664469	104.5323946	138.1100213	111.1126214	Cyclin-D3-1
Bradi4g03121	225.4435976	238.363912	220.9397993	49.8036074	44.88961296	46.77727454	23.37038905	26.52652493	15.47334438	Cyclin-D5-2
Bradi4g03470	134.9771557	149.2007709	127.5746109	36.77425878	35.36941332	32.53007851	27.35228988	58.39031041	29.10472027	cyclin-A3-1
Bradi4g06827	572.3238143	563.7702217	637.4161505	91.27075244	51.60492873	115.9693844	20.98419818	11.168249	8.393570304	Cyclin-A2-1
Bradi4g08357	29.34979195	35.95199743	39.85769006	0.715936015	1.189224476	0.898443765	1.664939197	0.86067827	0.195081252	Cyclin-D3-2
Bradi4g29467	274.8015872	291.4836524	304.9122104	157.5409246	128.3975609	171.6592326	38.92930559	23.04018165	27.59619392	Cyclin-D2-1
Bradi4g32556	248.3146872	242.5327401	246.6868987	61.8257462	54.23980735	49.00684557	14.85619917	4.43324001	4.689242808	Cyclin-D4-1
Bradi4g34440	149.3566859	140.5277372	155.1639171	192.7773508	211.7551398	204.2191857	320.9504972	561.4977602	357.3567738	Cyclin-C1-1
Bradi5g18397	520.2783922	416.8974224	550.0636426	63.32813914	44.8159026	70.53716003	20.85498514	18.82367782	7.466502685	Cyclin-B2-1

Table 4.6. List of Brachypodium genes annotated as CYCLIN (CYC) with their expression in each developmental zone in drought stress conditions. The gene expression is expressed in FPKM. (P) proliferation, (E) expansion and (M) mature cells in (S) stress conditions.

Bd ID	Ps_1	Ps_2	Ps_3	Es_1	Es_2	Es_3	Ms_1	Ms_2	Ms_3	Description
Bradi1g03640	126.57682	145.2647662	166.2586797	159.4295271	143.8849027	155.7395382	13.32580076	5.594976238	10.99988149	Expansin-A4
Bradi1g26990	3.183521631	2.186524943	1.307887662	13.20897577	12.60447261	20.99836995	1.87160123	3.47514052	1.378431265	Expansin-like B1
Bradi1g28130	87.16446654	105.9037637	115.0283546	114.3008957	125.8569499	163.8511237	51.38015892	57.41747536	41.34523721	Expansin-like A3
Bradi1g30050	1.803302013	1.733976207	1.498166163	0.594331455	0.598033559	0.322719033	0.070677752	0.114828536	0.091094586	Expansin-like A4
Bradi1g35830	16.32838514	17.50502374	14.66803045	27.28827527	19.85021988	25.14133416	6.399668723	6.277673198	5.758285445	Expansin-A16
Bradi1g51990	0	0	0	0	0	0	0	0	0	Expansin-A17
Bradi1g61190	11.02755925	13.26869824	8.829950039	89.47180305	75.96927689	59.48339003	21.20365783	13.38310385	16.31863847	Expansin-A4
Bradi1g74710	0	0	0	0.160343733	0.921957244	0.278610726	0	0.247835257	0.196610102	Putative expansin-A27
Bradi1g74720	0	0	0	0.09274642	0	0	0	0.286706969	0	Expansin-A25
Bradi1g74740	1.851121204	2.080469275	3.295486911	2.778096052	3.006817746	3.407418082	0	0.252586092	0	Expansin-A25
Bradi1g74750	0.423848527	0.582220248	0.580432954	3.891414549	1.63510837	3.7059099	0.07119478	0.11566854	0.275282908	Expansin-A12
Bradi1g76260	22.42693171	28.09279228	27.03942054	57.72195235	62.1069544	48.90707783	244.6674234	267.2120968	165.7313322	Expansin-like A1
Bradi1g76270	0.693616445	1.414744935	1.551442162	10.57283286	12.1585043	9.682111854	135.382641	147.5187444	111.0715271	Expansin-like A1
Bradi2g08760	0	0	0	0	0.209513347	0.079142317	0	0	0	Expansin-A8
Bradi2g08780	0	0	0	0	0	0	0	0.975182604	0	Expansin-A9
Bradi2g10320	13.49140004	11.95276951	14.50583776	2.7039463	3.627718988	3.327986713	4.716105303	2.43795651	4.696989354	Expansin-A11
Bradi2g22290	96.65497142	104.254627	148.803909	426.6828702	412.3098834	537.6621782	512.2686179	416.0092937	344.6518556	Expansin-A4
Bradi2g31760	0	0	0	0	0	0	0	0	0	Expansin-A8
Bradi2g53580	23.70514683	30.79628543	38.54267682	182.4229636	155.9869964	246.9425614	402.998389	272.2046777	284.0200914	Expansin-A4
Bradi3g09930	0	0.033008256	0	0	0	0	0	0	0	Expansin-A23
Bradi3g09940	0.343450466	0.375280592	0.164616566	0.106119608	0.122035004	0.092195873	0.100957743	0.328047497	0.130121624	Expansin-A23
Bradi3g09950	1.851121204	1.386979516	1.901242449	0	0.563778327	0.141975753	0.310936946	0.757758276	0	Expansin-A23
Bradi3g09960	0	0	0	0	0	0	0	0	0	Expansin-A23

Bd ID	Ps_1	Ps_2	Ps_3	Es_1	Es_2	Es_3	Ms_1	Ms_2	Ms_3	Description
Bradi3g09967	0	0	0	0	0	0	0	0	0	Expansin-A23
Bradi3g09990	0	0	0	0	0	0	0	0	0	Expansin-A23
Bradi3g10100	0	0	0	0	0	0	0	0	0	Expansin-A23
Bradi3g13720	0	0	0	0.087286094	0.20075383	0.227500397	0	0	0	Expansin-A4
Bradi3g19500	0	0	0	0	0	0	0	0	0	Expansin-A23
Bradi3g27440	0	0	0	0	0	0	0	0	0	Putative expansin-A27
Bradi3g27450	0	0	0	0	0	0	0	0	0	Putative expansin-A27
Bradi3g27460	0	0	0	0	0	0	0	0	0	Expansin-A25
Bradi3g27470	0	0	0	0	0	0	0	0	0	Expansin-A25
Bradi3g32070	0	0.07185114	0	0	0	0.176518017	0	0	0	Putative expansin-A30
Bradi3g32297	2.316280158	0.867753318	0.770341601	9.581430884	6.71854622	11.31897843	110.3849242	84.70332511	82.09656361	Expansin-like A1
Bradi3g43080	0	0	0	0	0	0	0	0	0	Expansin-A16
Bradi3g49850	66.99399185	71.82364284	84.9295967	100.199316	77.79534705	134.4880937	3.282162861	3.477688277	3.494586007	Expansin-B16
Bradi3g50730	0	0	0	0	0	0	0	0	0	Putative expansin-B14
Bradi3g50740	27.69140022	24.20621564	31.18686425	309.8902064	295.5022974	485.0042277	119.2076542	83.53996393	89.20491471	Putative expansin-B14
Bradi3g50750	20.95673438	12.12491262	25.00312747	226.9591065	194.1410207	341.0992043	37.40475173	39.74573284	21.24893223	Putative expansin-B14
Bradi3g59460	193.2490871	259.798641	384.5530228	125.1989362	124.779005	169.8824045	37.66695363	20.61940943	23.61789134	Expansin-A15
Bradi4g41110	0	0	0	0	0	0	0	0	0.280620235	Putative expansin-B14
Bradi4g41117	0	0	0	0	0	0	0	0	0	Putative expansin-B14
Bradi5g04120	0	0	0	0	0.120534574	0	0	0	0	Expansin-A15
Bradi5g16497	71.18354366	88.99554067	102.8511959	30.81766464	25.88118375	36.21730482	4.379546879	4.74356681	3.763117353	Expansin-B16
Bradi5g17760	9.513972689	13.3065008	12.76819067	37.03940234	34.81925191	41.11829966	0.279664552	1.363093911	0	Putative expansin-B14
Bradi5g17770	0	0	0	0.336510861	0	0	0.320142316	0.26006397	0.412622517	Putative expansin-B14

Bd ID	Ps_1	Ps_2	Ps_3	Es_1	Es_2	Es_3	Ms_1	Ms_2	Ms_3	Description
Bradi5g17780	0	0	0	0	0	0	0.158506945	0	0	Putative expansin-B14
Bradi5g19340	147.8063614	165.2633377	170.5406246	172.5470365	160.2295836	173.4252266	25.27876986	27.46545718	17.91960644	Expansin-A10

Table 4.7. List of Brachypodium genes annotated as EXPANSIN (EXP) with their expression in each developmental zone in drought stress conditions. The gene expression is expressed in FPKM. (P) proliferation, (E) expansion and (M) mature cells in (S) stress conditions.

Bd ID	Ps_1	Ps_2	Ps_3	Es_1	Es_2	Es_3	Ms_1	Ms_2	Ms_3	Description
Bradi1g21890	2.471983077	2.544243334	2.598975227	2.956627217	2.833375345	3.638983545	7.969631443	2.284955111	5.921411378	gibberellin receptor gID1C
Bradi1g23350	50.13399511	61.38333445	71.9912409	45.45249462	66.13761479	83.99943508	418.608722	241.6776586	782.6570224	Chitin-inducible gibberellin-responsive protein 2
Bradi1g25370	17.30273932	15.70802936	21.16818719	45.5172363	56.39852648	74.19663042	286.3499616	224.4382327	638.0230153	Chitin-inducible gibberellin-responsive protein 1
Bradi1g29515	111.7656707	101.6953675	103.5639186	49.96012408	33.51421786	45.60104366	3.536455813	3.217535627	2.370180503	gibberellin-regulated protein
Bradi1g32070	0	0	0	0	0.041805879	0	0	0	0	Chitin-inducible gibberellin-responsive protein
Bradi1g43850	410.4089969	504.7200802	578.5586396	1011.271222	1073.072439	1480.66316	108.474888	245.4136996	114.5485954	gibberellin-regulated protein
Bradi1g56200	0	0	0	0	0	0	0.087207226	0	0	gibberellin 20 oxidase 1
Bradi1g59570	0	0	0.11507641	0.29673474	0	0.257800788	0.917478196	0	0.363849877	gibberellin 2-beta-dioxygenase 8
Bradi2g04840	11.52708262	9.454860673	7.106992018	17.7611671	10.97027309	6.488553236	3.04508372	2.134120037	2.616482413	gibberellin 3-beta-dioxygenase 2-2
Bradi2g06670	0	0.132516663	0	0.093680679	0	0	1.158610285	0.86878513	0.918954177	gibberellin 2-beta-dioxygenase
Bradi2g12440	1.767734373	1.99973638	1.893917729	8.482102904	6.355018851	4.912789136	5.624208722	19.26825714	4.569949884	gibberellin 2-beta-dioxygenase
Bradi2g16727	0.076428035	0	0	0	0	0	0	0	0	gibberellin 2-beta-dioxygenase
Bradi2g16750	0	0	0.034438014	0	0.153179355	0	0.929302	0.823535905	1.415524467	gibberellin 2-beta-dioxygenase
Bradi2g19900	8.797347205	10.1643465	15.03305258	38.76406072	41.42468076	67.10939305	310.8587803	128.3071984	402.1643283	gibberellin 2-beta-dioxygenase 1

Bd ID	Ps_1	Ps_2	Ps_3	Es_1	Es_2	Es_3	Ms_1	Ms_2	Ms_3	Description
Bradi2g24320	0	0.524305059	1.149930215	0	0	0	0	0	0	gibberellin-regulated protein
Bradi2g24980	0	0.175050237	0.063988052	0.164998874	0.379489498	0.215024568	0.392432516	0.127515237	0.505795343	gibberellin 20 oxidase
Bradi2g25600	15.40184208	17.25677888	18.6855012	18.46399085	18.70539123	19.78435479	63.94811802	35.26588131	76.11404817	gibberellin receptor gID1
Bradi2g32577	7.368896859	8.089278049	3.531928519	18.53248219	24.60003349	19.32104818	14.10482087	10.47578592	17.40019756	gibberellin 2-beta-dioxygenase
Bradi2g34837	3.168748908	4.19687344	3.221672239	5.696480837	6.004915023	4.433530546	6.661337094	6.603573286	4.511084221	gibberellin 2-beta-dioxygenase
Bradi2g50280	8.824909226	7.334212676	5.417475857	40.8874835	35.89803227	18.15813215	0.511151597	0.415228187	0.790570872	gibberellin 2-beta-dioxygenase
Bradi2g56910	72.86149778	71.36968861	78.26565853	98.68055089	101.476008	123.5811044	236.753736	291.4980965	378.8716791	Chitin-inducible gibberellin-responsive protein 2
Bradi2g57027	0.726066337	0.423123381	0.580008661	3.813789756	2.665858241	2.338863727	9.817697682	9.015550955	8.160756443	gibberellin 20 oxidase 2
Bradi2g57940	0	0	0	0	0	0	0	0	0	Chitin-inducible gibberellin-responsive protein
Bradi2g60750	24.37064203	27.81062229	23.70161304	38.22532794	38.79406558	28.1665302	137.8572572	73.98068151	90.92185753	Chitin-inducible gibberellin-responsive protein
Bradi3g24210	148.4407814	153.2981805	177.3491689	125.5385266	126.6394576	148.5338663	145.984896	93.13852641	167.3928533	Chitin-inducible gibberellin-responsive protein 2
Bradi3g49390	0.084806929	0.148266594	0.081296296	0.524074291	0.482138296	1.183810124	3.091210229	0.972042379	5.654957771	gibberellin 2-beta-dioxygenase 8
Bradi3g60370	0	0	0	0	0	0	0	0	0	gibberellin-regulated protein
Bradi4g18390	0.108766836	0.095077658	0.208528738	0.537709864	0.618353452	0.408763306	0	0	0.082416061	Chitin-inducible gibberellin-responsive protein
Bradi4g21690	3.625531245	3.966519428	4.874373615	1.296354787	1.134286791	1.811813995	7.426596177	3.702508529	3.66290578	gibberellin receptor gID1C
Bradi4g23540	0	0	0	0	0	0	0	0	0	gibberellin 3-beta-dioxygenase 2-2
Bradi4g23570	0	0	0	0	0	0	0	0	0	gibberellin 3-beta-dioxygenase 2-2
Bradi4g26520	29.74919235	31.93133181	32.10667016	16.63301605	16.97032497	10.43053163	19.03633525	9.858268432	18.40155185	Chitin-inducible gibberellin-responsive protein
Bradi4g30250	23.22098131	25.53674051	26.56807095	24.07042393	26.08346367	31.36828999	0.44037676	1.430940214	1.135178689	gibberellin-regulated protein
Bradi5g16040	0	0	0	0	0	0	0.105328208	0	0	gibberellin 2-beta-dioxygenase 8

Table 4.8. List of Brachypodium genes annotated as GIBBERELLIN ACID (GA) with their expression in each developmental zone in drought stress conditions. The gene expression is expressed in FPKM. (P) proliferation, (E) expansion and (M) mature cells in (S) stress conditions.

Bd ID	Ps_1	Ps_2	Ps_3	Es_1	Es_2	Es_3	Ms_1	Ms_2	Ms_3	Description
Bradi1g09670	198.1055415	236.160838	277.1039958	3.635000568	2.687247967	2.255756894	9.633521054	6.019754835	10.5061652	gRF1-interacting factor 1
Bradi1g09900	213.2242079	254.0546008	242.5057058	49.70881561	47.05669773	34.92483554	11.65137667	10.68972802	5.653509638	gRF
Bradi1g12650	158.6292649	147.4321152	192.8554728	20.33950822	21.59072013	17.77536433	15.22822836	21.76460066	11.65828513	gRF
Bradi1g28400	32.4856132	38.43325211	34.72418305	31.12978751	33.26857931	32.77930088	44.05709047	41.995018	50.17489804	gRF
Bradi1g46427	21.11234108	27.19389667	25.33148638	0.345605749	0.695517069	0.225194649	0.739788324	1.469009992	0.529718096	gRF
Bradi1g50597	116.9806185	121.2872165	146.1923565	43.46242008	38.93057724	26.20068152	22.64312934	16.22318129	15.77028949	gRF
Bradi2g14320	77.27871272	83.28171933	92.87199555	33.82665697	32.97737684	41.59109845	28.72929303	28.22259429	28.70417508	gRF
Bradi3g51685	70.07815985	67.15292492	74.52870399	22.061351	15.78579317	22.57414479	5.441396548	1.515516553	2.604926815	gRF
Bradi3g52547	93.89677239	100.3621361	100.7811824	10.31242961	10.27784057	9.198273207	14.12757058	12.1139475	7.924127043	gRF
Bradi3g57267	76.11789982	82.06722864	87.44553733	6.414264897	7.092548894	5.072551717	4.068175022	1.65236786	0.907504185	gRF
Bradi4g07090	252.4980874	268.7811081	263.8155785	32.49941715	31.42775841	41.71114373	48.1346107	90.76138662	38.03873137	gRF1-interacting factor
Bradi4g13730	212.8038592	236.6914818	247.2966645	185.2359595	203.7391723	203.5475473	235.1723035	295.7870787	239.0034575	gRF1-interacting factor
Bradi4g16450	52.05871933	61.80409904	54.30698724	5.788426211	5.120424127	3.868414435	6.142273461	6.366049038	2.729863876	gRF
Bradi5g20607	161.3793114	192.9074963	216.626869	18.24545472	15.7812096	15.1740915	49.40342516	33.98592074	43.59709129	gRF

Table 4.9. List of Brachypodium genes annotated as GROWTH REGULATING FACTORS (GRF) with their expression in each developmental zone in drought stress conditions. The gene expression is expressed in FPKM. (P) proliferation, (E) expansion and (M) mature cells in (S) stress conditions.

Bd ID	Ps_1	Ps_2	Ps_3	Es_1	Es_2	Es_3	Ms_1	Ms_2	Ms_3	Description
Bradi1g14467	0.353724626	0.206137032	0.339081987	36.13992425	42.73311225	36.4622858	21.90466625	20.49689362	19.29803771	NAC
Bradi1g29857	0.135691086	0.553528619	0.47693827	0.279506289	0.064285106	0.58279883	0.797731672	0.86403767	0.959629198	NAC
Bradi1g48580	0	0	0	0	0	0	0	0	0	NAC
Bradi1g50057	1.73820281	1.953560649	1.190177773	35.49785769	32.93968841	30.395873	71.72724555	43.64081465	60.96250112	NAC
Bradi1g52187	9.336186331	8.77019371	7.61393188	27.72758851	30.30166141	26.33387308	2.785345939	2.395740813	6.335214399	NAC
Bradi1g52480	17.56084894	17.40991235	15.60215795	18.39534662	16.89292836	15.98173119	31.60173255	17.79604625	22.55598586	NAC
Bradi1g58057	0	0	0	0	0	0	0.331595448	0	0.64107621	NAC
Bradi1g58520	0.046763595	0.040878022	0	0	0.066464262	0.050212894	0	0	0	NAC
Bradi1g63600	0.12244314	0.214065379	0	0.151330328	0	0	4.031141112	0.935614755	5.010067482	NAC
Bradi1g63630	4.212293252	2.761606798	4.542663255	13.79608903	13.47042874	17.8658242	172.1111157	121.7072909	207.1470027	NAC
Bradi1g76207	0.111551971	0.195024523	0.320802634	0.068934839	0	0.419230291	0.459072	0.319647359	0	NAC
Bradi1g77217	10.01694067	9.332296094	9.854975189	57.99132389	55.63630265	60.14753056	28.6700698	23.16391436	37.75101803	NAC
Bradi2g03467	0	0	0	0	0	0	0.140539009	0.114165266	0.362273632	NAC
Bradi2g20590	0.333420191	0.51004903	1.038758714	1.442286227	0.71082625	0.805530105	0.882083964	0	1.010571965	NAC
Bradi2g24790	355.8113737	392.2149879	347.8785139	402.1874045	417.4140692	361.7876615	254.8744151	191.1308683	273.1684759	NAC
Bradi2g25150	20.39867888	16.28824483	18.42613298	69.20959866	48.08815378	54.54762276	20.75614635	7.681131091	16.19983379	NAC
Bradi2g46980	0.141853577	0.279000378	0.169976831	0.08766007	0	0.152316747	0.041698057	0	0	NAC
Bradi2g53260	0.880548536	0.577293336	0.633073283	0.408108916	1.407946408	0.236374526	9.835861785	2.312909349	13.34438778	NAC
Bradi3g13630	8.360763878	8.039344234	8.758884043	58.38293481	40.23245801	43.79716391	53.08541672	17.79693176	38.82581396	NAC
Bradi3g16480	136.9493123	130.347004	159.6521295	266.9081781	328.8621489	366.2802346	596.3261811	480.106459	1136.72752	NAC
Bradi3g33320	0	0	0.200366628	0.51666314	0.297075112	0	5.652613817	6.787932304	5.068171519	NAC
Bradi3g33680	0	0	0	0	0	0	0	0	0	NAC
Bradi3g36670	0.102694246	0	0	0.380766632	0.291914998	1.543766133	0	0	0	NAC

Bd ID	Ps_1	Ps_2	Ps_3	Es_1	Es_2	Es_3	Ms_1	Ms_2	Ms_3	Description
Bradi3g37067	0	0.144419358	0.237560434	1.429331561	0.234813861	0.177398846	0.48564503	1.735836158	1.251868714	NAC
Bradi3g41470	208.6846664	222.4705804	225.7731169	474.0900971	471.3987876	451.2069753	607.5331024	556.4507329	437.6366107	NAC
Bradi3g46900	0.468518278	0.273034332	0.598831584	2.509228155	3.77341444	1.006152698	1.6526592	1.790025211	4.260132853	NAC
Bradi3g54817	1.101988257	0.374614413	1.291119872	1.891629099	1.653249365	2.169330706	0.79183129	1.0525666	2.133917631	NAC
Bradi4g07527	9.87835339	14.10961352	9.840783457	10.45336078	12.29640697	12.89476507	74.09321813	102.3702666	69.17639024	NAC
Bradi4g13570	0	0	0	0	0	0	0	0	0	NAC
Bradi4g24060	0.160783921	0.196767167	0.184953811	0.158973274	0.045703863	0	0.45372151	0.552863265	0.341126929	NAC
Bradi4g24100	0.818362905	0.817560431	1.718398542	1.396741878	1.661606558	2.761709147	0.412386712	0.148887847	0.708685001	NAC
Bradi4g26600	0	0	0	0	1.311989714	0.165198553	1.447186081	1.175605157	1.632083115	NAC
Bradi4g34022	8.984868483	9.414101984	11.14962077	9.279193165	12.77003321	11.4978193	18.66870045	23.74722418	27.23247254	NAC
Bradi4g34157	0	0	0	4.172075926	2.206982153	3.842146449	6.826917375	4.385026415	7.264310279	NAC
Bradi4g34800	0.164993148	0.288454876	0.210884212	14.34229412	14.53911259	12.63763444	20.04665238	29.20734381	14.50237917	NAC
Bradi4g37327	2.824968	4.074548187	1.760217412	13.96577498	22.88593661	17.13836322	2.657290484	10.79309854	3.853021181	NAC
Bradi4g41200	0.060505528	0.079335634	0.174002598	0	0	0.032484218	0.035571368	0	0	NAC
Bradi4g44000	0	0.044091467	0.048351728	0	0	0	0	0	0.305758062	NAC
Bradi5g11247	0	0	0	0	0	0	0	0	0	NAC
Bradi5g12407	0.173889837	0.152004408	0.166691565	1.934230494	1.730025652	1.120296071	2.249067025	0.996547649	1.054094497	NAC
Bradi5g15587	0.103206437	0	0	0	0.293370933	0	0	0	0	NAC
Bradi5g27467	0.172680589	0.301894707	0.220709833	8.679078447	8.262737257	5.377109515	23.2817822	16.71354092	19.62682903	NAC

Table 4.10. List of Brachypodium genes annotated as NAC-domain protein (NAC) with their expression in each developmental zone in drought stress conditions. The gene expression is expressed in FPKM. (P) proliferation, (E) expansion and (M) mature cells in (S) stress conditions.

Bd ID	Ps_1	Ps_2	Ps_3	Es_1	Es_2	Es_3	Ms_1	Ms_2	Ms_3	Description
Bradi1g11060	0.071478033	0.031240975	0.137038316	0.044170683	0.101590453	0	0	0	0.054161159	TCP
Bradi2g06890	697.3660896	844.1311446	858.5960486	121.8679181	116.5277126	99.73393337	49.21460508	11.52950266	16.27358199	TCP
Bradi2g20060	80.07980427	98.6570397	88.33026677	66.71435296	60.8703799	55.94801083	16.84223732	8.264053676	12.82053144	TCP
Bradi2g50687	37.38829097	43.71393427	45.53331631	33.32477252	33.47665167	29.62560721	27.09568145	29.79702636	19.59956955	TCP
Bradi2g59240	6.812210631	6.720194871	7.267167344	4.8563136	3.763564576	4.448427089	26.96728212	14.48199362	24.85443866	TCP
Bradi3g36590	0	0	0	0	0	0	0	0	0	TCP
Bradi4g29980	0.049802384	0	0	0.369311558	0.07078324	0.160427476	0	0	0	Transcription factor TCP18
Bradi5g16270	24.26063036	32.37519168	33.80964773	29.31236149	22.60112329	28.60403455	2.477028886	2.596369354	3.501532293	Transcription factor TCP22

Table 4.11. List of Brachypodium genes annotated as TEOSINTE BRANCHED1/CYCLOIDEA/PCF (TCP) with their expression in each developmental zone in drought stress conditions. The gene expression is expressed in FPKM. (P) proliferation, (E) expansion and (M) mature cells in (S) stress conditions.

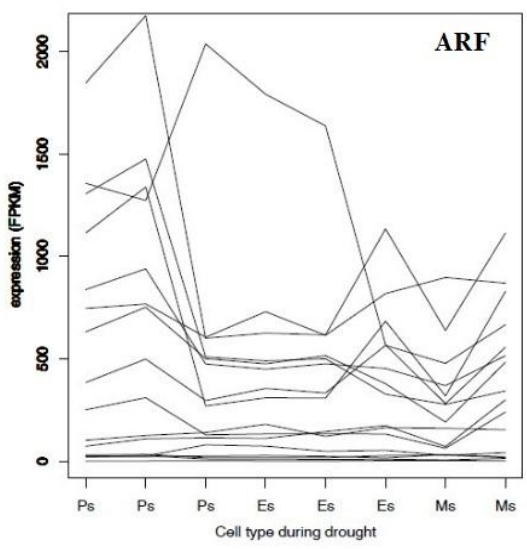
ARF
expression (FPKM)
0
500
1000
1500
2000
Ps Ps Ps Es Es Es Ms Ms
Cell type during drought

A

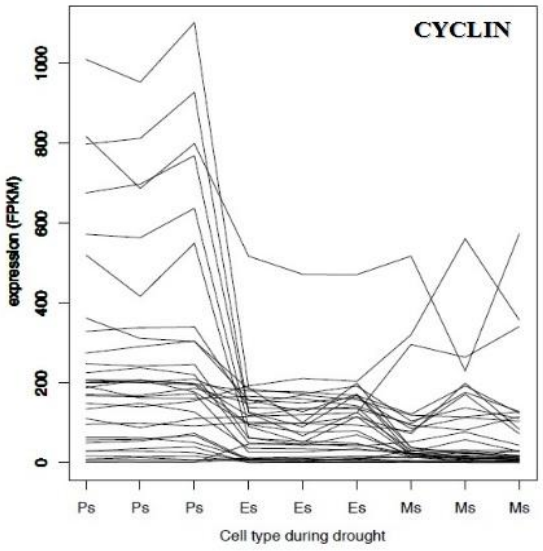
CYCLIN
expression (FPKM)
0
200
400
600
800
1000
Ps Ps Ps Es Es Es Ms Ms Ms
Cell type during drought

B

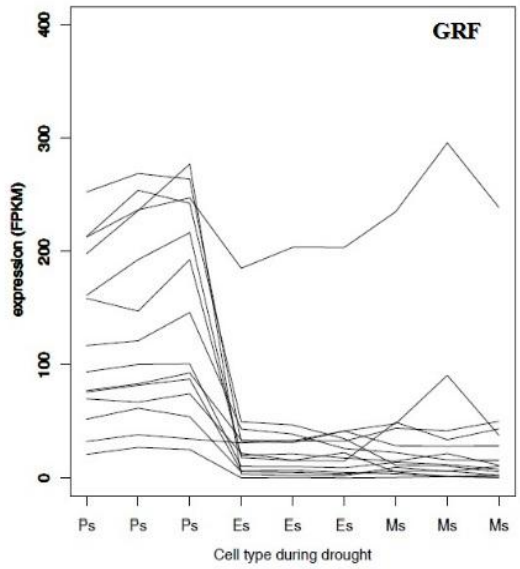
GRF
expression (FPKM)
0
100
200
300
400
Ps Ps Ps Es Es Es Ms Ms Ms
Cell type during drought

C

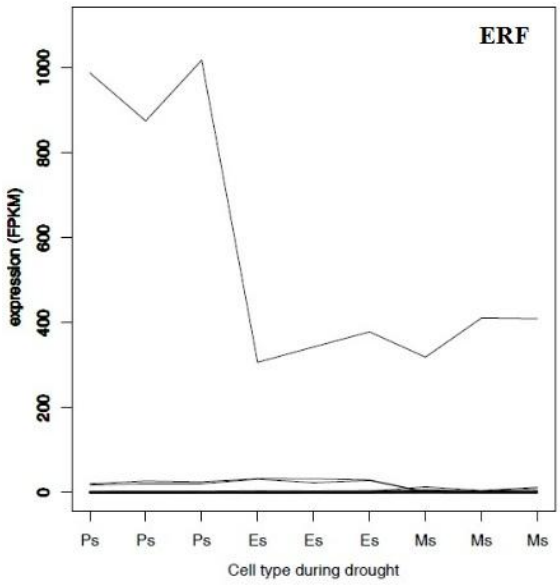
ERF
expression (FPKM)
0
200
400
600
800
1000
Ps Ps Ps Es Es Es Ms Ms Ms
Cell type during drought

D

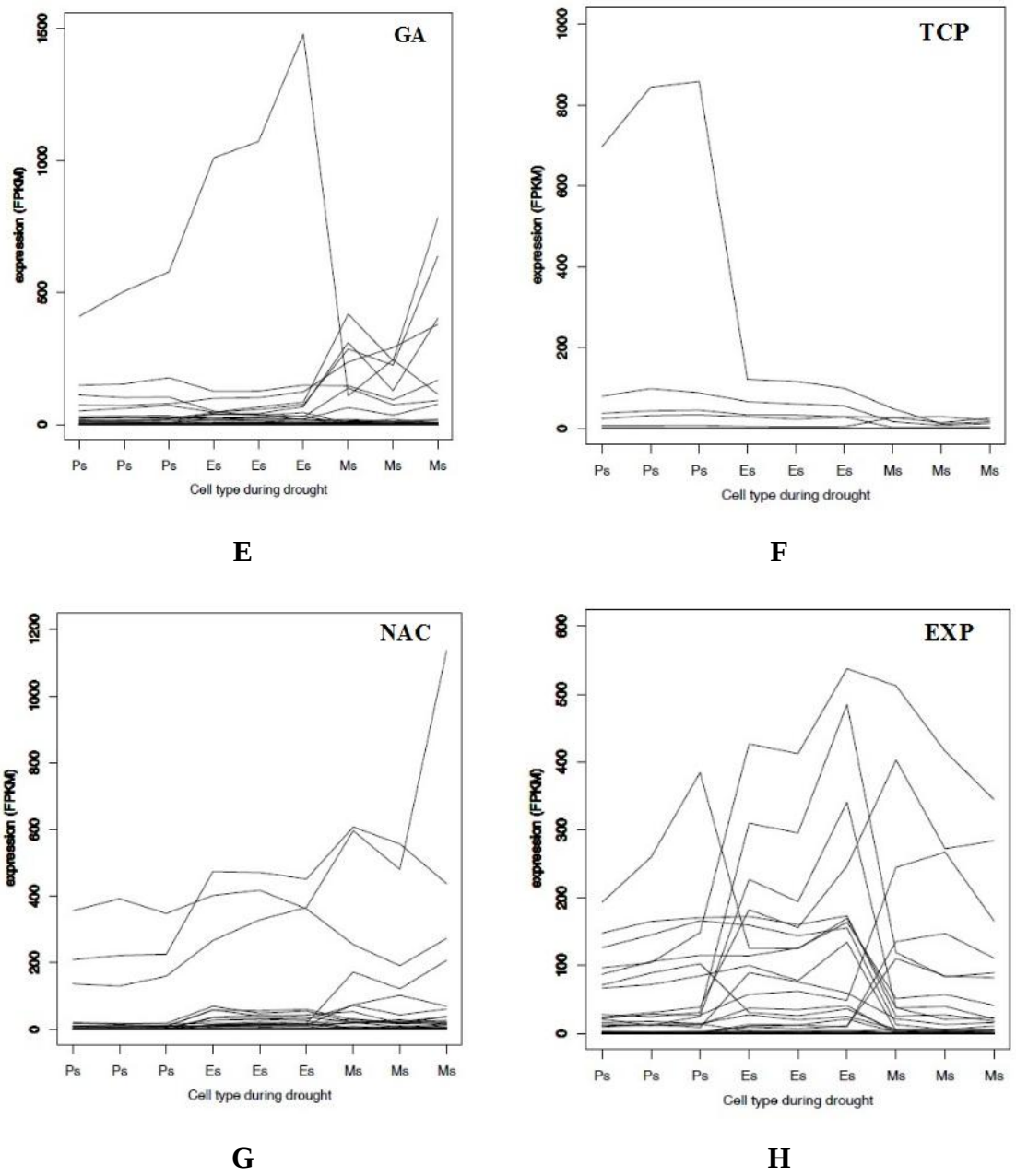

Figure 4.8. Plots show the expression level in each developmental zone during drought stress. y-axis shows expression level in FPKM, x-axis shows the three developmental leaf areas: (P) proliferation, (E) expansion and (M) mature cells in (S) stress conditions. Gene are (a) ARF, (b) CYCLYN, (c) GRF, (d) ERF, (e) GA, (f) TCP, (g) NAC, (h) EXP.

4.5 Gene Ontology analysis

Gene enrichment analysis based on gene ontology (GO) was performed on differentially expressed genes regulated in response to drought stress, in proliferating, expanding and mature leaf cells, (ei: Ps vs Pc, Es vs Ec, Ms vs Mc), using *GOseq* Bioconductor R package.

Applying a p-value < 0.05 we were able to identify 96 enriched GO terms in Proliferating cells a, 87 in expanding and 29 in mature cells. To have strong evidence We filtered these resulted by a FDR < 0.1 in order to increase the statistical significance. Proliferating cells were found to be enriched in GO terms related to translation, ribosome, nucleic acid binding, GTPase activity, helicase and methyltransferase activity, showing the main biological activities of the cells in active division. Whereas, expanding cells were enriched in GO terms referred to microtubule binding, DNA replication, translation, fatty acid biosynthetic process, GTP-catabolic process, transporter activity, DNA replication, sequence-specific DNA binding and protein polimerization. GO analys on mature cells was shown terms linked with contained GO terms related to glycerol metabolic process and phosphodiesterase activity.

We obtained 39 GO terms in proliferation cells (Tab. 3.14), 22 GO terms in expansion cells (Tab. 3.15) and 2 GO terms in mature cells (Tab. 3.16). Terms are related to translation, ribosome, nucleic acid binding, GTPase activity, helicase and methyltransferase activity .

This analysis clearly confirmed that the drought response of the three type of cells, also observed in the Venn diagram, is specific to each developmental stage

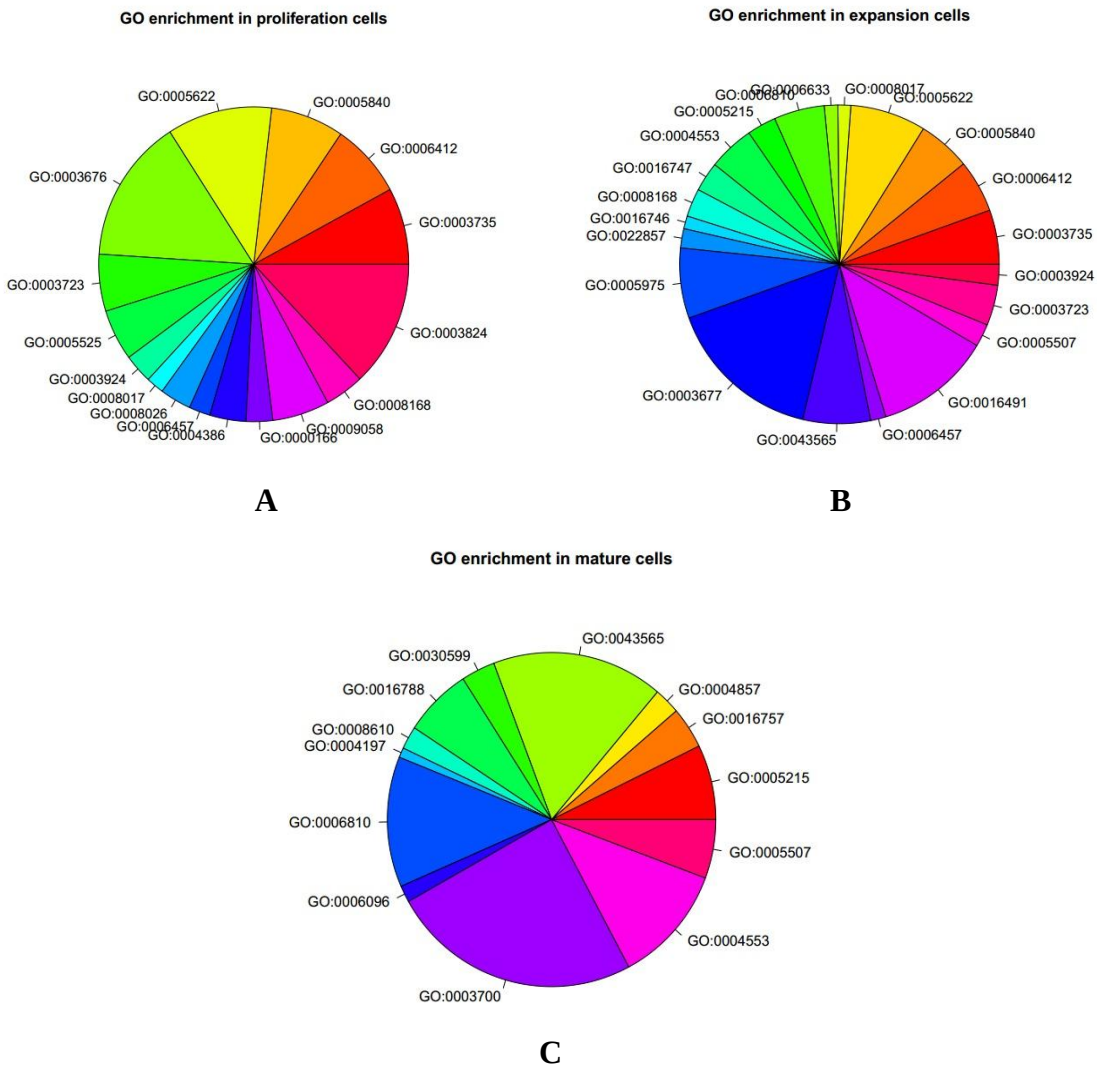

Figure 4.9. Gene ontology (GO) terms of differentially expressed genes in proliferation (A), expansion (B) and mature (C) cells. These terms are selected from list of genes differentially expressed in each leaf zones with a p-value < 0.05.

Category	Over represented pvalue	Under represented pvalue	NumDEInCat	NumInCat	Description
GO:0000166	**0.000889414**	**0.999611617**	**28**	**106**	**nucleotide binding**
GO:0003676	**8.31E-14**	**1**	**145**	**569**	**nucleic acid binding**
GO:0003723	**2.70E-11**	**1**	**69**	**224**	**RNA binding**
GO:0003735	**1.10E-77**	**1**	**174**	**302**	**structural constituent of ribosome**
GO:0003743	**0.002038242**	**0.999473852**	**11**	**32**	**translation initiation factor activity**
GO:0003746	0.031516786	0.991984343	6	16	NA
GO:0003777	**1.30E-07**	**0.999999973**	**25**	**54**	**microtubule motor activity**
GO:0003824	0.017252638	0.987447633	84	497	NA
GO:0003883	0.041257154	0.995864872	3	5	NA
GO:0003899	0.024315706	0.988852001	15	65	NA
GO:0003918	0.028202127	0.995879665	4	8	NA
GO:0003924	**3.67E-07**	**0.999999881**	**38**	**115**	**GTPase activity**
GO:0004055	0.022684495	1	2	2	NA
GO:0004066	0.006768815	0.999522145	4	6	NA
GO:0004097	0.00872951	0.999443213	3	6	NA
GO:0004152	0.024688638	1	2	2	NA
GO:0004386	**0.000225969**	**0.999897243**	**37**	**145**	**helicase activity**
GO:0004564	0.026898253	0.999061264	2	3	NA
GO:0004575	0.026898253	0.999061264	2	3	NA
GO:0004609	0.029846783	1	2	2	NA
GO:0004743	**0.002943096**	**0.999718277**	**5**	**9**	**pyruvate kinase activity**
GO:0004812	**1.72E-05**	**0.999995963**	**19**	**46**	**aminoacyl-tRNA ligase activity**
GO:0005525	**1.13E-07**	**1**	**57**	**201**	**GTP binding**
GO:0005544	0.006663451	0.99911114	5	11	NA
GO:0005576	**4.44E-05**	**0.999997044**	**7**	**12**	**extracellular region**
GO:0005622	**8.50E-31**	**1**	**146**	**419**	**intracellular**
GO:0005643	0.03432939	0.992429305	5	13	NA
GO:0005730	**0.002493224**	**1**	**3**	**3**	**nucleolus**
GO:0005741	**0.000865036**	**0.999932567**	**6**	**9**	**mitochondrial outer membrane**
GO:0005750	0.049962107	0.997525287	2	3	NA
GO:0005759	0.040828121	0.994466609	3	8	NA
GO:0005840	**7.98E-76**	**1**	**169**	**292**	**ribosome**
GO:0005852	**5.02E-05**	**0.999999106**	**5**	**6**	**eukaryotic translation initiation factor 3 complex**
GO:0005985	0.010768784	0.998459049	5	10	NA
GO:0005992	0.033143402	0.991079859	6	19	NA
GO:0006096	0.003432766	0.998979846	12	36	NA

Category	Over represented pvalue	Under represented pvalue	numDEInCat	numInCat	Description
GO:0006122	0.049962107	0.997525287	2	3	NA
GO:0006164	0.016109629	0.998897011	3	5	NA
GO:0006184	**1.37E-05**	**0.999998834**	**9**	**16**	**GTP catabolic process**
GO:0006221	0.041257154	0.995864872	3	5	NA
GO:0006222	0.024688638	1	2	2	NA
GO:0006265	0.00745814	0.998802002	6	12	NA
GO:0006303	0.02501025	1	2	2	NA
GO:0006310	0.046510156	0.978898767	12	49	NA
GO:0006334	0.042839384	0.98934621	5	16	NA
GO:0006364	**2.39E-05**	**0.999996767**	**12**	**22**	**rRNA processing**
GO:0006396	0.01704663	0.993775092	11	40	NA
GO:0006412	**8.14E-77**	**1**	**170**	**292**	**translation**
GO:0006414	0.006780424	0.998231114	9	25	NA
GO:0006418	**3.20E-05**	**0.999992424**	**18**	**44**	**tRNA aminoacylation for protein translation**
GO:0006452	0.028217428	1	2	2	NA
GO:0006457	**0.000137358**	**0.999950245**	**26**	**85**	**protein folding**
GO:0006479	**0.001549637**	**0.999698087**	**9**	**21**	**protein methylation**
GO:0006526	0.004066313	1	3	3	NA
GO:0006529	0.006768815	0.999522145	4	6	NA
GO:0006541	0.033932344	0.992541249	5	13	NA
GO:0007018	**1.30E-07**	**0.999999973**	**25**	**54**	**microtubule-based movement**
GO:0008017	**1.07E-06**	**0.999999713**	**28**	**71**	**microtubule binding**
GO:0008026	**3.17E-06**	**0.999998849**	**38**	**125**	**ATP-dependent helicase activity**
GO:0008168	0.004081091	0.997823154	34	156	NA
GO:0008173	0.029427593	0.995346296	4	9	NA
GO:0008276	0.012369343	0.997084224	7	19	NA
GO:0008479	0.027449612	1	2	2	NA
GO:0008536	**1.26E-05**	**0.999999356**	**8**	**11**	**Ran GTPase binding**
GO:0008616	0.027449612	1	2	2	NA
GO:0008716	0.025134358	0.99794625	3	5	NA
GO:0009058	0.003313789	0.998083245	45	228	NA
GO:0009116	0.008360554	0.998209583	7	18	NA
GO:0009405	**0.000525867**	**1**	**3**	**3**	**pathogenesis**
GO:0015093	**3.93E-06**	**0.999999468**	**14**	**26**	**ferrous iron transmembrane transporter activity**
GO:0015684	**3.93E-06**	**0.999999468**	**14**	**26**	**ferrous iron transport**
GO:0015934	0.020367933	0.997137662	4	9	NA
GO:0016702	0.026908201	0.995515058	4	11	NA

Category	Over represented pvalue	Under represented pvalue	numDEInCat	numInCat	Description
GO:0016740	0.003693955	0.999148052	9	23	NA
GO:0016818	0.047802497	0.982396437	8	31	NA
GO:0016831	0.044333627	0.986710655	6	23	NA
GO:0016841	**0.0003908**	**0.999976721**	**5**	**9**	**ammonia-lyase activity**
GO:0016876	0.03786499	0.993493469	4	9	NA
GO:0019752	0.044333627	0.986710655	6	23	NA
GO:0019843	**1.56E-08**	**0.999999999**	**12**	**17**	**rRNA binding**
GO:0019867	0.044263722	0.994152595	3	7	NA
GO:0030688	0.014641066	1	2	2	NA
GO:0030955	**0.002943096**	**0.999718277**	**5**	**9**	**potassium ion binding**
GO:0031369	0.018503181	0.999474133	2	3	NA
GO:0032040	**0.000259476**	**0.99998713**	**6**	**8**	**small-subunit processome**
GO:0032259	0.037567222	0.993561595	4	9	NA
GO:0042254	**8.96E-05**	**0.999991685**	**8**	**14**	**ribosome biogenesis**
GO:0043022	0.016582894	0.999203777	3	4	NA
GO:0043039	0.041905812	0.990220833	5	13	NA
GO:0043234	**3.23E-05**	**0.999997425**	**8**	**14**	**protein complex**
GO:0044267	**7.73E-11**	**1**	**19**	**27**	**cellular protein metabolic process**
GO:0045901	0.028217428	1	2	2	NA
GO:0045905	0.028217428	1	2	2	NA
GO:0046907	0.021892882	0.998307647	3	5	NA
GO:0051082	**9.81E-05**	**0.999979755**	**14**	**32**	**unfolded protein binding**
GO:0051258	**3.23E-05**	**0.999997425**	**8**	**14**	**protein polymerization**

Table 4.12. List of enrichment of GO terms in proliferation leaf zones. Terms are selected by a p-value < 0.05. The ontology description (in bold) is shown only for terms which passes the statistically test with a FDR < 0.1. NA indicates terms which does not pass the statistically test.

Category	Over represented pvalue	Under represented pvalue	numDEInCat	numInCat	Description
GO:0000786	0.046061188	0.990607688	4	12	NA
GO:0001671	0.014121345	1	2	2	NA
GO:0003677	0.008109073	0.993887357	128	867	NA
GO:0003723	0.036116683	0.976620019	36	224	NA
GO:0003735	**7.44E-63**	**1**	**153**	**302**	**structural constituent of ribosome**
GO:0003777	**1.71E-10**	**1**	**25**	**54**	**microtubule motor activity**
GO:0003883	0.01244453	0.999229304	3	5	NA
GO:0003924	0.046412128	0.973824974	20	115	NA
GO:0004175	0.033276639	0.994061616	4	11	NA
GO:0004553	**0.000175307**	**0.999909195**	**51**	**255**	**hydrolase activity, hydrolyzing O-glycosyl compounds**
GO:0004564	0.043241454	0.998028918	2	3	NA
GO:0004575	0.043241454	0.998028918	2	3	NA
GO:0005215	**0.000174115**	**0.999921926**	**36**	**161**	**transporter activity**
GO:0005507	0.026054043	0.985606273	23	126	NA
GO:0005542	0.014592106	1	2	2	NA
GO:0005576	**0.001652405**	**0.99980824**	**6**	**12**	**extracellular region**
GO:0005618	0.018892866	0.991851839	14	63	NA
GO:0005622	**1.67E-30**	**1**	**137**	**419**	**intracellular**
GO:0005759	0.009551006	0.999007517	4	8	NA
GO:0005840	**5.67E-60**	**1**	**147**	**292**	**ribosome**
GO:0005886	0.025979392	0.997475191	3	6	NA
GO:0005975	0.0072551	0.995197575	63	389	NA
GO:0006073	0.021349897	0.993339346	8	30	NA
GO:0006184	**0.001612071**	**0.99975911**	**7**	**16**	**GTP catabolic process**
GO:0006221	0.01244453	0.999229304	3	5	NA
GO:0006260	**4.43E-05**	**0.999990404**	**15**	**42**	**DNA replication**
GO:0006269	0.036120656	0.998513482	2	3	NA
GO:0006270	0.017640766	1	2	2	NA
GO:0006306	0.02061982	0.996950201	4	10	NA
GO:0006334	0.00762438	0.998605095	6	16	NA
GO:0006352	0.026777564	0.990476323	9	37	NA
GO:0006364	0.038382272	0.988979335	6	22	NA
GO:0006412	**9.80E-62**	**1**	**149**	**292**	**translation**
GO:0006457	0.01837662	0.99130959	17	85	NA

Category	Over represented pvalue	Under represented pvalue	numDEInCat	numInCat	Description
GO:0006479	0.029670508	0.992064158	6	21	NA
GO:0006541	0.012770635	0.997841527	5	13	NA
GO:0006633	**3.45E-05**	**0.999989475**	**23**	**75**	**fatty acid biosynthetic process**
GO:0006729	0.015356139	1	2	2	NA
GO:0006810	7.71E-05	0.999960374	56	280	transport
GO:0006814	0.046207996	0.990567777	4	12	NA
GO:0006950	0.006969506	0.997164787	16	70	NA
GO:0007018	**1.71E-10**	**1**	**25**	**54**	**microtubule-based movement**
GO:0008017	**3.91E-11**	**1**	**30**	**71**	**microtubule binding**
GO:0008124	0.015356139	1	2	2	NA
GO:0008134	0.0311643	0.994555332	4	11	NA
GO:0008168	**0.000633979**	**0.9997032**	**33**	**156**	**methyltransferase activity**
GO:0008184	0.036910801	0.998462282	2	3	NA
GO:0008536	0.035469321	0.993537536	4	11	NA
GO:0008610	**2.93E-05**	**0.999992907**	**18**	**49**	**lipid biosynthetic process**
GO:0009116	0.003504329	0.999366447	7	18	NA
GO:0009186	0.02090814	1	2	2	NA
GO:0009228	0.029214271	0.997024039	3	6	NA
GO:0009405	0.049256628	0.997580233	2	3	NA
GO:0009415	0.016158644	0.997888251	4	9	NA
GO:0009690	0.0369195	0.993184634	4	11	NA
GO:0010309	0.005684168	0.999819837	3	4	NA
GO:0015934	0.002219649	0.999801617	5	9	NA
GO:0015995	**7.46E-07**	**0.99999997**	**9**	**12**	**chlorophyll biosynthetic process**
GO:0016429	0.005993678	0.999806186	3	4	NA
GO:0016491	0.021177976	0.984099154	95	645	NA
GO:0016740	0.043477737	0.987030421	6	23	NA
GO:0016746	**0.001329609**	**0.999507637**	**19**	**71**	**transferase activity, transferring acyl groups**
GO:0016747	**0.000299535**	**0.999858834**	**38**	**164**	**transferase activity, transferring acyl groups other than**
GO:0016762	0.021349897	0.993339346	8	30	NA
GO:0016830	0.043648106	0.997999701	2	3	NA
GO:0016851	**1.29E-05**	**0.99999924**	**8**	**12**	**magnesium chelatase activity**
GO:0019139	0.0369195	0.993184634	4	11	NA
GO:0019538	0.006224718	0.998934809	6	15	NA
GO:0019773	0.033276639	0.994061616	4	11	NA

Category	Over represented pvalue	Under represented pvalue	numDEInCat	numInCat	Description
GO:0019843	0.002177243	0.999647389	7	17	NA
GO:0022857	0.002763805	0.998751655	24	107	NA
GO:0030488	0.005993678	0.999806186	3	4	NA
GO:0031515	0.005993678	0.999806186	3	4	NA
GO:0036355	0.0493711	0.997571355	2	3	NA
GO:0042254	**6.59E-05**	**0.99999416**	**8**	**14**	**ribosome biogenesis**
GO:0042626	0.008792384	0.996727547	13	54	NA
GO:0042802	0.008600942	0.996457169	16	63	NA
GO:0042823	0.020786058	1	2	2	NA
GO:0043086	0.008600942	0.996457169	16	63	NA
GO:0043169	0.013719937	0.997637518	5	13	NA
GO:0043234	**0.000532346**	**0.999939195**	**7**	**14**	**protein complex**
GO:0043565	0.013276458	0.991017637	60	374	NA
GO:0044267	0.031361258	0.990310618	7	27	NA
GO:0048037	0.033579865	0.99074614	6	21	NA
GO:0048046	0.021349897	0.993339346	8	30	NA
GO:0051258	**0.000532346**	**0.999939195**	**7**	**14**	**protein polymerization**
GO:0080019	0.023713923	0.997777532	3	6	NA

Table 4.13. List of enrichment of GO terms in expansion leaf zones. Terms are selected by a p-value < 0.05. The ontology description (in bold) is shown only for terms which passes the statistically test with a FDR < 0.1. NA indicates terms which does not pass the statistically test.

Category	Over represented pvalue	Under represented pvalue	NumDEInCat	NumInCat	Description
GO:0000015	0.026457085	0.999718899	1	5	NA
GO:0003700	0.029816637	0.98710962	11	546	NA
GO:0004144	0.039645204	0.999339226	1	6	NA
GO:0004197	0.021613105	0.998541247	2	21	NA
GO:0004356	0.023393052	0.999780514	1	5	NA
GO:0004553	0.038769936	0.987496306	6	255	NA
GO:0004634	0.026457085	0.999718899	1	5	NA
GO:0004857	0.007153451	0.999017257	4	57	NA
GO:0005215	0.000359585	0.999937506	8	161	NA
GO:0005507	0.049207506	0.987671187	4	126	NA
GO:0006071	**0.000147351**	**0.999996975**	**3**	**14**	**glycerol metabolic process**
GO:0006096	0.028963154	0.997643335	2	36	NA
GO:0006542	0.017540274	0.999884557	1	4	NA
GO:0006810	0.021936345	0.993059394	7	280	NA
GO:0008610	0.020458719	0.997299134	3	49	NA
GO:0008889	**0.000128523**	**0.999997518**	**3**	**13**	**Glycerophosphodiester phosphodiesterase activity**
GO:0009405	0.042213923	0.999398593	1	3	NA
GO:0009415	0.004605903	0.999876102	2	9	NA
GO:0016757	0.002323802	0.999676305	5	89	NA
GO:0016788	0.014520725	0.996831268	5	148	NA
GO:0019310	0.004252307	1	1	1	NA
GO:0030036	0.048673925	0.999000348	1	6	NA
GO:0030599	0.014310829	0.997572543	4	74	NA
GO:0043565	0.007804545	0.997388338	10	374	NA
GO:0045017	0.035291515	0.999498007	1	5	NA
GO:0046658	0.012886454	0.999958496	1	2	NA
GO:0050113	0.004252307	1	1	1	NA
GO:0051716	0.012886454	0.999958496	1	2	NA
GO:0080019	0.043053537	0.999219656	1	6	NA

Table 4.14. List of enrichment of GO terms in mature leaf zones. Terms are selected by a p-value < 0.05. The ontology description (in bold) is shown only for terms which passes the statistically test with a FDR < 0.1. NA indicates terms which does not pass the statistically test.

4.6 Identification of miRNAs target genes

We tried to investigate the link between microRNAs and their putative target genes, integrating mRNA-Seq data with small RNA-Seq data, previously produced by the lab, in order to characterized the regulatory network underlying the response to drought stress

Small RNA data was produced during a previous work in the laboratory. It was realized a *in vivo* drought assay of Brachypodium plants described by Verelst (2012) and was collected the third leaf of Brachypodium plants grown in control and stress condition . Leaves were sectioned and eight small RNA libraries were generated from proliferating (P), expanding (E) leaf zones of plants grown under drought stress (s) and control conditions (c), considering for each condition, two biological replicates. The libraries (Ps1, Ps2, Pc1, Ps2, Es1, Es2, Ec1, Ec2) were sequenced with a next generation small RNA sequencing and data were analyzed using an *ad hoc* miRNA pipeline, based on the the properties of know plant miRNAs and their precursors. It was identified a list of 213 miRNAs Brachypodium. The expression of miRNAs was calculated as the sum of the abundances off all libraries and expressed as number of tags per five million (TP5M) (Bertolini et al., 2013). Moreover based on high base pairing between plant miRNAs and their putative targets, putative target genes of *B. distachyon* microRNAs were predicted by TARGET FINDER and psRNATarget. This analysis allowed to identify of at least one potential target gene for 233 of the miRNA sequences analyzed (Bertolini et al., 2013).

Thus we combined these data with mRNA-Seq data to investigated the presence of putative targets genes in our dataset of gene differentially expressed. Therefore we joined the list of gene differentially expressed produced through mRNA-Seq with the list of predicted targets and afterwards. The resulting list had been combined with the list of Brachypodium miRNAs annotated in order to verified if the target identified are really targeted by microRNAs, analyzing the relationship between the expression level of targets genes and miRNAs abundance.

During this analysis, we focused on comparison between drought stress and control condition in proliferating and expansion leaf zones to identify some targets and miRNAs involved in response to stress. Based on Venn diagram, we considered unique genes differentially expressed of each leaf developmental zone, which have a pvalue

≤0.05 and a FDR ≤0.1. Moreover these genes are divided into down and up-regulated genes.

In proliferation leaf zone, 23 genes differentially expressed down-regulated are target genes (Tab. 4.15), and 32 genes up-regulated are putative target (Tab. 4.16). Instead in expansion leaf zone, 15 genes down-regulated are putative targets (Tab. 4.17) and 20 genes up-regulated are putative targets (Tab. 4.18). Tables shown that a single miRNA could have more than on target genes.

Bd ID	miRNA	miRNA position	Score	Range	Target seq	miRNA seq	Target gene annotation
Bradi1g06460	miR319b	MIR319b_p1	2.5	943-962	AGGGGG-ACCCUUCAGUCCAA	UUGGACUGAAGGGUGCUCCCU	TCP2;-transcription-factor
Bradi1g06460	miR319b	MIR319b_p3	2.5	943-962	AGGGGG-ACCCUUCAGUCCAA	UUGGACUGAAGGGUGCUCCCU	TCP2;-transcription-factor
Bradi1g06460	miR319b	MIR319b_p2	2.5	943-962	AGGGGG-ACCCUUCAGUCCAA	UUGGACUGAAGGGUGCUCCCU	TCP2;-transcription-factor
Bradi1g39270	miR5181a	MIR5181a_m	2	943-963	UCUGAUCCAUAAUAAUUGUCG	CGGCACUUAUUAUGGAUCAGA	Ubiquitin-protein-ligase-activity
Bradi1g60160	miR5174e	MIR5174e_np1	1.5	653-673	AAUUAUGGAACAGAGGGGGUA	UACUCCCUCUGUUCCAUAAAG	Ribosomal-protein
Bradi1g60160	miR5174e	MIR5174e_np2	1.5	653-673	AAUUAUGGAACAGAGGGGGUA	UACUCCCUCUGUUCCAUAAAG	Ribosomal-protein
Bradi2g37800	miR172a	MIR172a_m	0.5	1361-1381	CUGCAGCAUCAUCAGGAUUCU	AGAAUCUUGAUGAUGCUGCAU	AP2-(APETALA-2); -transcription-factor
Bradi2g37800	miR172a	MIR172a_m	0.5	1316-1336	CUGCAGCAUCAUCAGGAUUCU	AGAAUCUUGAUGAUGCUGCAU	AP2-(APETALA-2);-transcription-factor
Bradi3g28060	miRCB5185i	MIR5185i_m	2.5	1624-1644	GAGUUGAAAAUUGAACUGGAA	UUCUAGUUCAUUUUUCAAAUC	SAP-domain
Bradi3g28060	miRCB5185d	MIR5185d_m	2.5	1624-1644	GAGUUGAAAAUUGAACUGGAA	UUCUAGUUCAUUUUUCAAAUC	SAP-domain
Bradi3g28060	miRCB5185e	MIR5185e_m	2.5	1624-1644	GAGUUGAAAAUUGAACUGGAA	UUCUAGUUCAUUUUUCAAAUC	SAP-domain
Bradi3g28060	miRCB5185c	MIR5185c_m	2.5	1624-1644	GAGUUGAAAAUUGAACUGGAA	UUCUAGUUCAUUUUUCAAAUC	SAP-domain
Bradi3g28060	miR5185a	MIR5185a_m	2.5	1624-1644	GAGUUGAAAAUUGAACUGGAA	UUCUAGUUCAUUUUUCAAAUC	SAP-domain
Bradi3g28060	miRCB5185g	MIR5185g_m	2.5	1624-1644	GAGUUGAAAAUUGAACUGGAA	UUCUAGUUCAUUUUUCAAAUC	SAP-domain
Bradi3g28060	miR5185b	MIR5185b_m	2.5	1624-1644	GAGUUGAAAAUUGAACUGGAA	UUCUAGUUCAUUUUUCAAAUC	SAP-domain
Bradi3g28060	miRCB5185j	MIR5185j_m	2.5	1624-1644	GAGUUGAAAAUUGAACUGGAA	UUCUAGUUCAUUUUUCAAAUC	SAP-domain
Bradi3g28060	miRCB5185h	MIR5185h_m	2.5	1624-1644	GAGUUGAAAAUUGAACUGGAA	UUCUAGUUCAUUUUUCAAAUC	SAP-domain
Bradi3g28060	miRCB5185f	MIR5185f_m	2.5	1624-1644	GAGUUGAAAAUUGAACUGGAA	UUCUAGUUCAUUUUUCAAAUC	SAP-domain
Bradi3g28060	miRCB5185k	MIR5185k_m	2.5	1624-1644	GAGUUGAAAAUUGAACUGGAA	UUCUAGUUCAUUUUUCAAAUC	SAP-domain
Bradi3g29840	miRCB47	MIR7757	2.5	275-295	UGGGUUGCUGGCGGUUUUGUG	CACAAAACCUUCAGCUACCCA	Unknown
Bradi4g07090	miRCB118	MIR5049_m	1.5	1204-1227	CCUUCCUCCGAUCCAUAUUAGUUG	CAAGUAAUAUGGAUCGGAGGAAGU	GRF-interacting-factor.-putative
Bradi4g33020	miRCB5174b	MIR5174b_m	2.5	2363-2382	CCCUCUGUUCC-UAAAGGUUG	CAACCUUUAUGGAACGGAGGG	RNA-binding

Bd ID	miRNA	miRNA position	Score	Range	Target seq	miRNA seq	Target gene annotation
Bradi5g13350	miRCB13	MIR7725b	2.5	1479-1499	CAACUAUGAAUAUGGUUUUUA	UGAAAACCAUAUUCCUAGCUC	Copper-ion-binding

Table 4.15. List of putative target down-regulated of *B. distachyon* microRNAs in proliferation leaf zone. Range, complementary site of the microRNA with the target gene.

Bd ID	miRNA	miRNA position	Score	Range	Target seq	miRNA seq	Target gene annotation
Bradi1g08070	miR395c	MIR395c_m	2.5	414-434	CAUGGAGUUCUUGCAGGGAAG	GUUCCCUGCAAGCACUUCAUG	Glycosyl-transfearse
Bradi1g08070	miR395k	MIR395k_m	2.5	414-434	CAUGGAGUUCUUGCAGGGAAG	GUUCCCUGCAAGCACUUCAUG	Glycosyl-transferase
Bradi1g09030	miR395n	MIR395n_m	1	609-628	GAGUUCCUCCAAGCACUUCA	UGAAGUGUUUGGGGGAACUC	APS4;-sulfate-adenylyltransferase-(ATP)
Bradi1g09030	miR395f	MIR395f_m	1	609-628	GAGUUCCUCCAAGCACUUCA	UGAAGUGUUUGGGGGAACUC	APS4;-sulfate-adenylyltransferase-(ATP)
Bradi1g09030	miR395e	MIR395e_m	1	609-628	GAGUUCCUCCAAGCACUUCA	UGAAGUGUUUGGGGGAACUC	APS4;-sulfate-adenylyltransferase- (ATP)
Bradi1g09030	miRCB395p	MIR395p_m	0.5	609-628	GAGUUCCUCCAAGCACUUCA	UGAAGUGUUUGGAGGAACUC	APS4;-sulfate-adenylyltransferase-(ATP)
Bradi1g09030	miR395l	MIR395l_m	1	609-628	GAGUUCCUCCAAGCACUUCA	UGAAGUGUUUGGGGGAACUC	APS4;-sulfate-adenylyltransferase-(ATP)
Bradi1g09030	miR395h	MIR395h_m	1	609-628	GAGUUCCUCCAAGCACUUCA	UGAAGUGUUUGGGGGAACUC	APS4;-sulfate-adenylyltransferase-(ATP)
Bradi1g09030	miR395j	MIR395j_m	1	609-628	GAGUUCCUCCAAGCACUUCA	UGAAGUGUUUGGGGGAACUC	APS4;-sulfate-adenylyltransferase-(ATP)
Bradi1g09030	miR395c	MIR395c_m	1	609-628	GAGUUCCUCCAAGCACUUCA	UGAAGUGUUUGGGGGAACUC	APS4;-sulfate-adenylyltransferase-(ATP)
Bradi1g09030	miRCB395o	MIR395o_m	1	609-628	GAGUUCCUCCAAGCACUUCA	UGAAGUGUUUGGGGGAACUC	APS4;-sulfate-adenylyltransferase-(ATP)
Bradi1g09030	miR395b	MIR395b_m	1	609-628	GAGUUCCUCCAAGCACUUCA	UGAAGUGUUUGGGGGAACUC	APS4;-sulfate-adenylyltransferase-(ATP)
Bradi1g09030	miR395g	MIR395g_m	1	609-628	GAGUUCCUCCAAGCACUUCA	UGAAGUGUUUGGGGGAACUC	APS4;-sulfate-adenylyltransferase-(ATP)
Bradi1g09030	miR395k	MIR395k_m	1	609-628	GAGUUCCUCCAAGCACUUCA	UGAAGUGUUUGGGGGAACUC	APS4;-sulfate-adenylyltransferase-(ATP)
Bradi1g11800	miR169e	MIR169e_m	2.5	1111-1131	CAGGCAAUUCAUUCUUGGCUU	UAGCCAAGGAUGACUUGCCUG	NF-YA4-(nuclear-factor-Y.-subunit-A4); -transcription-factor
Bradi1g11800	miR169k	MIR169k_m	2.5	1111-1132	UCAGGCAAUUCAUUCUUGGCUU	UAGCCAAGGAUGAUUUGCCUGU	NF-YA9-(nuclear-factor-Y.-subunit-A9);-transcription-factor
Bradi1g11800	miR169h	MIR169h_m	2.5	1111-1131	CAGGCAAUUCAUUCUUGGCUU	UAGCCAAGGAUGACUUGCCUA	NF-YA4-(nuclear-factor-Y.-subunit-A4);-transcription-factor
Bradi1g11800	miR169k	MIR169k_m	2.5	1137-1158	UCAGGCAAUUCAUUCUUGGCUU	UAGCCAAGGAUGAUUUGCCUGU	NF-YA9-(nuclear-factor-Y.-subunit-A9);-transcription-factor
Bradi1g11800	miR169e	MIR169e_m	2.5	1138-1158	CAGGCAAUUCAUUCUUGGCUU	UAGCCAAGGAUGACUUGCCUG	NF-YA9-(nuclear-factor-Y.-subunit-A9);-transcription-factor
Bradi1g11800	miR169h	MIR169h_m	2.5	1138-1158	CAGGCAAUUCAUUCUUGGCUU	UAGCCAAGGAUGACUUGCCUA	NF-YA9-(nuclear-factor-Y.-subunit-A9);-transcription-factor
Bradi1g11800	miR169e	MIR169e_m	2.5	1112-1132	CAGGCAAUUCAUUCUUGGCUU	UAGCCAAGGAUGACUUGCCUG	NF-YA9-(nuclear-factor-Y.-subunit-A9);-transcription-factor

Bd ID	miRNA	miRNA position	Score	Range	Target seq	miRNA seq	Target gene annotation
Bradi1g11800	miR169h	MIR169h_m	2.5	1112-1132	CAGGCAAUUCAUUCUUGGCUU	UAGCCAAGGAUGACUUGCCUA	NF-YA9-nuclear-factor-Y.-subunit-A9);-transcription-factor
Bradi1g11800	miR169k	MIR169k_m	2.5	1110-1131	UCAGGCAAUUCAUUCUUGGCUU	UAGCCAAGGAUGAUUUGCCUGU	NF-YA4-(nuclear-factor-Y.-subunit-A4);-transcription-factor
Bradi1g17910	miRCB118	MIR5049_m	2.5	573-596	GCUUUCUCCGAUUCAUAUUAAUUG	CAAGUAAUAUGGAUCGGAGGAAGU	Helix-loop-helix-domain
Bradi1g52550	miRCB5163	MIR5163b	1.5	1203-1223	UUUGAAUUUUUCAGUUGGGUG	CACCCAACUGAAAUAUUUAAA	Unknown
Bradi1g52550	miRCB5163	MIR5163b	1.5	1192-1212	UUUGAAUUUUUCAGUUGGGUG	CACCCAACUGAAAUAUUUAAA	Unknown
Bradi2g24380	miRCB118	MIR5049_m	1	2079-2102	ACUUCCUCCGACCCAUAUUACUUG	CAAGUAAUAUGGAUCGGAGGAAGU	Unknown
Bradi2g28000	miRCB8	MIR7775_m	2.5	1049-1072	ACUGGUGUUUGAAAAUAAACCGGU	ACCGGUUUAUUCUGAAGCACCAGU	Unknown
Bradi4g21830	miRCB17	MIR7739_m	2.5	543-565	CGGCAACUACUUCUCAGGCUCAA	UUGAGUCUGAGAAGUAUUU-CUG	NBS-LRR
Bradi4g21830	miRCB17	MIR7739_m	2.5	744-766	CGGCAACUACUUCUCAGGCUCAA	UUGAGUCUGAGAAGUAUUU-CUG	NBS-LRR
Bradi4g27570	miRCB137a	MIR7729a_m	2.5	585-607	CCUCUCCAGGGCCUAUGGAAACA	UGUUUUCAUAGGCCAUGUAGAGC	ADP-glucose-pyrophosphorylase
Bradi4g27570	miRCB137b	MIR7729b_m	2.5	585-607	CCUCUCCAGGGCCUAUGGAAACA	UGUUUUCAUAGGCCAUGUAGAGC	ADP-glucose-pyrophosphorylase

Table 4.16. List of putative target up-regulated of *B. distachyon* microRNAs in proliferation leaf zone. Score, Range, complementary site of the microRNA with the target gene

Bd ID	miRNA	miRNA position	Score	Range	Target seq	miRNA seq	Target gene annotation
Bradi1g06460	miR319b	MIR319b_p3	2.5	943-962	AGGGGG-ACCCUUCAGUCCAA	UUGGACUGAAGGGUGCUCCCU	TCP2;-transcription-factor
Bradi1g06460	miR319b	MIR319b_p1	2.5	943-962	AGGGGG-ACCCUUCAGUCCAA	UUGGACUGAAGGGUGCUCCCU	TCP2;-transcription-factor
Bradi1g06460	miR319b	MIR319b_p2	2.5	943-962	AGGGGG-ACCCUUCAGUCCAA	UUGGACUGAAGGGUGCUCCCU	TCP2;-transcription-factor
Bradi1g14820	miR5168	MIR166g_np2	2.5	876-896	CCUUGAUCCAGACACCAACCC	GGGUUGUUGUCUGGUUCAAGG	Cyclin-(CYCA3;1)
Bradi1g14820	miR5168	MIR166g_np1	2.5	876-896	CCUUGAUCCAGACACCAACCC	GGGUUGUUGUCUGGUUCAAGG	Cyclin-(CYCA3;1)
Bradi1g45220	miR408	MIR408_m	2.5	423-442	CAUGCUCUCCUCCAUCCCGG	CAGGGAUGGAGCAGAGCAUG	TCP14;-transcription-factor
Bradi1g58450	miR319b	MIR319b_p1	2.5	1587-1606	AGGGGG-ACCCUUCAGUCCAA	UUGGACUGAAGGGUGCUCCCU	TCP2;-transcription-factor
Bradi1g58450	miR319b	MIR319b_p2	2.5	1587-1606	AGGGGG-ACCCUUCAGUCCAA	UUGGACUGAAGGGUGCUCCCU	TCP2;-transcription-factor
Bradi1g58450	miR319b	MIR319b_p3	2.5	1587-1606	AGGGGG-ACCCUUCAGUCCAA	UUGGACUGAAGGGUGCUCCCU	TCP2;-transcription-factor
Bradi1g60160	miR5174e	MIR5174e_np2	1.5	653-673	AAUUAUGGAACAGAGGGGGUA	UACUCCCUCUGUUCCAUAAAG	Ribosomal-protein
Bradi1g60160	miR5174e	MIR5174e_np1	1.5	653-673	AAUUAUGGAACAGAGGGGGUA	UACUCCCUCUGUUCCAUAAAG	Ribosomal-protein
Bradi2g37800	miR172a	MIR172a_m	0.5	1316-1336	CUGCAGCAUCAUCAGGAUUCU	AGAAUCUUGAUGAUGCUGCAU	AP2-(APETALA-2);-transcription-factor
Bradi2g55320	miRCB35	MIR7754_m	2.5	1766-1786	CAAGUUUUUUAGCUGAGAGAA	UUCUCUCGGCUAAGGAACUGC	CDC6
Bradi3g29840	miRCB47	MIR7757	2.5	275-295	UGGGUUGCUGGCGGUUUUGUG	CACAAAACCUUCAGCUACCCA	Unknown
Bradi3g53720	miRCB75	MIR7773_m	1.5	985-1005	CUGUGUCAGUUGAAGGAAAAA	UUUUUCCUUCGGCUGACACGU	Binding-protein

Table 4.17. .List of putative target down-regulated of *B. distachyon* microRNAs in expansion leaf zone.

Bd ID	miRNA	miRNA position	Score	Range	Target seq	miRNA seq	Target gene annotation
Bradi1g08070	miR395c	MIR395c_m	2.5	414-434	CAUGGAGUUCUUGCAGGGAAG	GUUCCCUGCAAGCACUUCAUG	Glycosyl-transfearse
Bradi1g08070	miR395k	MIR395k_m	2.5	414-434	CAUGGAGUUCUUGCAGGGAAG	GUUCCCUGCAAGCACUUCAUG	Glycosyl-transferase
Bradi1g11800	miR169h	MIR169h_m	2.5	1138-1158	CAGGCAAUUCAUUCUUGGCUU	UAGCCAAGGAUGACUUGCCUA	NF-YA9;-transcription factor
Bradi1g11800	miR169h	MIR169h_m	2.5	1111-1131	CAGGCAAUUCAUUCUUGGCUU	UAGCCAAGGAUGACUUGCCUA	NF-YA4;-transcription-factor
Bradi1g11800	miR169k	MIR169k_m	2.5	1111-1132	UCAGGCAAUUCAUUCUUGGCUU	UAGCCAAGGAUGAUUUGCCUGU	NF-YA9;-transcription-factor
Bradi1g11800	miR169e	MIR169e_m	2.5	1111-1131	CAGGCAAUUCAUUCUUGGCUU	UAGCCAAGGAUGACUUGCCUG	NF-YA4;-transcription-factor
Bradi1g11800	miR169k	MIR169k_m	2.5	1137-1158	UCAGGCAAUUCAUUCUUGGCUU	UAGCCAAGGAUGAUUUGCCUGU	NF-YA9;-transcription-factor
Bradi1g11800	miR169h	MIR169h_m	2.5	1112-1132	CAGGCAAUUCAUUCUUGGCUU	UAGCCAAGGAUGACUUGCCUA	NF-YA9;-transcription-factor
Bradi1g11800	miR169k	MIR169k_m	2.5	1110-1131	UCAGGCAAUUCAUUCUUGGCUU	UAGCCAAGGAUGAUUUGCCUGU	NF-YA4;-transcription-factor
Bradi1g11800	miR169e	MIR169e_m	2.5	1138-1158	CAGGCAAUUCAUUCUUGGCUU	UAGCCAAGGAUGACUUGCCUG	NF-YA9;-transcription-factor
Bradi1g11800	miR169e	MIR169e_m	2.5	1112-1132	CAGGCAAUUCAUUCUUGGCUU	UAGCCAAGGAUGACUUGCCUG	NF-YA9;transcription-factor
Bradi3g57320	miR169e	MIR169e_m	2	888-908	CAGGCAAUUCAUCCUUGGCUU	UAGCCAAGGAUGACUUGCCUG	NF-YA5;-transcription-factor
Bradi3g57320	miR169k	MIR169k_m	2	887-908	UCAGGCAAUUCAUCCUUGGCUU	UAGCCAAGGAUGAUUUGCCUGU	NF-YA5;-transcription-factor
Bradi3g57320	miR169h	MIR169h_m	2	888-908	CAGGCAAUUCAUCCUUGGCUU	UAGCCAAGGAUGACUUGCCUA	NF-YA5;-transcription-factor
Bradi4g27570	miRCB137a	MIR7729a_m	2.5	585-607	CCUCUCCAGGGCCUAUGGAAACA	UGUUUUCAUAGGCCAUGUAGAGC	ADP-glucose-pyrophosphorylase
Bradi4g27570	miRCB137b	MIR7729b_m	2.5	585-607	CCUCUCCAGGGCCUAUGGAAACA	UGUUUUCAUAGGCCAUGUAGAGC	ADP-glucose-pyrophosphorylase
Bradi4g30710	miR5174e	MIR5174e_np1	1	1163-1183	CUACUCCCUCCGUUCCAUAAU	UUUAUGGAACGGAGGGAGUAG	Tetraspanin-family
Bradi4g30710	miR5174e	MIR5174e_np2	1	1163-1183	CUACUCCCUCCGUUCCAUAAU	UUUAUGGAACGGAGGGAGUAG	Tetraspanin-family
Bradi4g30710	miR5174e	MIR5174e_np1	1	1265-1285	AUACUCCCUUCGUUUCAUAAU	UUUAUGGAACGGAGGGAGUAG	Tetraspanin-family
Bradi4g30710	miR5174e	MIR5174e_np2	1	1265-1285	AUACUCCCUUCGUUUCAUAAU	UUUAUGGAACGGAGGGAGUAG	Tetraspanin-family

Table 4.18. List of putative target up-regulated of *B. distachyon* microRNAs in expansion leaf zone

Considering that the cleavage of the target genes is the predominant mechanism used by the plant miRNAs to negatively regulate the expression of target genes (Voinnet et al., 2009), this mode of action was indagated. The expression patterns of miRNA target genes generally show an opposite profile with those of miRNAs. Therefore in order to validate putative target genes after miRNAs cleavage, we focused on the lists of putative targets down-regulated looking for a negative correlation between target and miRNA expression, which is often considered an indication of miRNA regulation (Jeong and Green, 2013).

Both in the list of differential expressed genes, down-regulated in proliferation and expansion cells were found targets genes related to:TEOSINTE BRANCHED1/CYCLOIDEA/PCF2 (TCP2), APETALA2 (AP2). In proliferating cells were found know mirna target genes like GROWTH-REGULATION FACTOR (GRF)., SAP-domain, RNA-binding and Copper-ion-binding. While in expanding cells there are TCP14, Binding-protein, as CYCLIN (CYCA3;1) and Cell Division Cycle 6 (CDC6). The latter two target genes are involved in the control of cell cycle.

Taking into account the effect of drought stress on the activity of cell proliferation, the expression profile of four miRNA and their target genes were investigated deeply: miR319b, miR5049, miR166g and miR7754 which seem to target Bradi1g06460 (TCP2), Bradi1g12650 (GRF2), Bradi1g14820 (CycA3), Bradi2g55320 (CDC6), respectively. By plotting the expression profile of both miRNAs and targets genes, interesting opposite expression profiles have been highlight. CycA3 and miR166g have a similar expression trend in proliferating cells, while they have an opposite expression in expanding cells where the expression level of miRNA is greater than its target gene (Fig.4.10a). This expression profile suggests that miR166g might acts on the target through two modes of action: translation inhibition to finely regulation the activity of the target in proliferating cells and endonucleolytic cleavage of the target in expanding cells.

CDC6 showed an opposite expression profile to miR7754 in proliferation and expansion cells. The target is down regulated in expansion cells while miR7754 is up-regulated (Fig.4.10b). Moreover, TCP was found down-regulated in expansion leaf zone. Specifically in expansion cells grown in control condition there is an opposite expression pattern with miR319b, while in stress conditions the expression of miRNA and was approximately equal suggesting a translation inhibition by miRNA (Fig.4.10c).

To further investigate the relation between miRNA and target genes Bradi1g12650

(GRF2), Bradi1g14820 (CycA3) and Bradi2g55320 (CDC6) has been selected in order to validate the cleavage mediated by miRNAs on the target using a 5'RACE approach.

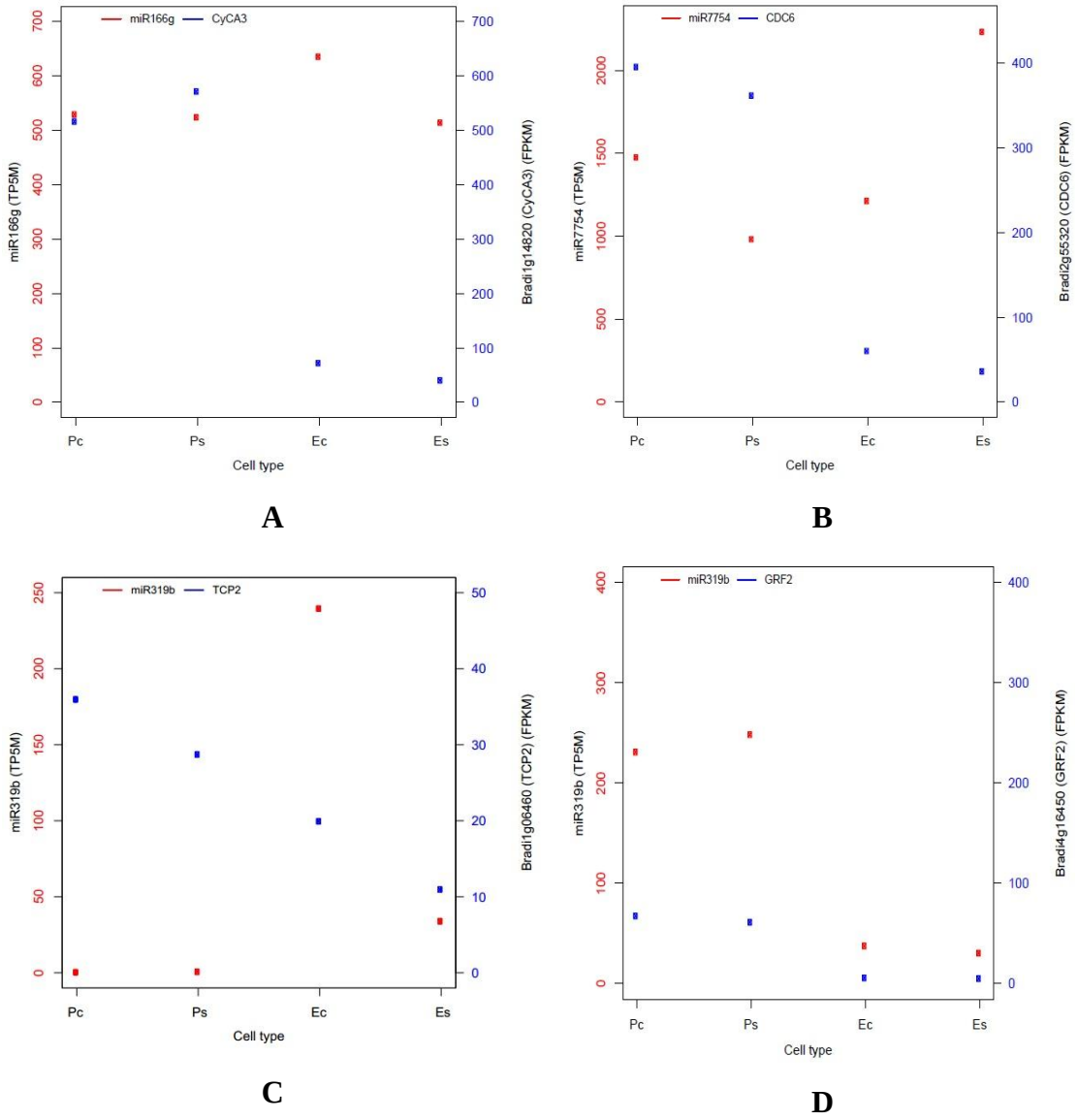

Figure 4.10. Plot showing expression of miRNAs and their targets in proliferating (P) and expanding (E) cells under control (C) and drought stress (S) conditions. (a) miR166g and CycA;3 target. (b) miR7754 and CDC6 target. (c) miR319b and TCP2 target. (d) miR5049 and GRF2 target.. miRNAs expression in TP5M: . Target expression in FPKM.

4.7 Validation of predicted miRNAs target by 5'-RACE

Modified 5’-RACE allows to validate reliably the cleavage of the mRNA of target genes between 10 and 11 position by the action of miRNAs.

In this work, we have been started the validation of predicted target genes, performing a 5’-RACE. Based on RNA-seq data, we have been focused on: Bradi1g12650 (GRF2), Bradi1g14820 (CycA3), Bradi2g55320 (CDC6), Bradi4g30710 (TETRA) and Bradi4g16450 (NAM).

We predict the appropriate size of amplification products with Primer3 (Tab. 4.19).

	Primer	
Gene	**Fad.inn - Rinn**	**Fc+ - Rinn**
Bradi1g12650	403	315
Bradi1g14820	160	320
Bradi2g55320	142	190
Bradi4g16450	260	309
Bradi4g30710	144	280

Table 4.19. List of product size of nested 5’RACE predicted by Primer3. Fad.inn: GeneRacer 5' Nested Primer. Fc+: forward primer for the positive control. Rinn: gene-specific inner reverse primer.

The products size of the gene-specific inner primer (Rinn) might correspond to the size of putative targets after the action of the miRNA cleavage. Has shown in the agarose gel the expected band were obtained for three putative target genes: Bradi1g12650 (GRF2), Bradi1g14820 (CycA3) and Bradi2g55320 (CDC6) (Fig.4.11, Fig.4.12). This results support the expression data showing a post-transactional regulation mediated by the miRNA.

In order to confirm these observations, the agarose bands were excised from the gel and successively cloned into a bacterial vector and sequenced. This last activity have been not completed yet and will be done in the coming months.

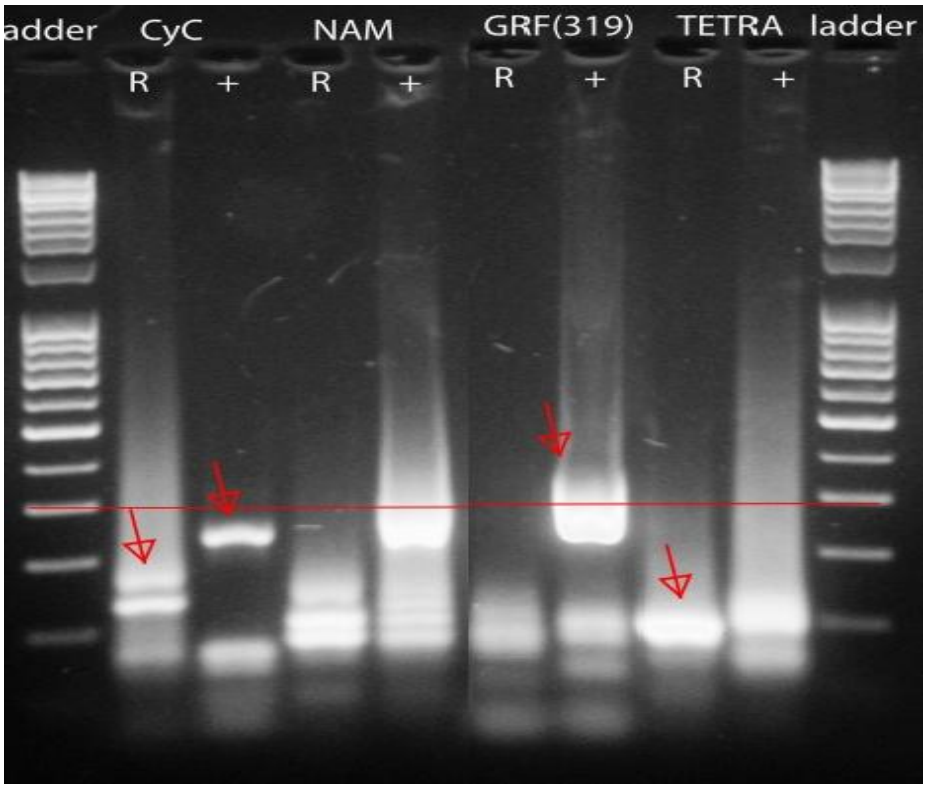

Figure 4.11. Electrophoresis gel of 5'-RACE of CyC, NAM and GRF genes. Red line indicates bands with 300 bp size and red arrows indicate bands analysed (R): nested 5'-RACE.(+): positive control.

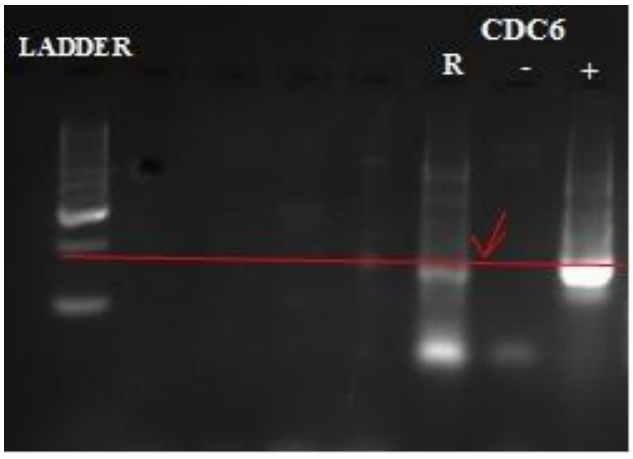

Figure 4.12. Electrophoresis gel of 5'-RACE of CDC6 gene. Red line indicates bands with 200 bp size and red arrows indicate the band excised. (R): nested 5'-RACE. (-): negative control. (+): positive control.

5 Discussion

Plants are able to redistribute resources during adverse conditions. Hence, dissecting the transcriptional and post-transcriptional mechanisms controlling gene expression during stress responses is pivotal to understand of how plants adapt to the environment (Bertolini et al., 2013).

The present project investigates the molecular network controlling leaf development during drought stress in *Brachypodium distachyon.*

We conducted a whole transcriptome analysis, based on next generation sequencing, in order to dissect the complex regulatory network involved in the reprogramming of leaf growth during drought stress. We focused on three developmental leaf zones (from basal portion to the tip: Proliferation, Expansion and Mature cells) in order to study individual cell types to gain insight into finely regulated processes connecting leaf development to drought stress response.

5.1 The Molecular response to drought stress

In this study, we analyzed leaf development during drought stress, which has been showed to be plastic and dependent on environmental conditions (Andriankaja et al., 2012).

Previous works conducted in *Arabidopsis* have been shown that drought response is highly dependent on leaf developmental stage (Skirycz et al., 2010).

With the aim to understand better drought stress response, we investigated the expression of the entire *Brachypodium* transcriptome in three developmental zones: proliferation, expansion and maturation.

Differential expression analysis was performed taking into account comparisons between different cell types in the same growth conditions (drought or control) and same developmental areas between drought versus control condition. We observed that genes modulated in response to drought stress shown high dependence on cell type. This observation is highlighted in the venn diagrams were a limited overlap between the three developmental zone is shown, highlighting that the modulation of gene expression in proliferation, expansion and mature zone. Gene ontology analysis confirmed that the

drought stress is specific to each developmental zone. Proliferation cells are characterized by terms involved in cell cycle, ribosomal factor, anabolism, highlighting that in this leaf stage the synthesis of new proteins and macromolecules occurs (Johnson and Lenhard, 2011). In expansion cells, were found terms involved in production and transport of fatty acid, DNA replication, transporter activity, indeed at this stage cell begin to expand mainly by loosening of the cell wall and deposition of new cell material (Clays and Inzè, 2014) involving the activity of many carriers.

The actual state of art in *Arabidopsis,* shows that drought stress reduces leaf size due to a negative effect on both cell expansion and cell proliferation. Whereas, in *Brachypodium* leaf size reduction in response to drought stress is nearly entirely caused by a reduction in cell expansion, showing proliferation cells unaffected by drought (Verelst et al., 2012).

To better understand the molecular mechanisms underlying drought stress response, we focused on the several transcription factors (TFs) which are mainly involved in the molecular pathways controlling leaf growth.

Our data shows an over expression in proliferating cells of different TFs: GROWTH-REGULATING FACTOR (GRF), Cyclin (CYC) and AUXIN RESPONSE FACTORS (ARF2).

The strong expression of GRFs in the proliferating cells is in accordance with the recent literatures, indicating the main role of GRF in controlling cell proliferation and affecting leaf growth and shape (Gonzalez et al., 2012). These functions were confirmed by experiment where loss of function in different GRF genes lead to a reduction of leaf size leaf, in contrast over expression of GRF generates slightly bigger leaves (Debernardi et al., 2014).

Similarly, ARF were found strongly expressed in proliferating cells. ARF is a transcription factors that have main role in affecting cell division and cell expansion (Gonzalez et al., 2012).

In our data set we found A-type Cyclins (CYCAs) which is a mitotic cyclin with important roles in cell cycle progression (Masaki Ito, 2014). This gene has important role in meristematic tissues, contributing to fine tuning local proliferation during plant development. In particular, CYCD3 is a G1-type cyclin of which the expression is induced in response to growth stimuli and which is involved in cell cycle initiation and progression in plants (Gonzalez et al., 2012). A strong expression of this class of genes in proliferation cells was observed in our data both in control and drought stress,

highlighting that drought stress did not affected cyclin activity, hence the progression of cell cycle in *Brachypodium*.

Again in accordance with the literature TEOSINTE BRANCHED1/CYCLOIDEA/PCF (TCP) was found down regulated in the proliferation cells.

TCP transcription factors family are involved in controlling both proliferation and differentiation in leaves (Endriankaja et al., 2014). Analysis of single, double and triple mutants of TCP genes showed an increase in leaf size underlining the activity of TCP in cell proliferation (Gonzalez et al., 2012).

Our data shows an expression of EXPANSINs during cell expansion. It is well known that during cell expansion loosening of the cell wall and deposition of new cell wall material occur (Claeys and Inzè, 2014) mediated by EXPANSINs (EXP). The over-expression of EXP10 under the control of its own promoter results in the production of larger leaves containing larger cells (Gonzalez et al., 2012).

Moreover we investigated the role of gibberellin (GA), is a crucial plant hormone in controlling growth regulation networks.

The expression of GA biosynthesis genes is associated with growing tissues, suggesting that biosynthesis is the first regulatory step controlling GA levels and consequently plant growth (Claeys et al., 2014). Based on transcript expression profile, GA synthesis appears to be drought-repress in the growing parts of the leaf. Moreover we observed that the gibberellin-2-beta-dioxygenase (GA2ox, Bradi2g50280, involved in gibberellin catabolism) was down-regulated in the proliferation and expansion zones.

5.2 Role of miRNAs in leaf growth during drought stress conditions

The expression of a large number of miRNAs in leaves reflects the complexity of regulatory activities required for fine-tuning growth and development of this organ (Bertolini et al., 2013). Several miRNA-target nodes have been described as coordinating gene expression programs to support phenotypic plasticity (Rubio-Somoza and Weigel, 2011).

In the lab has been shown that miRNAs are involved in reprogramming leaf growth under drought stress conditions (Bertolini et al 2013). In this thesis, we also focused on

analysis of target node controlling cell proliferation described in Arabidopsis leaves by Rubio-Somoza and Weigel, 2011 (Fig 5.1).

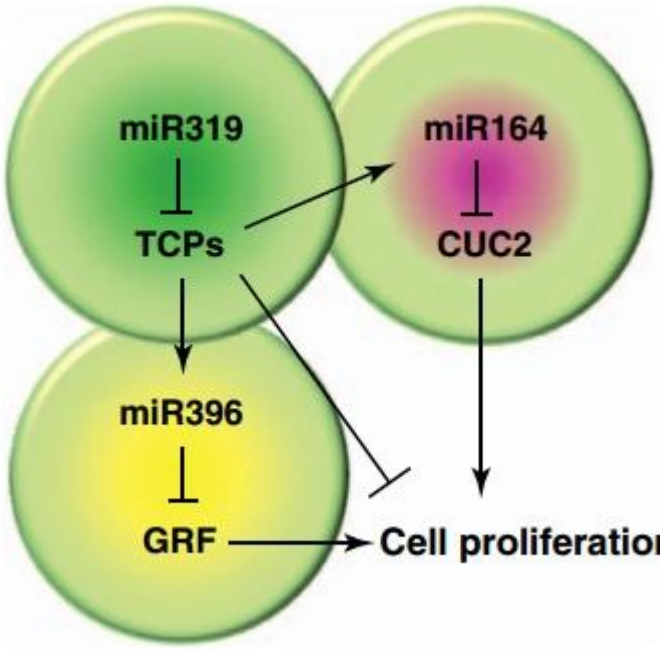

Figure 5.1. Interplay of miRNA nodes regulating cell proliferation in leaves (from Rubio-Somoza and Weigel, 2011).

In proliferation cells GROWTH-REGULATING FACTORS (GRFs) show an high expression level, while in expansion cells their expression is down-regulated by miR396. In our data we observed a similar expression profile of both GRFs and miR396, our *in silico* target prediction data also shown a putative role of miR319b in controlling GRF2, adding a new function to miR319 which is well known to be involved in controlling five members of the TCP transcription factor family (TCP2, 2, 3, 4, 10, 24) that, in turn, inhibit cell proliferation (Bertolini et al., 2013). In our experiment during drought stress in proliferating cell, TCPs are low expressed. Moreover Cell Division Cycle 6 (CDC6), an essential regulator of DNA replication that play important role in the activation and maintenance of the checkpoint mechanism in the cell cycle, seams to be targeted by a species specific *Brachypodium* miR7754. Our data show an inverse expression profile in which target is down regulated in expansion cells while miR7754 is up-regulated. Also CYCLIN (CYCA3;1), targetd by miR166g, shows an inverse trend in expansion cells, while in proliferation cell they have a similar

expression. This two non canonical targets involved directly in cell proliferation might contribute in keeping active cell division during drought stress.

6 Conclusions

Brachypodium distachyon (Bd), a drought-tolerant wild grass, is an interesting model species to deeply study the molecular mechanisms involved in drought-stress response. In this study we take benefit from a reproducible soil assay to subject Bd to drought stress was applied, which resulted in a drastically leaf size reduction. This effect was mainly caused by a reduction in cell expansion instead of a reduction of cell proliferation, underlining the insensitivity of the meristem to drought stress.

In order to investigate molecular mechanism underlying this phenomenon we used a Next Generation Sequencing (NGS) approach.

We show differences in expression profiles of coding and non coding genes between proliferating leaf cells, cells expansion and mature cell in both normal and drought-stressed conditions, emphasizing the importance of the study of individual cell types to gain insight into processes which occur during abiotic stress responses. Differential expression analyses shows that the response to drought stress is cell specific. Such hypotheses are the subject of ongoing experimental work and are expected to lead to further insights into lineage-specific and widely conserved responses to drought stress, one of the most relevant objectives in modern plant biology.

7 References

Anders, Simon, and Wolfgang Huber. "Differential Expression Analysis for Sequence Count Data." *Genome Biology* 11, no. 10 (October 27, 2010): R106. doi:10.1186/gb-2010-11-10-r106.

Andriankaja, Megan, Stijn Dhondt, Stefanie De Bodt, Hannes Vanhaeren, Frederik Coppens, Liesbeth De Milde, Per Mühlenbock, et al. "Exit from Proliferation during Leaf Development in Arabidopsis Thaliana: A Not-so-Gradual Process." *Developmental Cell* 22, no. 1 (January 17, 2012): 64–78. doi:10.1016/j.devcel.2011.11.011.

Baldos Uris Lantz C and Thomas W. Hertel. "Global Food Security in 2050: The Role of Agricultural Productivity and Climate Change." *Australian Journal of Agricultural and Resource Economics*, March 1, 2014, n/a–n/a. doi:10.1111/1467-8489.12048.

Bertolini, Edoardo, Wim Verelst, David Stephen Horner, Luca Gianfranceschi, Viviana Piccolo, Dirk Inzé, Mario Enrico Pè, and Erica Mica. "Addressing the Role of microRNAs in Reprogramming Leaf Growth during Drought Stress in Brachypodium Distachyon." *Molecular Plant* 6, no. 2 (March 2013): 423–43. doi:10.1093/mp/sss160.

Bevan Michael W., David F. Garvin, and John P. Vogel. "Brachypodium Distachyon Genomics for Sustainable Food and Fuel Production." *Current Opinion in Biotechnology* 21, no. 2 (April 2010): 211–17. doi:10.1016/j.copbio.2010.03.006.

Bonnet, Eric, Yves Van de Peer, and Pierre Rouzé. "The Small RNA World of Plants." *The New Phytologist* 171, no. 3 (2006): 451–68. doi:10.1111/j.1469-8137.2006.01806.x.

Boyer, J. S. "Plant Productivity and Environment." *Science* 218, no. 4571 (October 29, 1982): 443–48. doi:10.1126/science.218.4571.443.

Brkljacic Jelena, Erich Grotewold, Randy Scholl, Todd Mockler, David F. Garvin, Philippe Vain, Thomas Brutnell, et al. "Brachypodium as a Model for the Grasses:

Today and the Future." *Plant Physiology* 157, no. 1 (September 1, 2011): 3–13. doi:10.1104/pp.111.179531.

Chinnusamy V, Schumaker K, Zhu JK (2004) Molecular genetic perspectives on cross-talk and specificity in abiotic stress signalling in plants. J Exp Bot 55: 225–236.

Chinnusamy, Viswanathan, and Jian-Kang Zhu. "Epigenetic Regulation of Stress Responses in Plants." *Current Opinion in Plant Biology* 12, no. 2 (April 2009): 133–39. doi:10.1016/j.pbi.2008.12.006.

Chinnusamy, Viswanathan, and Jian-Kang Zhu. "Epigenetic Regulation of Stress Responses in Plants." *Current Opinion in Plant Biology* 12, no. 2 (April 2009): 133–39. doi:10.1016/j.pbi.2008.12.006.

Claeys, H., S. Van Landeghem, M. Dubois, K. Maleux, and D. Inze. "What Is Stress? Dose-Response Effects in Commonly Used in Vitro Stress Assays." *PLANT PHYSIOLOGY* 165, no. 2 (June 1, 2014): 519–27. doi:10.1104/pp.113.234641.

Claeys, Hannes, and Dirk Inzé. "The Agony of Choice: How Plants Balance Growth and Survival under Water-Limiting Conditions." *Plant Physiology* 162, no. 4 (August 2013): 1768–79. doi:10.1104/pp.113.220921.

Claeys, Hannes, Stefanie De Bodt, and Dirk Inzé. "Gibberellins and DELLAs: Central Nodes in Growth Regulatory Networks." *Trends in Plant Science* 19, no. 4 (January 4, 2014): 231–39. doi:10.1016/j.tplants.2013.10.001.

Cramer, Grant R., Kaoru Urano, Serge Delrot, Mario Pezzotti, and Kazuo Shinozaki. "Effects of Abiotic Stress on Plants: A Systems Biology Perspective." *BMC Plant Biology* 11, no. 1 (November 17, 2011): 163. doi:10.1186/1471-2229-11-163.

Dalmais Marion, Sébastien Antelme, Séverine Ho-Yue-Kuang, Yin Wang, Olivier Darracq, Madeleine Bouvier d' Yvoire, Laurent Cézard, et al. "A TILLING Platform for Functional Genomics in Brachypodium Distachyon." *PLoS ONE* 8, no. 6 (June 19, 2013): e65503. doi:10.1371/journal.pone.0065503.

Danquah, Agyemang, Axel de Zelicourt, Jean Colcombet, and Heribert Hirt. "The Role of ABA and MAPK Signaling Pathways in Plant Abiotic Stress Responses."

Biotechnology Advances, Plant Biotechnology 2013: "Green for Good II"., 32, no. 1 (January 2014): 40–52. doi:10.1016/j.biotechadv.2013.09.006.

Dempewolf Hannes, Ruth J. Eastwood, Luigi Guarino, Colin K. Khoury, Jonas V. Müller, and Jane Toll. "Adapting Agriculture to Climate Change: A Global Initiative to Collect, Conserve, and Use Crop Wild Relatives." *Agroecology and Sustainable Food Systems* 38, no. 4 (February 18, 2014): 369–77. doi:10.1080/21683565.2013.870629.

Draper John, Luis A.J. Mur, Glyn Jenkins, Gadab C. Ghosh-Biswas, Pauline Bablak, Robert Hasterok, and Andrew P.M. Routledge. "Brachypodium Distachyon. A New Model System for Functional Genomics in Grasses." *Plant Physiology* 127, no. 4 (December 2001): 1539–55.

Gentile, Agustina, Thais H. Ferreira, Raphael S. Mattos, Lara I. Dias, Andrea A. Hoshino, Monalisa S. Carneiro, Glaucia M. Souza, et al. "Effects of Drought on the Microtranscriptome of Field-Grown Sugarcane Plants." *Planta* 237, no. 3 (March 2013): 783–98. doi:10.1007/s00425-012-1795-7.

Gentleman, Robert C., Vincent J. Carey, Douglas M. Bates, Ben Bolstad, Marcel Dettling, Sandrine Dudoit, Byron Ellis, et al. "Bioconductor: Open Software Development for Computational Biology and Bioinformatics." *Genome Biology* 5, no. 10 (September 15, 2004): R80. doi:10.1186/gb-2004-5-10-r80.

Gonzalez, Nathalie, Hannes Vanhaeren, and Dirk Inzé. "Leaf Size Control: Complex Coordination of Cell Division and Expansion." *Trends in Plant Science* 17, no. 6 (June 2012): 332–40. doi:10.1016/j.tplants.2012.02.003.

Hands Philip, and Sinéad Drea. "A Comparative View of Grain Development in Brachypodium Distachyon." *Journal of Cereal Science*, Cereal Grain Development: Molecular Mechanisms and Impacts on Grain Composition and Functionality, 56, no. 1 (July 2012): 2–8. doi:10.1016/j.jcs.2011.12.010.

Humbeck, Klaus. "Epigenetic and Small RNA Regulation of Senescence." *Plant Molecular Biology* 82, no. 6 (August 1, 2013): 529–37. doi:10.1007/s11103-012-0005-0.

J. Bot, F.O. Nachtergaele and A. Young. “Land resource potential and constraints at regional and country levels” World Soil Resources Report 2000, 90. FAO.

Jeong Dong-Hoon, Skye A. Schmidt, Linda A. Rymarquis, Sunhee Park, Matthias Ganssmann, Marcelo A. German, Monica Accerbi, et al. “Parallel Analysis of RNA Ends Enhances Global Investigation of microRNAs and Target RNAs of Brachypodium Distachyon.” *Genome Biology* 14, no. 12 (December 24, 2013): R145. doi:10.1186/gb-2013-14-12-r145.

Jeong, Dong-Hoon, Skye A. Schmidt, Linda A. Rymarquis, Sunhee Park, Matthias Ganssmann, Marcelo A. German, Monica Accerbi, et al. “Parallel Analysis of RNA Ends Enhances Global Investigation of microRNAs and Target RNAs of Brachypodium Distachyon.” *Genome Biology* 14, no. 12 (December 24, 2013): R145. doi:10.1186/gb-2013-14-12-r145.

Jiang, Qian, Feng Wang, Meng-Yao Li, Hua-wei Tan, Jing Ma, and Ai-Sheng Xiong. “High-Throughput Analysis of Small RNAs and Characterization of Novel microRNAs Affected by Abiotic Stress in a Local Celery Cultivar.” *Scientia Horticulturae* 169 (April 16, 2014): 36–43. doi:10.1016/j.scienta.2014.02.007.

Johnson, Kim, and Michael Lenhard. “Genetic Control of Plant Organ Growth.” *New Phytologist* 191, no. 2 (July 1, 2011): 319–33. doi:10.1111/j.1469-8137.2011.03737.x.

Kasschau, K.D., Xie, Z., Allen, E., Llave, C., Chapman, E.J., Krizan, K.A., and Carrington, J.C. (2003). P1/HC-Pro, a viral suppressor of RNA silencing, interferes with Arabidopsis development and miRNA function. Dev. Cell 4, 205–217

Khraiwesh, Basel, Jian-Kang Zhu, and Jianhua Zhu. “Role of miRNAs and siRNAs in Biotic and Abiotic Stress Responses of Plants.” *Biochimica Et Biophysica Acta* 1819, no. 2 (February 2012): 137–48. doi:10.1016/j.bbagrm.2011.05.001.

Kidner, Catherine A. “The Many Roles of Small RNAs in Leaf Development.” *Journal of Genetics and Genomics* 37, no. 1 (January 2010): 13–21. doi:10.1016/S1673-8527(09)60021-7.

Love MI, Huber W and Anders S (2014). "Moderated estimation of fold change and dispersion for RNA-Seq data with DESeq2. " *bioRxiv*. http://dx.doi.org/10.1101/002832, http://dx.doi.org/10.1101/002832.

Moon, J. and Hake, S. (2011) How a leaf gets its shape. Curr. Opin. Plant Biol.1, 24–30.

Mur Luis A. J., Joel Allainguillaume, Pilar Catalán, Robert Hasterok, Glyn Jenkins, Karolina Lesniewska, Ianto Thomas, and John Vogel. "Exploiting the Brachypodium Tool Box in Cereal and Grass Research." *New Phytologist* 191, no. 2 (July 1, 2011): 334–47. doi:10.1111/j.1469-8137.2011.03748.x.

Nakashima, Kazuo, Yusuke Ito, and Kazuko Yamaguchi-Shinozaki. "Transcriptional Regulatory Networks in Response to Abiotic Stresses in Arabidopsis and Grasses." *Plant Physiology* 149, no. 1 (January 1, 2009): 88–95. doi:10.1104/pp.108.129791.

Ortiz R, Jarvis A, Fox P, Aggarwal PK and Campbell BM. 2014. *Plant Genetic Engineering, Climate Change and Food Security*. CCAFS Working Paper no. 72. CGIAR Research Program on Climate Change, Agriculture and Food Security (CCAFS). Copenhagen, Denmark. Available online at: www.ccafs.cgiar.org.

Peleg, Zvi, and Eduardo Blumwald. "Hormone Balance and Abiotic Stress Tolerance in Crop Plants." *Current Opinion in Plant Biology* 14, no. 3 (June 2011): 290–95. doi:10.1016/j.pbi.2011.02.001.

Priest, Henry D., Samuel E. Fox, Erik R. Rowley, Jessica R. Murray, Todd P. Michael, and Todd C. Mockler. "Analysis of Global Gene Expression in Brachypodium Distachyon Reveals Extensive Network Plasticity in Response to Abiotic Stress." *PLoS ONE* 9, no. 1 (January 29, 2014): e87499. doi:10.1371/journal.pone.0087499.

Pulido, Amada, and Patrick Laufs. "Co-Ordination of Developmental Processes by Small RNAs during Leaf Development." *Journal of Experimental Botany* 61, no. 5 (March 1, 2010): 1277–91. doi:10.1093/jxb/erp397.

Richard M. Adams, Brian H. Hurd, Stephanie Lenhart, Neil Leary.(1998) "Effects of global climate change on agriculture: an interpretative review". CLIMATE RESEARCH, 11:19–30.

Roberts Adam, Harold Pimentel, Cole Trapnell, and Lior Pachter. “Identification of Novel Transcripts in Annotated Genomes Using RNA-Seq.” *Bioinformatics*, June 21, 2011, btr355. doi:10.1093/bioinformatics/btr355.

Schapire, Arnaldo L., Nicolas G. Bologna, Belen Moro, Jixian Zhai, Blake C. Meyers, and Javier F. Palatnik. “Reprint of: Construction of Specific Parallel Amplification of RNA Ends (SPARE) Libraries for the Systematic Identification of Plant microRNA Processing Intermediates.” *Methods (San Diego, Calif.)* 67, no. 1 (May 1, 2014): 36–44. doi:10.1016/j.ymeth.2014.04.001.

Shinozaki, Kazuo, and Kazuko Yamaguchi-Shinozaki. “Gene Networks Involved in Drought Stress Response and Tolerance.” *Journal of Experimental Botany* 58, no. 2 (January 1, 2007): 221–27. doi:10.1093/jxb/erl164.

Skirycz, Aleksandra, and Dirk Inzé. “More from Less: Plant Growth under Limited Water.” *Current Opinion in Biotechnology* 21, no. 2 (April 2010): 197–203. doi:10.1016/j.copbio.2010.03.002.

Skirycz, Aleksandra, Hannes Claeys, Stefanie De Bodt, Akira Oikawa, Shoko Shinoda, Megan Andriankaja, Katrien Maleux, et al. “Pause-and-Stop: The Effects of Osmotic Stress on Cell Proliferation during Early Leaf Development in Arabidopsis and a Role for Ethylene Signaling in Cell Cycle Arrest.” *The Plant Cell* 23, no. 5 (May 2011): 1876–88. doi:10.1105/tpc.111.084160.

Skirycz, Aleksandra, Stefanie De Bodt, Toshihiro Obata, Inge De Clercq, Hannes Claeys, Riet De Rycke, Megan Andriankaja, et al. “Developmental Stage Specificity and the Role of Mitochondrial Metabolism in the Response of Arabidopsis Leaves to Prolonged Mild Osmotic Stress.” *Plant Physiology* 152, no. 1 (January 1, 2010): 226–44. doi:10.1104/pp.109.148965.

Skirycz, Aleksandra, Stefanie De Bodt, Toshihiro Obata, Inge De Clercq, Hannes Claeys, Riet De Rycke, Megan Andriankaja, et al. “Developmental Stage Specificity and the Role of Mitochondrial Metabolism in the Response of Arabidopsis Leaves to Prolonged Mild Osmotic Stress.” *Plant Physiology* 152, no. 1 (January 1, 2010): 226–44. doi:10.1104/pp.109.148965.

Trapnell, Cole, Adam Roberts, Loyal Goff, Geo Pertea, Daehwan Kim, David R. Kelley, Harold Pimentel, Steven L. Salzberg, John L. Rinn, and Lior Pachter. “Differential Gene and Transcript Expression Analysis of RNA-Seq Experiments with TopHat and Cufflinks.” *Nature Protocols* 7, no. 3 (March 2012): 562–78. doi:10.1038/nprot.2012.016.

Trapnell, Cole, Brian A. Williams, Geo Pertea, Ali Mortazavi, Gordon Kwan, Marijke J. van Baren, Steven L. Salzberg, Barbara J. Wold, and Lior Pachter. “Transcript Assembly and Quantification by RNA-Seq Reveals Unannotated Transcripts and Isoform Switching during Cell Differentiation.” *Nature Biotechnology* 28, no. 5 (May 2010): 511–15. doi:10.1038/nbt.1621.

Trapnell, Cole, Lior Pachter, and Steven L. Salzberg. “TopHat: Discovering Splice Junctions with RNA-Seq.” *Bioinformatics (Oxford, England)* 25, no. 9 (May 1, 2009): 1105–11. doi:10.1093/bioinformatics/btp120.

Vaucheret, Hervé. “Post-Transcriptional Small RNA Pathways in Plants: Mechanisms and Regulations.” *Genes & Development* 20, no. 7 (April 1, 2006): 759–71. doi:10.1101/gad.1410506.

Verelst, Wim, Edoardo Bertolini, Stefanie De Bodt, Klaas Vandepoele, Marlies Demeulenaere, Mario Enrico Pè, and Dirk Inzé. “Molecular and Physiological Analysis of Growth-Limiting Drought Stress in Brachypodium Distachyon Leaves.” *Molecular Plant* 6, no. 2 (March 2013): 311–22. doi:10.1093/mp/sss098.

Vogel, John P., David F. Garvin, Todd C. Mockler, Jeremy Schmutz, Dan Rokhsar, Michael W. Bevan, Kerrie Barry, et al. “Genome Sequencing and Analysis of the Model Grass Brachypodium Distachyon.” *Nature* 463, no. 7282 (February 11, 2010): 763–68. doi:10.1038/nature08747.

Voinnet, Olivier. “Origin, Biogenesis, and Activity of Plant MicroRNAs.” *Cell* 136, no. 4 (February 20, 2009): 669–87. doi:10.1016/j.cell.2009.01.046.

Wu, Gang. “Plant MicroRNAs and Development.” *Journal of Genetics and Genomics*, Epigenetics: Plant Developmental Variations and Memories, 40, no. 5 (May 20, 2013): 217–30. doi:10.1016/j.jgg.2013.04.002.

Xin-Chum MO (2014). “Recent Progress in Model Grass Brachypodium distachyon (Poaceae)”. Plant Diversity and Resources 2014 – 36(2): 197-207.

Young MD, Wakefield MJ, Smyth GK and Oshlack A (2010). “Gene ontology analysis for RNA-seq: accounting for selection bias.”*Genome Biology*, 11, pp. R14.

Young, Matthew D., Matthew J. Wakefield, Gordon K. Smyth, and Alicia Oshlack. “Gene Ontology Analysis for RNA-Seq: Accounting for Selection Bias.” *Genome Biology* 11, no. 2 (February 4, 2010): R14. doi:10.1186/gb-2010-11-2-r14.